mapquest

Notes

Boise to Snake River Plains stop, to Bruneau Dunes

Trip to:

Bruneau Dunes Rd

Bruneau, ID 83604

68.41 miles / 1 hour 15 minutes

A **1455 S Capitol Blvd**, Boise, ID 83706

Download Free App

1. Start out going **southwest** on **S Capitol Blvd** toward **W Crescent Rim Dr**. Map	**0.2 Mi**	*0.2 Mi Total*
2. **S Capitol Blvd** becomes **S Federal Way**. Map	**5.3 Mi**	*5.5 Mi Total*
3. Turn **left** onto **ID-21 / E Gowen Rd**. Continue to follow **ID-21**. Map *ID-21 is 0.1 miles past E Lake Forest Dr* *If you reach E Hospitality Ln you've gone a little too far*	**3.4 Mi**	*8.9 Mi Total*
4. **9760 E HIGHWAY 21** is on the **left**. Map *Your destination is 0.2 miles past Warm Springs Ave* *If you reach E Discovery State Park Rd you've gone about 1.7 miles too far*		

A to **B** Travel Estimate: **8.86 mi - about 12 minutes**

B **9760 E Highway 21**, Boise, ID 83716-9393

1. Start out going **northwest** on **E Highway 21 / ID-21** toward **Warm Springs Ave**. Continue to follow **ID-21**. Map	**3.6 Mi**	*12.4 Mi Total*
2. Stay **straight** to go onto **E Gowen Rd**. Map	**0.2 Mi**	*12.6 Mi Total*
3. Merge onto **I-84 E / US-20 E / US-30 E / US-26 E** via the ramp on the **left** toward **Mountain Home / Twin Falls**. Map *If you reach S Eisenman Rd you've gone about 0.1 miles too far*	**33.2 Mi**	*45.8 Mi Total*
4. Merge onto **I-84 Bus Loop E / US-30 Bus E** via **EXIT 90** toward **ID-51 / ID-67 / Mountain Home / Bruneau**. Map	**4.1 Mi**	*49.9 Mi Total*
5. Stay **straight** to go onto **N Main St / ID-51**. Continue to follow **ID-51**. Map	**1.5 Mi**	*51.4 Mi Total*
6. Turn **left** onto **S 18th W / ID-51**. Continue to follow **ID-51**. Map *ID-51 is 0.2 miles past SW Autumn Ave* *If you reach Mountain Home Airport you've gone about 0.5 miles too far*	**14.2 Mi**	*65.6 Mi Total*
7. Turn **left** onto **ID-78**. Map *ID-78 is just past Oregon Trail Rd*	**2.8 Mi**	*68.4 Mi Total*
8. **BRUNEAU DUNES RD**. Map *If you reach Bruneau Dunes Rd you've gone about 0.6 miles too far*		

B to **C** Travel Estimate: **59.55 mi - about 1 hour 3 minutes**

C **Bruneau Dunes Rd**, Bruneau, ID 8360442.895139, -115.700859

(Address is approximate)

Entire Route

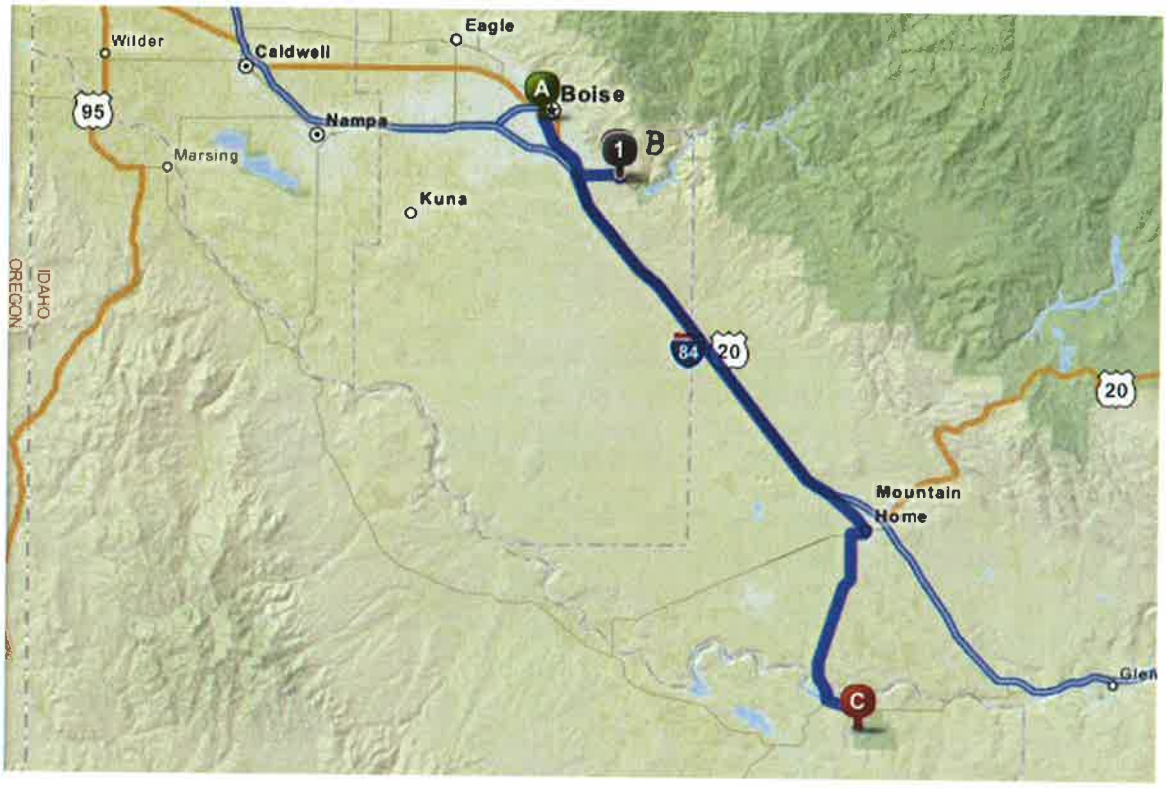

to SRP stop

Bruneau Dunes State Park

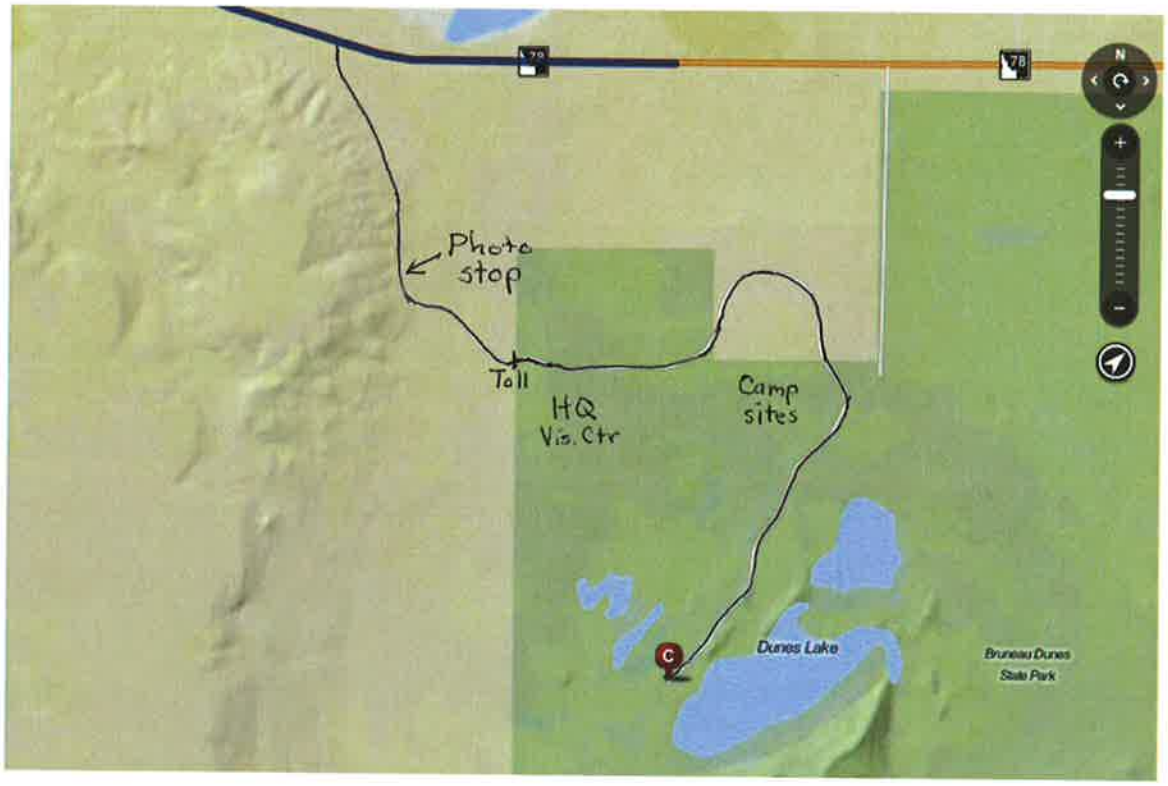

Take right-hand turn to the park
(Brown road sign)

From Google Earth:

1455 S Capitol Blvd, Boise
43° 36' 14" N, 116° 12' 49" W

SRP stop, 9760 E Highway 21
43° 32' 19.7" N, 116° 5' 33.8" W

Bruneau Dunes, parking lot
42° 53' 44.8" N, 115° 41' 50.0" W

VOLCANISM OF THE EASTERN SNAKE RIVER PLAIN, IDAHO:

A Comparative Planetary Geology Guidebook

Edited by

Ronald Greeley
Department of Geology and Center for Meteorite Studies
Arizona State University
Tempe, Arizona 85281

and

John S. King
Department of Geological Sciences
State University of New York at Buffalo
Amherst, New York 14226

August 1977

Prepared for the Office of Planetary Geology
National Aeronautics and Space Administration
Washington, D.C.

Cover:
Low oblique aerial view of King's Bowl lava field.

3. BASALTIC "PLAINS" VOLCANISM

Ronald Greeley
Department of Geology and
Center for Meteorite Studies
Arizona State University
Tempe, Arizona 85281

Analysis of the morphology of the central Snake River Plain and comparisons with other basaltic regions lead to the conclusion that the plain may represent a distinctive style of volcanism that combines aspects of both flood basalts and classic basaltic shield volcanoes. Although traditionally included in the Columbia Plateau and generally considered a plateau basalt region, the central Snake River Plain—and regions similar to it—is considered sufficiently different from flood basalts in the characteristics of the flows and the resulting surface morphology (and, therefore, also different in the style of volcanism involved in its formation) to warrant its consideration as a distinctive class. The expression *basaltic "plains"* has been tentatively proposed (Greeley, 1976) for this intermediate type of volcanic region.

Several authors have recognized the distinctive character of the central and eastern Snake River Plain in comparison to the Columbia Plateau. In many respects, the Snake River Plain is more akin to southeastern Oregon and the Modoc Plateau of California (Fig. 3-1) than to the flood basalts of the Columbia Plateau. The geochemical uniqueness (Figs. 3-2 and 3-3) of the plain has been addressed by Waters (1961), Powers (1960), Jones (1970), Leeman (1974, 1975) and others. The differences in the lava flow morphology of the plain and the Columbia Plateau are discussed by Greeley and King (1975) and in Chapter 4 of this guidebook. Thus, there are several independent lines of evidence that show the Snake River Plain is unlike the Columbia Plateau and the inference

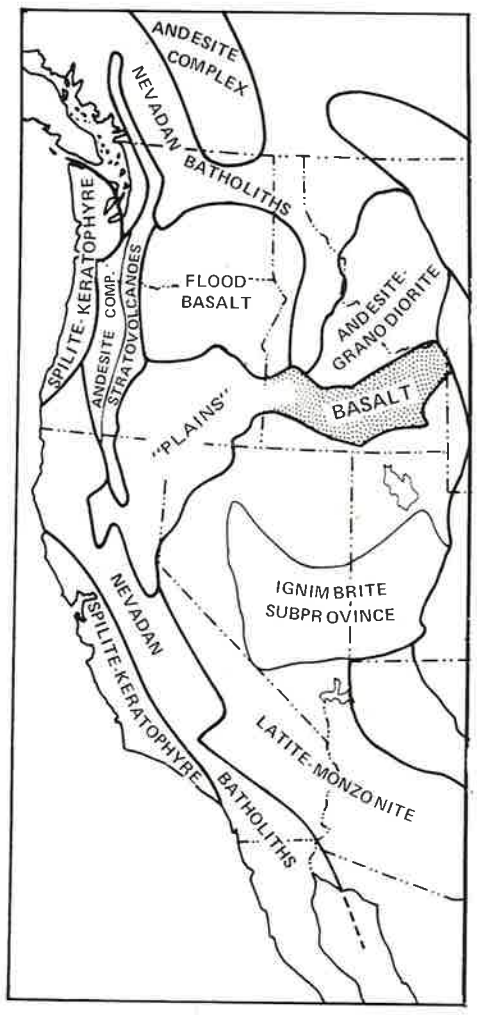

FIGURE 3-1. Map of the western United States showing major igneous provinces; note that the Snake River Plain of Idaho (shaded area) is more closely related to the basaltic regions of southeast Oregon and northeastern California than to the flood basalts of southeastern Washington and northeastern Oregon. (Modified from Eardley, 1962.)

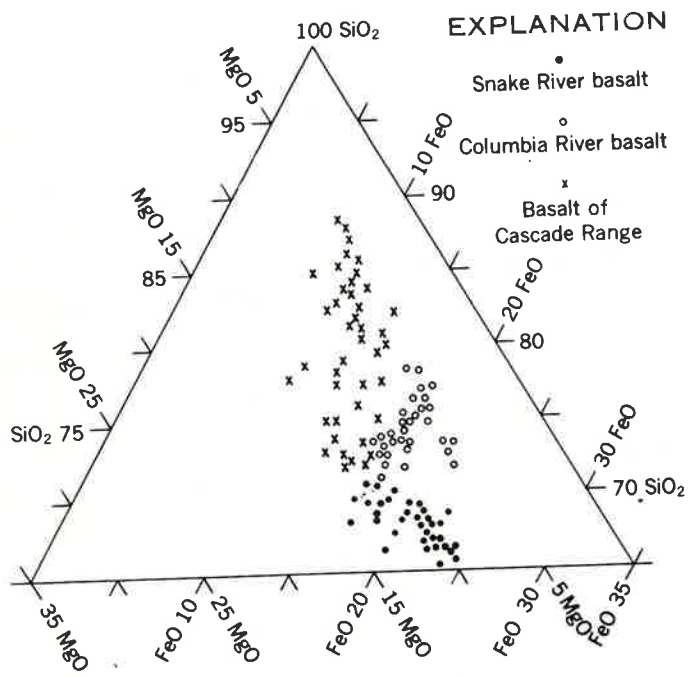

FIGURE 3-2. Ratios between SiO_2, MgO, and total iron plus manganese in some basalts of the northwestern United States. Data plotted are weight percent of SiO_2, MgO, and sum of FeO + 0.9 Fe_2O_3 + MnO computed to 100 percent. (after Powers, 1960).

is drawn that the style of volcanism and modes of lava flow emplacement were also different.

Investigations of basalt regions outside the Snake River Plain suggest that not all basaltic plains are the result of "typical" flood-type eruptions. Walker (1972), for example, proposed the terms *compound lava flows* and *simple lava flows* to distinguish differences in modes of emplacement and in morphology. Walker builds on the recognition by Nichols (1936) that many lava flows can be separated into *flow units* that represent individual "gushes" of lava, but which are all part of the same eruptive sequence. Compound lava flows consist of multiple flow units that range from 5 cm to more than 10 m thick, although most are in the 50 cm to 5 m range. Most pahoehoe lavas are of the compound type; aa lavas occur in both compound and simple flows. Although the interval between emplacement of flow units can be very short, lava crusts typically develop that are sufficiently thick to preserve the individuality of the unit. Thus, compound lava flows are made up of a sequence of thin units which, to some degree, behave as individual cooling units (Fig. 3-4).

In contrast to compound lava flows, simple lava flows consist of single, typically thicker, flow units that are essentially single cooling bodies. Walker (1972) attributes the difference primarily to the rate of effusion; a low rate leads to the development of compound flows, a high rate (flood eruptions) produces simple flows. Thus, determination of the predominant flow type in any one region would enable the prevailing rate (high versus low) of effusion to be estimated.

Another difference between the proposed "plain" type province and classic flood basalts and basaltic shields is the proposal of Noe-Nygaard (1968) to distinguish a sub-category of shield volcanoes for which he proposed the term *shield volcano of scutulum type* (from the Latin *scutulum*, the diminutive of *scutum*, = shield). In studies of the basalt flows of the Faroe Islands, Noe-Nygaard identified very flat shield volcanoes having slope angles of about $1/2^{o}$. The shields described are about 15 km across and are estimated to consist of less than 7 km^3 of lava, made up of compound lava flows. Similar flat shields occur in Iceland. Mauna Iki in Hawaii, constructed from eruptions in 1926, has a similar morphology and is of comparable dimensions. Macdonald (1972, p. 195-196) uses the term *lava cone* to describe Mauna Iki and similar low-profile shields.

It is primarily the small size and low profile of these shields that led Noe-Nygaard and Macdonald to separate the "scutulum" or "lava cone" type shields from Hawaiian and major Icelandic shield volcanoes. To prevent confusion with composite *cones* and to avoid the awkward phrase *shield volcano of scutulum type*, the term *low shield* is proposed to describe this category of volcano. Low shield volcanoes are

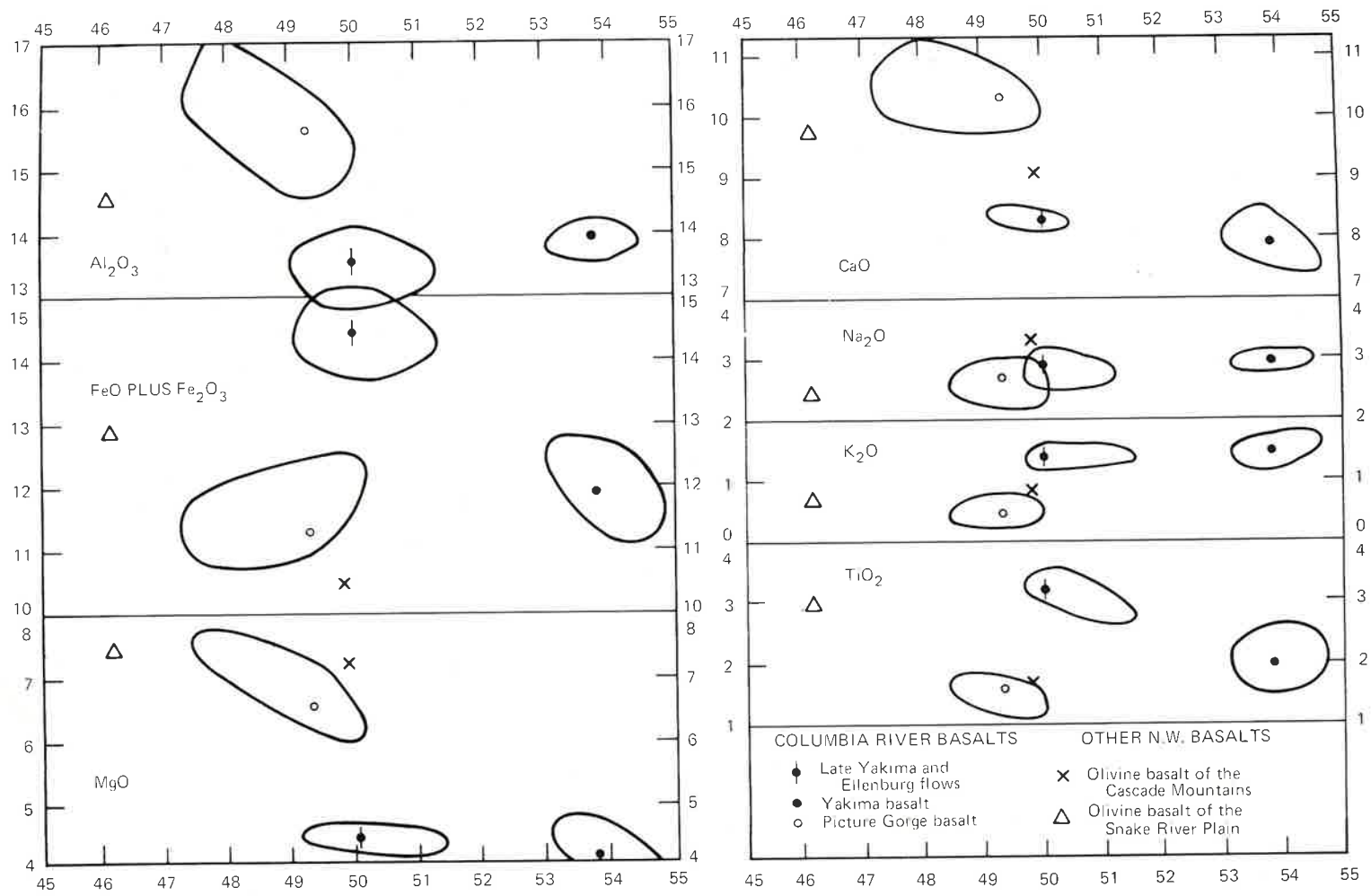

FIGURE 3-3. Variation diagram for basaltic rocks of the Pacific northwest, showing the distinctive character of the Snake River Plain basalts. Spaces enclosed by lines show areas within which chemical analyses fall. (from Waters, 1961.)

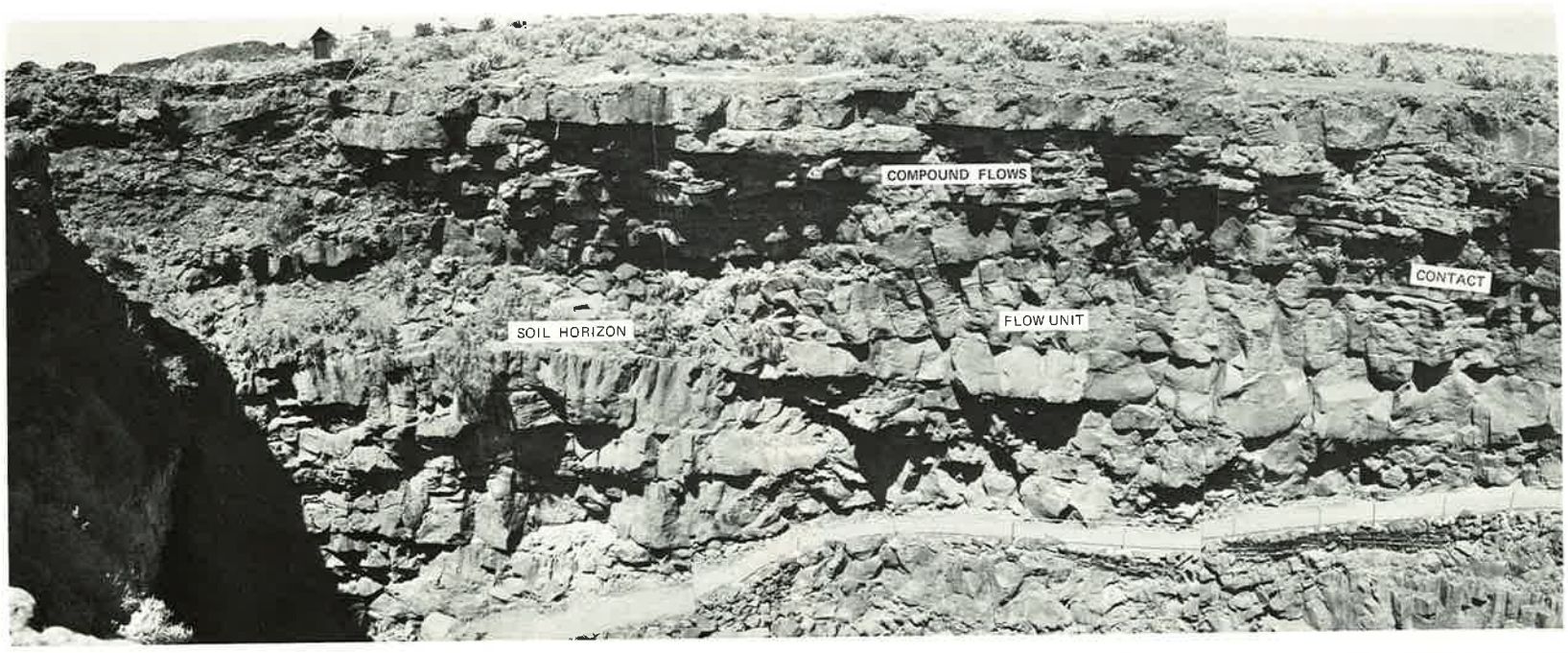

FIGURE 3-4. Panoramic view of the east wall of King's Bowl, showing lava flows typical of the Snake River Plain; compound lava flows consist of multiple, typically thin flow units.

typical of the Snake River Plain, and regardless of the term applied, they appear to represent a distinctive form of volcanism.

The foregoing discussion suggests that, first, the Snake River Plain is petrologically and morphologically distinct from the Columbia Plateau, and hence is not a classic flood basalt region, and second, that the shields making up most of the plain are not of the classic Hawaiian or Icelandic type, but are distinctive constructs. Moreover, other basaltic regions, such as parts of the Modoc Plateau of California, appear to share characteristics with the Snake River Plain and may also represent a style of volcanism intermediate between flood basalt eruptions and major shield-building eruptions. In the sections that follow, the Snake River Plain is described and compared with flood basalts and shield volcanoes.

FLOW TYPES

The prevailing flow type in the Snake River Plain is pahoehoe basalt that was emplaced as compound lava flows in the form described by Walker (Fig. 3-4). Cross sectional exposures of lava flows are rather limited in the central and eastern Snake River Plain because of the lack of erosion. Although some flows are exposed in the walls of summit craters, they are probably not typical for the main bodies of the flows that make up the plains away from the vents. When rare exposures are found away from the vents, flow units average about 1 to 5 m thick. Compound flow thicknesses, or the total of all flow units for a given eruptive sequence, may be 35 m or more thick, as in the Hell's Half Acre field (see Chapter 7) or the Wapi Field (see Champion, 1973, and Chapter 8).

Fresh surfaces of the pahoehoe flows are typically rather hummocky, with local relief as much as 10 m (Fig. 3-5). So-called *collapse depressions* (Hatheway, 1971) are common on some flows (Fig. 3-6). Also present are *pressure plateaus, pressure ridges, and flow ridges* (Fig. 3-7; see also Chapter 8). These structures are all typical of compound lava flows and apparently result from the manner in which the flows advance through a series of budding toes, described by Wentworth and Macdonald (1953) and others. Weathering of the flow surface features and accumulation of wind-blown sediments in low-lying parts result in a smoothing of the surface relief to the degree that in older flows only remnants of the prominent features, such as some ridges, are visible.

Local relief is also formed by flow fronts. Flows that encroach topographically high structures, such as tuff cones and other constructs "freeze" in place, and a shallow depression results between the flow front and the pre-flow feature.

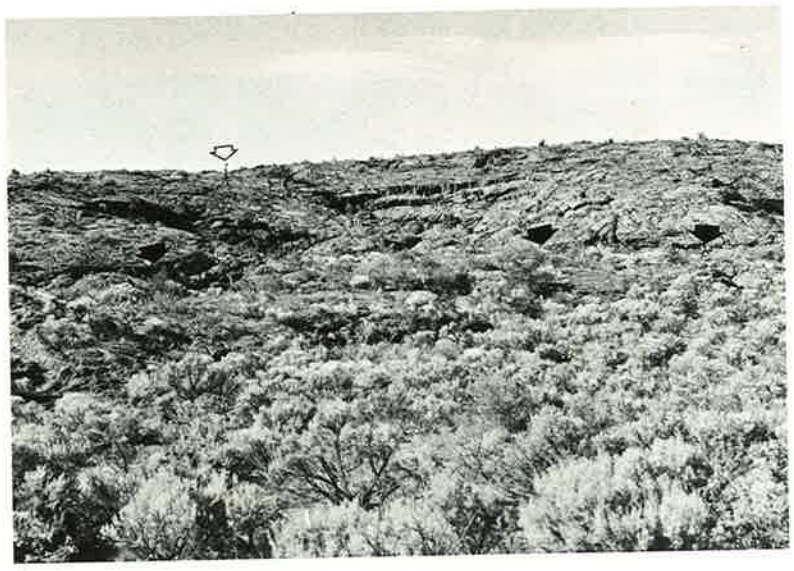

FIGURE 3-5. Photograph of the flow front of the Wapi lava field, showing typical surface relief of 5 to 10 m; arrows mark flow front contact; open arrow indicates figure for scale.

FIGURE 3-6. Vertical aerial photograph of part of the Wapi lava field showing pressure plateau (flat, upper surface) and some collapse depressions (arrows) formed on the plateau. (NASA-Ames photograph 878-3A-3, October, 1968.)

Aa flows are also present in the Snake River Plain. Some are of considerable extent, such as the aa flow complex erupted from fissures in Craters of the Moon (Fig. 3-8) that covers 150 km^2. Some aa flows appear to be of the simple lava flow type, emplaced as a single surge of lava. However, they are relatively thin, similar to the individual pahoehoe flow units of the compound lava flows and emplacement of comparatively viscous aa over so large an area is problematical. Observations made on Mt. Etna in collaboration with J. Guest on active flows suggest the process involved. In 1975, a series of pahoehoe flows was erupted on the north flank of the volcano. In the final stages of emplacement, however, the texture of the flow surface changed abruptly to aa. Moreover, some of the active flow on Etna was through lava tubes and

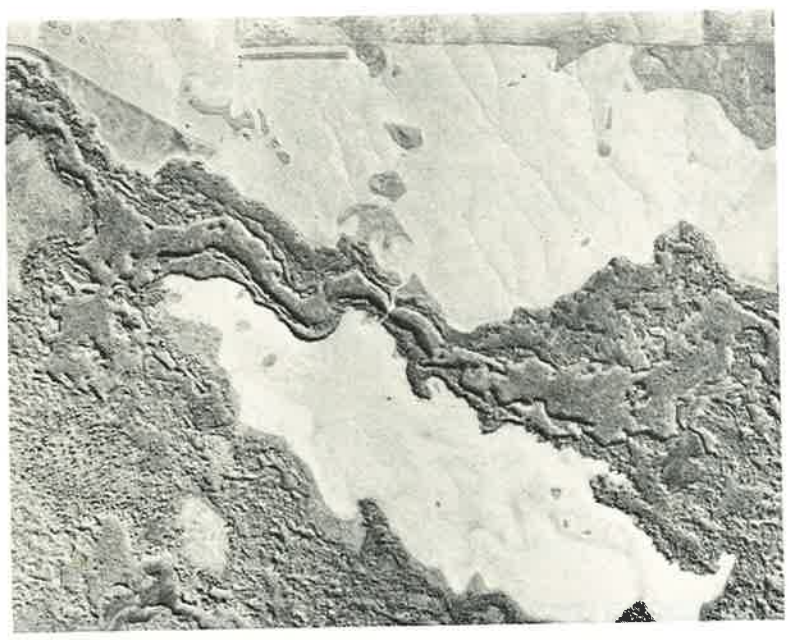

FIGURE 3-7. Vertical aerial photograph of the eastern margin of the Wapi flow, showing 'flow ridge' (Champion, 1973, and Chapter 8), which formed parallel to the direction of flow. Dark areas are flow units of the Wapi field; light areas are the older flows. (NASA-Ames photograph 878-5-7; October, 1968).

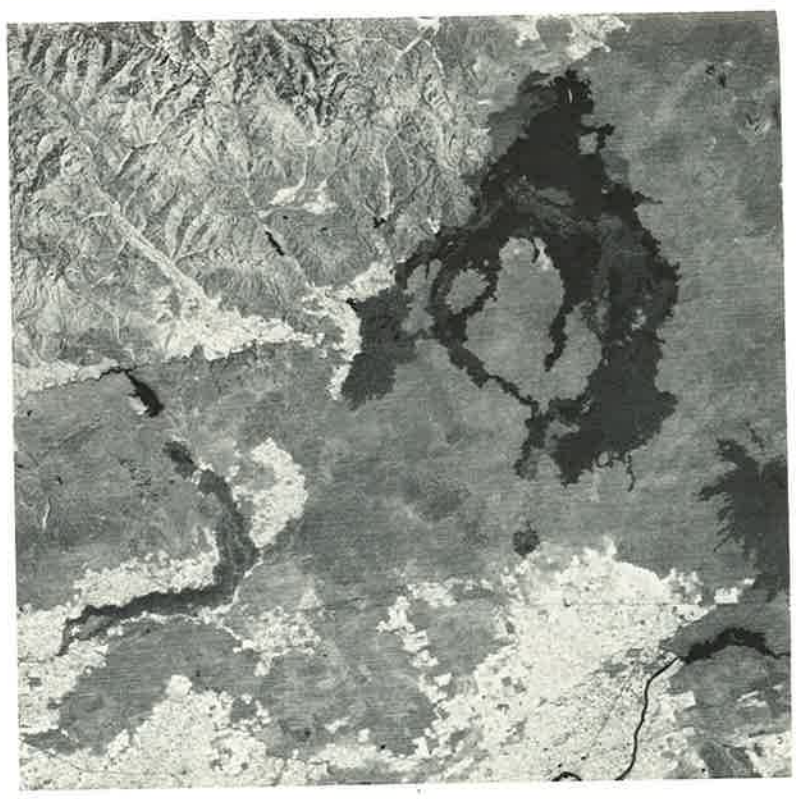

FIGURE 3-8. ERTS images of the central Snake River Plain; youngest flows show as dark patches: Craters of the Moon flows (upper right corner) are mostly fissure-fed; 'angle-shaped' flow on the left is the Shoshone Ice Cave lava field, emplaced mostly through lava tubes and channels; and the Wapi lava field (right-hand side), a low shield. All of the flows are compound flows, composed of multiple flow units.

after the flows cooled, it appeared that lava tubes had formed in aa—in conflict with widely held views that lava tubes form nearly exclusively in pahoehoe flows. The tubes, however, formed during the pahoehoe stage and were preserved within the flow after the surface texture had converted to aa. Such tubes appear to be very infrequent, but their occurrence does explain the presence of lava tubes in aa.

Some of the large, thin aa flows in the Snake River Plain may, like those on Etna, have been erupted and essentially emplaced as pahoehoe but transformed to aa in the final stages of flow. Although the concept is difficult to substantiate for prehistoric flows, some flows on the plain suggest this possibility, as shown in Figure 3-9.

LAVA TUBES

The role of lava tubes and channels in the emplacement of some basalt flows is poorly understood. A recent study (Greeley and others, 1976) of Mauna Loa shows that more than 80 percent of the flows exposed on the surface at least partly involved flow through lava tubes and channels in their

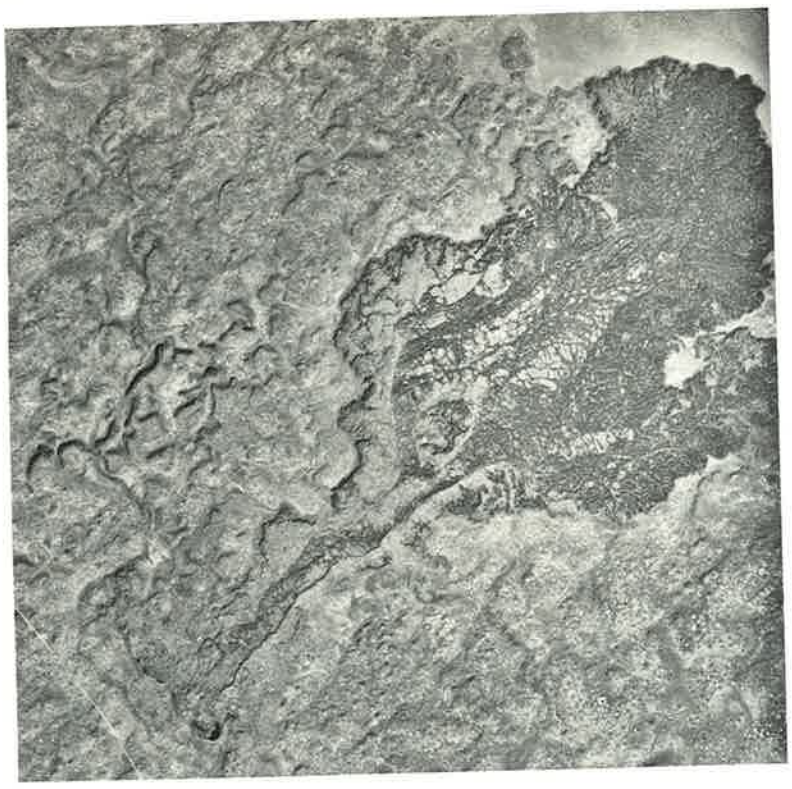

FIGURE 3-9. Vertical aerial photograph of a small basalt flow erupted southeast of Big Southern Butte; vent area is marked with an arrow. Flow surface exhibits both pahoehoe and aa flow textures; emplacement of most of the flow is considered to have taken place essentially in the pahoehoe state, then in the final stages of emplacement, the lava transformed to aa. Incomplete transition is indicated by irregular slabs of pahoehoe (light-toned surfaces). Similar flow transition has been observed in active flows on Mt. Etna and in Hawaii. (U.S. Department of Agriculture photograph CXN-4R-106; October, 1968).

emplacement. Lava tubes, and to a lesser extent channels, transport lavas efficiently great distances from their vents. Lava tube systems longer than 20 km are common in many areas on Earth and structures interpreted as lava tube systems on the Moon and Mars exceed 100 km in length.

The distinction between tubes and channels is that tubes are hollow tunnels within flows and have free-standing roofs upon cooling and draining of the lava; channels typically are non-roofed, open rivers of lava that frequently have crustal slabs on their surfaces, but the slabs do not form free-standing roofs after the lava drains. In active flows, tube roofs and channel crusts prevent heat loss and enable the flow to remain mobile longer than in flows lacking these features.

Lava tubes and channels develop in Hawaiian-type eruptions in which the rate of effusion is moderately high (e.g., 10 to 100 m^3s^{-1}; Walker, 1973) but not as high as in flood eruption. Predictably, there are no known lava tubes in the Yakima Basalt or comparable flood lava flows of the Columbia Plateau. Tube formation also seems enhanced by sporadic eruption, involving multiple flow units with intervening periods of quiescence. This kind of activity was typical for the approximately six-year history of Mauna Ulu, Hawaii, a low shield having complex networks of lava tubes (Greeley, 1970, 1971; Peterson and Swanson, 1974).

Although lava tubes and channels are predominantly constructional features in that they emplace lava flows, they can also erode by melting and "plucking" of flows previously emplaced by the lava tube and also pre-flow terrain. Complex sequences of construction and erosion by multiple flow units can develop in this type of flow, illustrated in Figure 3-10. Although hypothetical, this diagram is based on surveys of lava tube systems in the western United States and on observations of active flows on Mt. Etna and in Hawaii (Greeley, 1970, 1971).

Lava tubes also played an important role in the emplacement of some of the flows in the Snake River Plain. Although they are not as common as in Hawaiian flows, some of the tubes in the plain appear to be larger than those in Hawaii. A preliminary survey of part of the central plain indicates that more than a fifth of the flows involved lava tubes and channels.

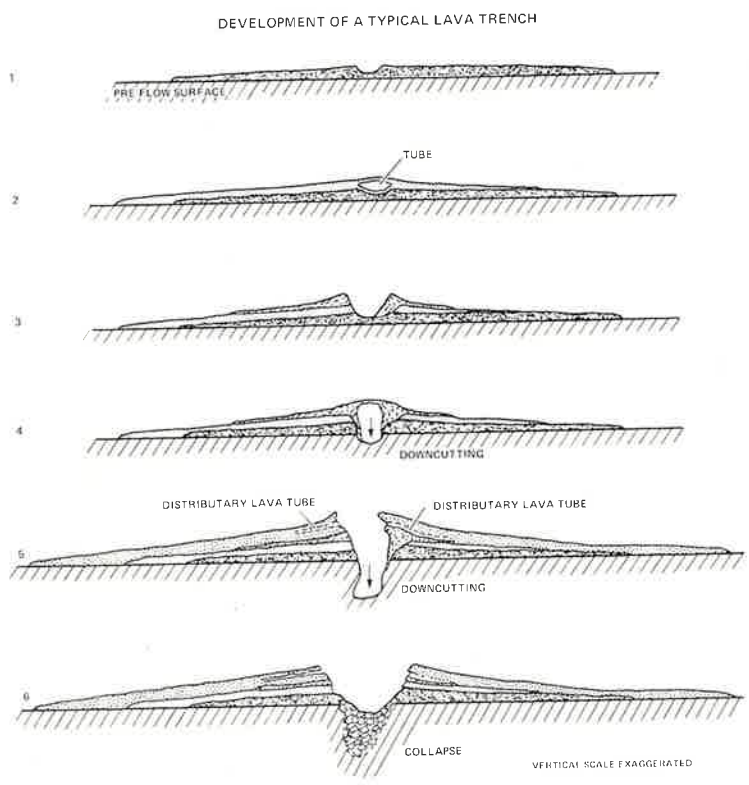

FIGURE 3-10. Sequence to show some of the stages in the development of a tube-fed compound lava flow. Stage 1 is a single flow unit emplaced by a shallow lava channel; stage 2 involves a second flow unit, in which lavas flowed down the previous channel and formed a roof. Stage 3 includes a third flow unit that was turbulent and formed a large channel; continued eruption of the same flow resulted in the formation of a roof, with downward erosion by melting and physical removal of some of the previous flow and preflow rocks. In stage 5 a fourth flow unit was erupted at a high rate; it initially used the previous tube as the feeding conduit, but because the volume of lava was large, the previous tube was destroyed and an open-flow channel developed, segments of which may have become roofed; overflow from the channel formed distributary lava tubes and small channels. Stage 6 marks the end of eruption with collapse of roofed segments by bank collapse.

Although this sequence is hypothetical, elements of each stage are based on observations of active lava tubes and channels and studies of cooled structures.

TYPES OF CONSTRUCTS ON THE SNAKE RIVER PLAIN

The regional geology of the eastern and central Snake River Plain is described in several reports, including Russell (1902) and Stearns and others (1938, 1939) and summarized in Chapter 4. Aspects of the plain pertinent to this discussion are described by Stearns (1928), Murtaugh (1961), Trimble and Carr (1961), Niccum (1969), Prinz (1970), Greeley and King (1975a,b), and LaPointe (1975, 1977).

The central and eastern Snake River Plain is formed by the accumulation of lavas in four main types of constructs. The term *construct* refers to any major accumulation of lava flows and other volcanic products. The four types are: 1) *low shields,* 2) *fissure flows,* 3) *major tube flows,* and 4) *intracanyon flows.* The relationships of these constructs are shown diagrammatrically in Figures 3-11 and 3-12. Although flood-type flows may also be present in the plain, none are exposed or documented.

Low Shields

Most of the central and eastern Snake River Plain is built up of multiple low shields, typified by the Wapi and Hell's Half Acre lava field. These fields are simply the uppermost and youngest of a complex series of coalescing low shields and other constructs that have an accumulated thickness of more than 1500 m (LaFehr and Pakiser, 1962) in some parts of the plain.

The Wapi lava field covers more than 300 km^2 and is a compound lava flow consisting of pahoehoe lavas of the "degassed" variety (Swanson, 1973). Lava toes, collapse depressions, flow ridges, and pressure ridges are common, but no lava tubes have been found on the main part of the field (Champion, 1971). The areal extent of the Wapi, one of the larger young flows on the plain, is considerably less than the 40,000 km^2 Roza Member of the Yakima Basalt (Swanson and others, 1975), a classic flood basalt.

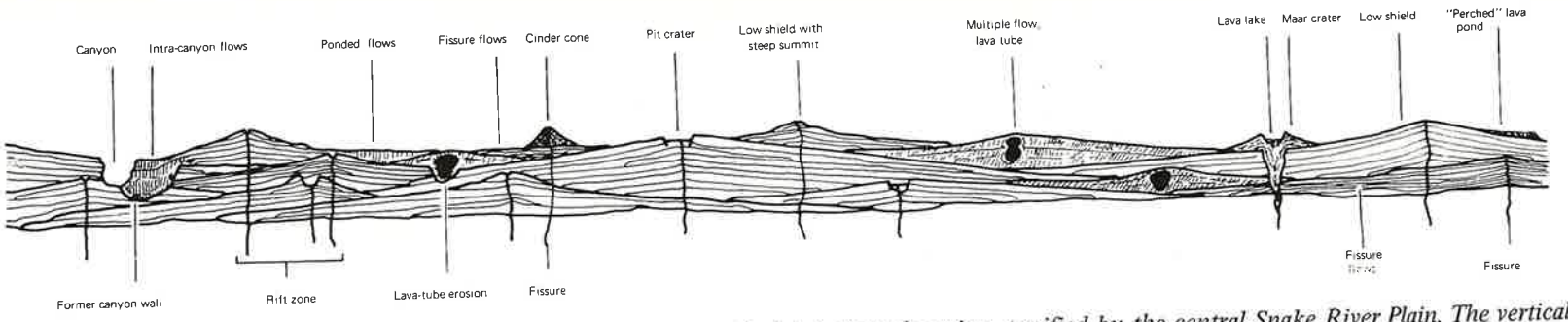

FIGURE 3-11. Schematic cross section to show the salient features of a 'plains' basalt region, typified by the central Snake River Plain. The vertical scale and surface relief are greatly exaggerated in order to show detail that would otherwise be lost. The predominant lava is pahoehoe basalt in the form of flow units that seldom exceed 5 to 10 m in thickness. The primary constructional forms are: 1) low shields, many of which have summit pit craters; the summits of most low shields are marked by steeper profiles than the rest of the construct, resulting partly from last-stage, low volume eruptions of aa lava; 2) flows fed by large lava tubes that wind between coalescing low shields; multiple eruptions often use the same lava tube as the conduit to feed advancing flow fronts and to add 'second stories' above previous flows and tubes; in some instances lava tubes may entrench into older flows by erosion; 3) fissures produce thin flows with relatively low surface gradients; the flows may be pahoehoe or aa, some of which are emplaced by networks of small tubes and channels; 'point source' eruptions along fissures can result in infrequent cinder-and-spatter cones; 4) flows more than 10 m thick are occasionally found in 'plains' type regions; these may represent flood-type eruptions, but more frequently, they are the result of lava ponding in low-lying regions and as intracanyon flows (left side of diagram); regardless of origin, thick flows are infrequent and appear to contribute comparatively little to the total volume of the 'plains' region; and 5) maar craters that result from ground water and magma interactions.

In profile (Fig. 3-13) the Wapi low shield displays two prominent slopes; the main part of the shield has slopes less than $1/2^{o}$, whereas the summit region steepens to about 5^{o}. The same type of profile is seen at Hell's Half Acre and older low shields on the plain. As older shields are encroached by subsequent flows from other sources, the steeper "upper story" often remains unburied.

The steeper summit for low shields can be explained partly by the nature of the flows that make up the summit region. As at Pillar Butte, the summit region for the Wapi low shield (see Chapter 8), has a high proportion of short, low-volume aa flows that piled up, elevating the vent. In comparison to the pahoehoe flow of the main field, the aa flows were more viscous and may represent the final stages of eruption. However, the complex sequence of development from steep cone to low shield to spatter rampart, observed during the short history of Mauna Ulu, would caution against assuming that earlier, steeper summit regions might not be buried at Pillar Butte.

In addition to steeper profiles, the summits of many of the low shields are marked by one or more irregular craters, commonly pit craters. Many of these show evidence of multiple collapse (Fig. 3-14) and were source vents for large lava tubes or channels (Fig. 3-15). Rarely, spatter ramparts, built of pasty agglutinate, occur at the summit (Fig. 3-16).

The summit vent regions in the Snake River Plain show an asymmetry toward the northside of the low shield. This is accounted for by the regional topographic slope to the south. Flows erupted from central vents tended to flow south, rather than north, resulting in the "offset" of the vent and summit region with respect to the shield in plan view.

Many low shields appear to be aligned in distinctive rift zones, with shields along each zone roughly contemporaneous in age. An example is the Inferno Chasm rift zone (Greeley and King, 1975b and Fig. 3-17). The aligned shields may represent a style of fissure eruption in which effusion was localized at various points along the fissure. Individual shields, however, are built of flow units of a magnitude akin

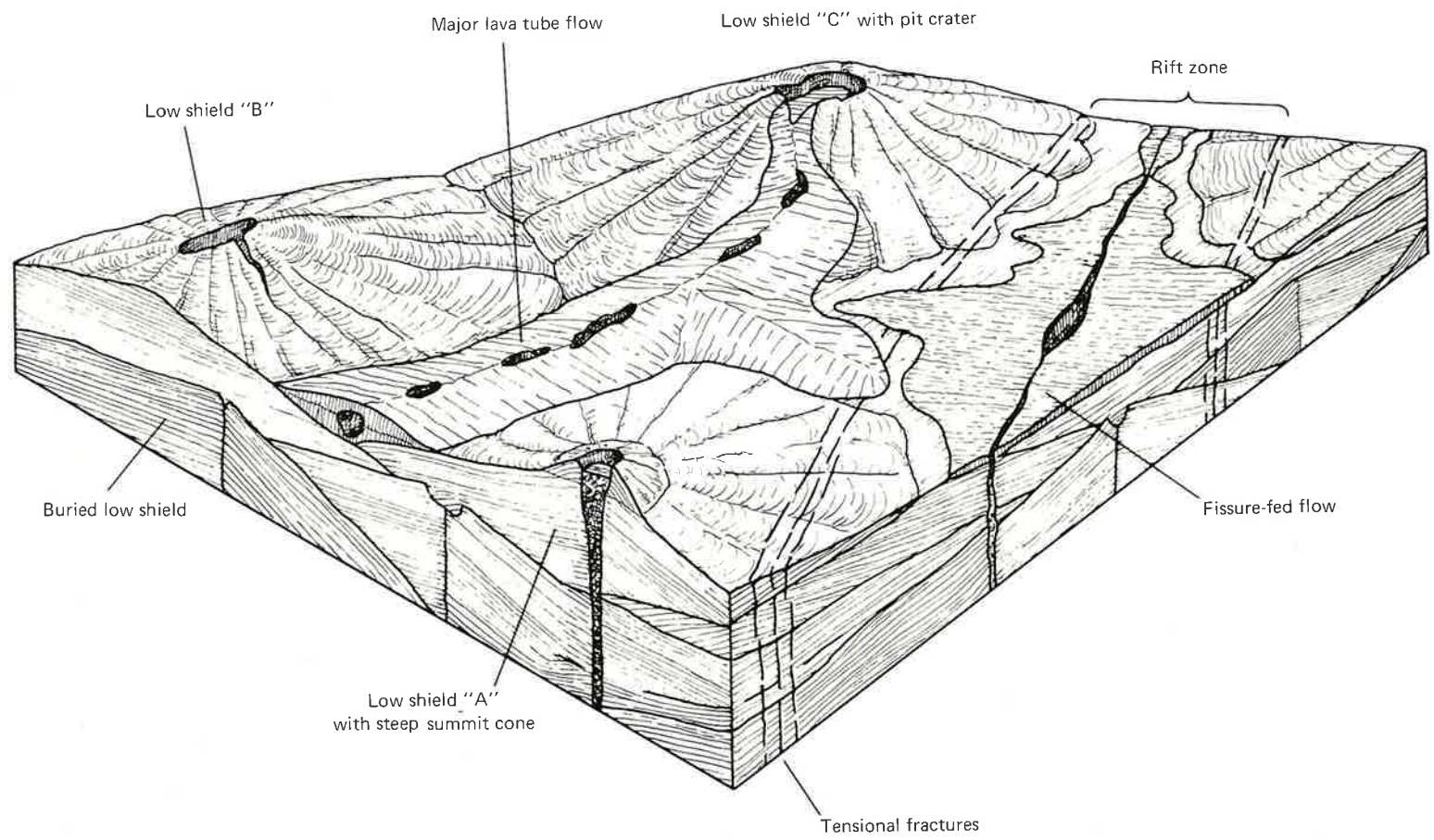

FIGURE 3-12. Block diagram showing the relationship of low shields, major lava tube flows, and fissure flows.

to Hawaiian activity. For some unknown reason, once the low shields on the plain reached a maximim size, the eruption vent shut off, with subsequent eruptions occurring elsewhere.

Fissure Flows

Most fissure vents are associated with rift zones. Typically, fissure flows in the central and eastern Snake River Plain are compound, or multiple flow units. The two youngest fissure flows on the plain are the King's Bowl flow, and flows in the Craters of the Moon where two flow units have been dated by C^{14} methods at 2085 ± 85 and 2255 ± 60 years before present (Bullard, 1971). The King's Bowl Flow has been dated by C^{14} methods at 2130 ± 130 years before present (Prinz, 1970). Craters of the Moon flows (see Chapter 13) consist of several aa and pahoehoe flows erupted from the fissures along the Great Rift (Fig. 3-8) and cover nearly 1500 km^2. This is the largest fissure flow identified on the plain, but its magnitude is much less than that of typical flood basalt flows on the Columbia Plateau.

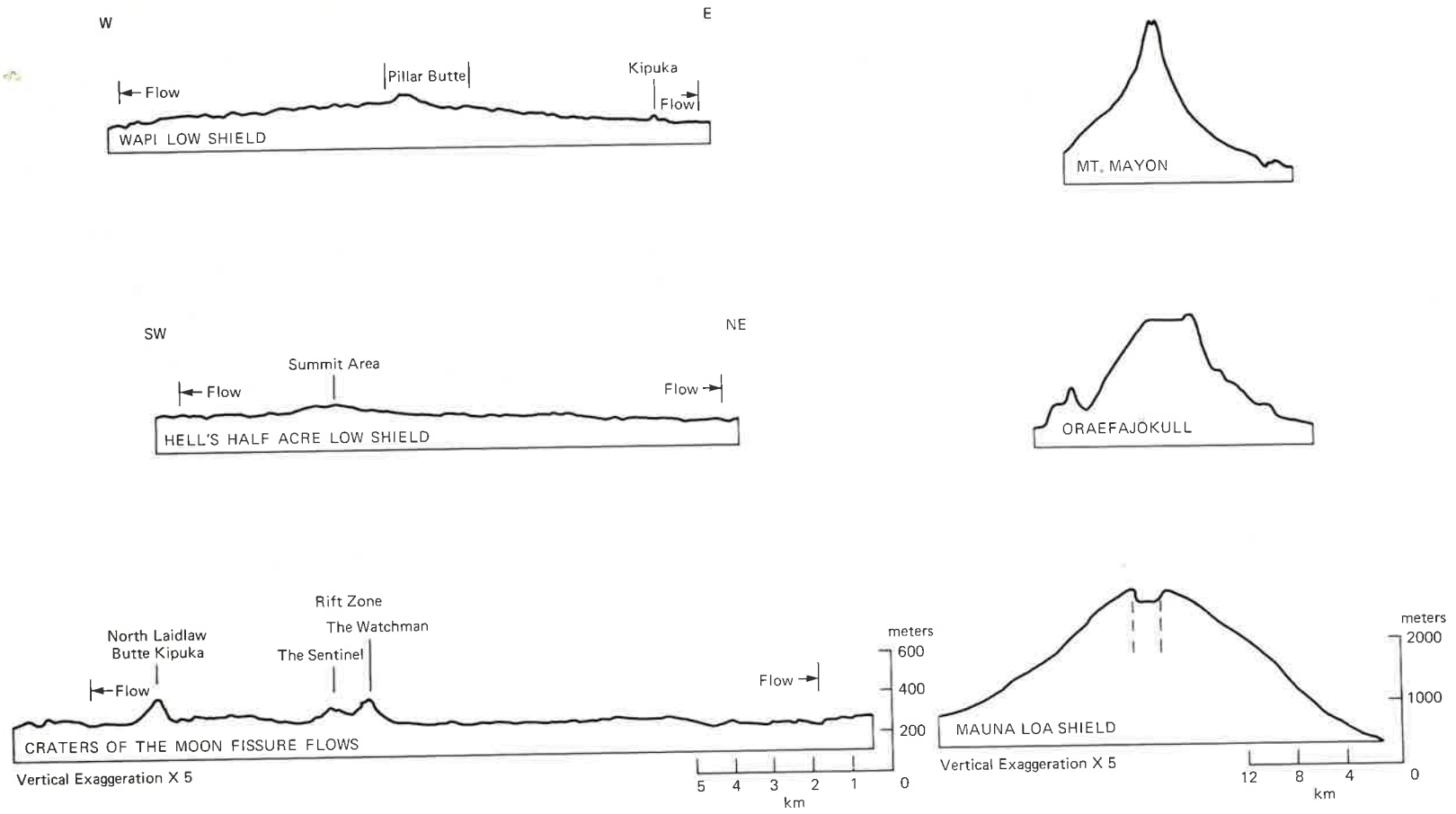

FIGURE 3-13a. Topographic profiles comparing Icelandic and Hawaiian shield volcanoes, a composite cone, and low shield volcanoes of the Snake River Plain; note the difference in scales for comparisons.

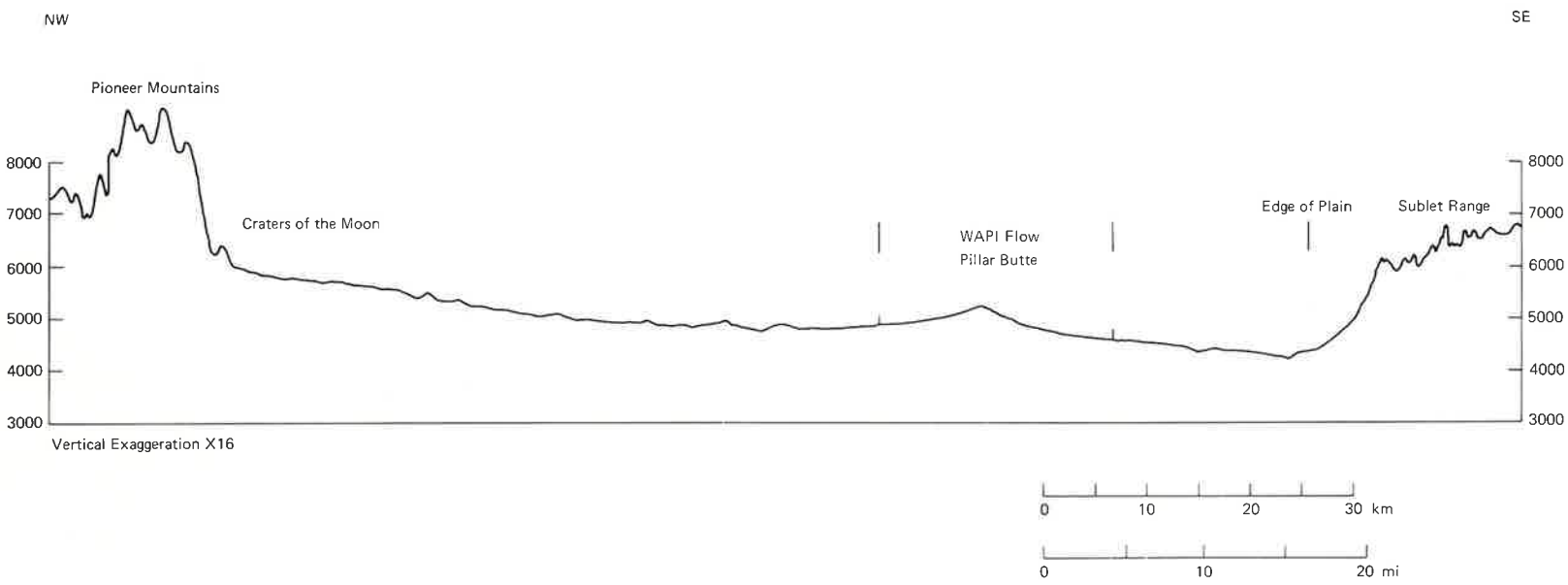

FIGURE 3-13b. Topographic profile across the Snake River Plain showing the region slope to be southeast and the Wapi low shield.

The King's Bowl flow covers only about 3 km^2 and consists of several flow units (Greeley and King, 1975a), some of which were ponded as small lava lakes (see Chapter 11). Thickness of individual flows is less than about 1.5 m, although some of the lava lakes may have been more than 4 m deep in places. The King's Bowl flow was erupted from a prominent fissure (Fig. 3-18); in some places the feeder dike is exposed (Fig. 3-19).

Although the main characteristic of fissure flows is the nearly continuous effusion of lava along several kilometers or more of the fissure, eruption at "point-sources" along the fissure may occur either independently or contemporaneously with fissure effusion, producing small spatter cones, or rarely, substantial cinder cones, as in Craters of the Moon (Fig. 3-20). Phreatic eruption may also occur along fissures when rising magma encounters ground water, as at King's Bowl (Fig. 3-18). Such "point source" structures are scarce on the plain and contribute little to the total accumulation of volcanic materials.

Major Lava Tube Flows

Lava tubes 0.5 to 5 m across are abundant in low shield and fissure flows. Major lava tube flows, however, are emplaced by tubes typically larger than 10 m across. The resulting construct is a compound flow that is long, narrow,

FIGURE 3-14. *Vertical aerial photograph of Wildhorse Corral (illumination from the east, or right side of the photograph). The vent is about 52 m deep and 1 km long, its length being oriented north-south on the Inferno Chasm rift zone. Wildhorse Corral appears to have a complex eruptive history, indicated by terraces within the crater walls and multiple flow units, some of which were tube-fed. (from Greeley and King, 1975a; NASA-Ames photograph 951, 8-15, 17; May, 1969).*

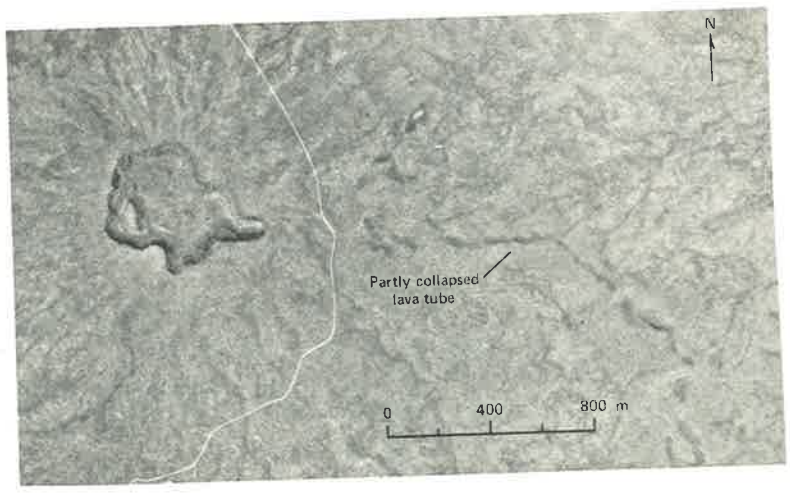

FIGURE 3-15a. *Vertical aerial photograph of an unnamed pit crater (left side of photograph), about 2.5 km north of Mosby Well, Idaho, that was the source for a major lava tube flow; lava tube can be traced eastward more than 5 km through a series of collapses that show as dark holes. (U.S. Geological Survey photograph GS SWEZ 6-206; September, 1971).*

FIGURE 3-15b. *Irregular pit crater, shown in Figure 3-15a; illumination is from the lower left. (photograph by Ronald Greeley, University of Santa Clara, 1971).*

FIGURE 3-16. *Low-altitude oblique view northward to the Pillar Butte area, the summit vent region for the Wapi low shield. The knob on the horizon is Pillar Butte, a spatter rampart associated with the summit vents. Dark patches are aa flows; a large pressure ridge is visible at the bottom of the photograph. (NASA-Ames photograph by Mike Lovas, 1969).*

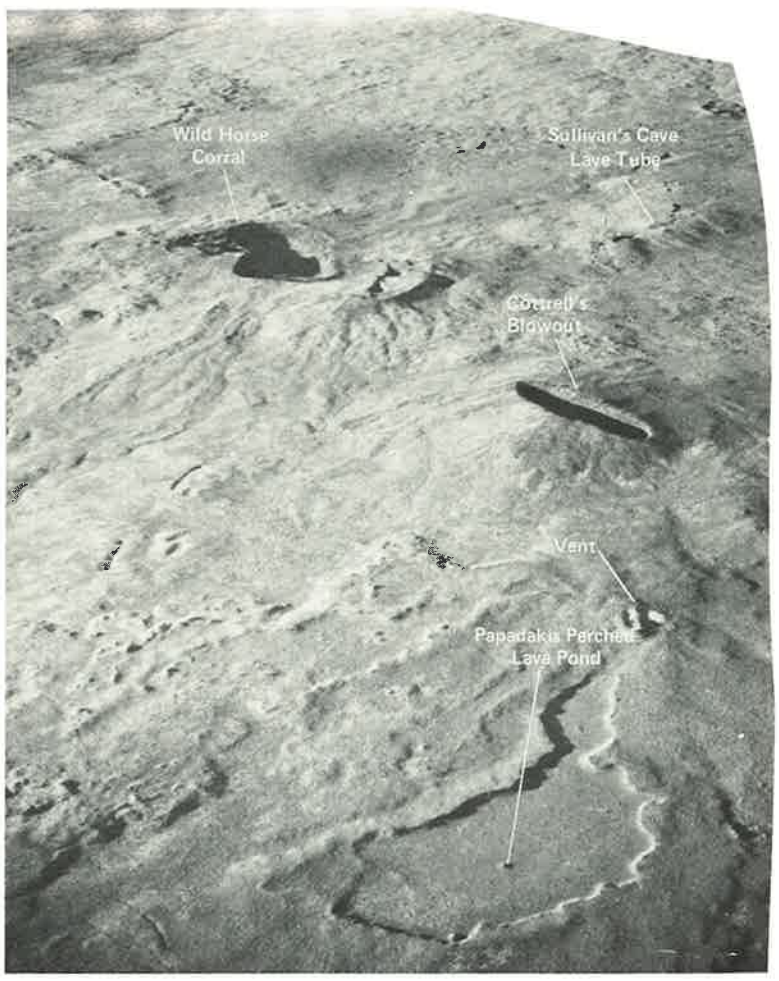

FIGURE 3-17. *Oblique aerial view northeastward across vents of the Inferno Chasm rift zone (Inferno Chasm vent is just out of view to the right). (from Greeley and King, 1975a).*

and somewhat sinuous, demonstrating the control exerted by pre-flow topography. Although the sources for the tubes are not always obvious, examples can be cited in which low shields, pit craters (Fig. 3-15), and possibly fissures were sources for major lava tube flows.

Bear Trap lava tube northwest of King's Bowl and Shoshone Ice Cave (lava tube) and their associated flows are examples of this class of construct on the plain. Bear Trap is an older, partly buried compound flow, whereas Shoshone Ice Cave flow (Fig. 3-21) is one of the youngest, fresh flows on the plain. The name Shoshone Ice Cave refers to a segment of the lava tube that has been developed as a tourist attraction; it is part of a complex lava tube–lava channel system, which during active flow, involved both roofed and and unroofed segments. Many of the formerly roofed parts, however, have collapsed, leaving open trenches that are continuous with the open channel segments. The compound flows associated with the Shoshone lava tube system cover

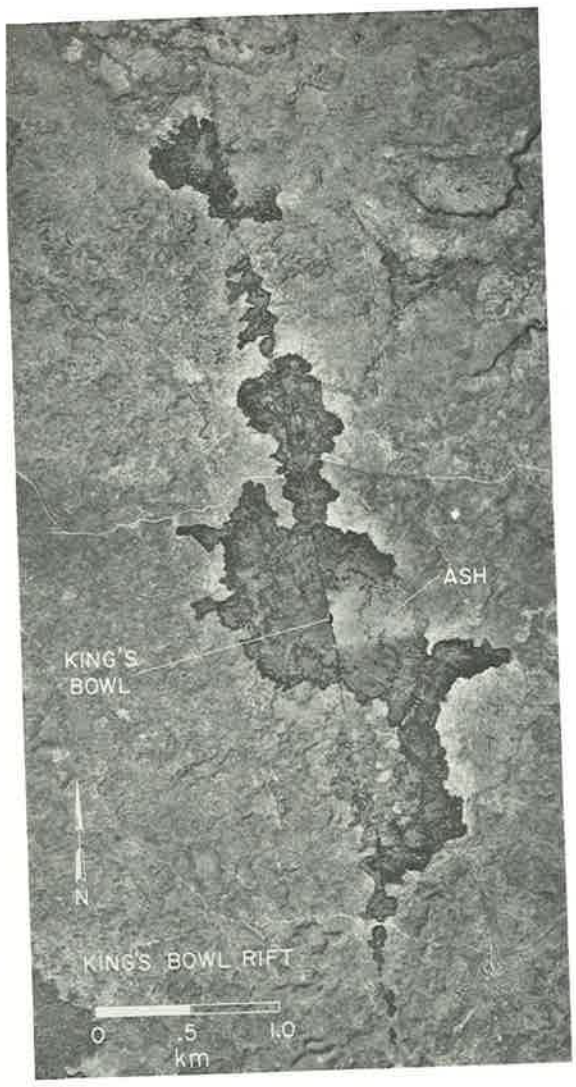

FIGURE 3-18. Vertical aerial photograph of the King's Bowl rift and the King's Bowl lava field, a compound lava flow fed by the main fissure. A phreatic eruption and subsequent collapse created King's Bowl (see Chapter 9), the elongate crater on the fissure; prevailing winds from the west (left) at the time of the eruptions carried ash and other fine particles eastward from the fissure. (U. S. Department of Agriculture Photograph.)

FIGURE 3-19. View of one of the feeding dikes along the main fissure at King's Bowl lava field. (photograph by James Papadakis).

about 210 km^2 and consist of both aa and pahoehoe flow units. Numerous small distributary lava tubes are preserved, some of which can be traced directly from the main tube. Small distributary lava tubes and channels were important in the conduction of lavas away from the main tube and contributed to the development of a subtle topographic arch along the axis of the main tube, typical of many lava tubes.

Bear Trap lava tube and the flows associated with it (Fig. 3-22) make up one of several tube-flow systems that originate in the vicinity of the King's Bowl rift and flow westward. The tube can be traced more than 21 km by a series of collapsed segments and is then buried by Holocene basalt flows from Craters of the Moon (Greeley and King, 1975). The axial trace of the tube is defined by a broad topographic swell which, to some degree, has controlled the emplacement of subsequent lava flows. Although most of the lava tube system

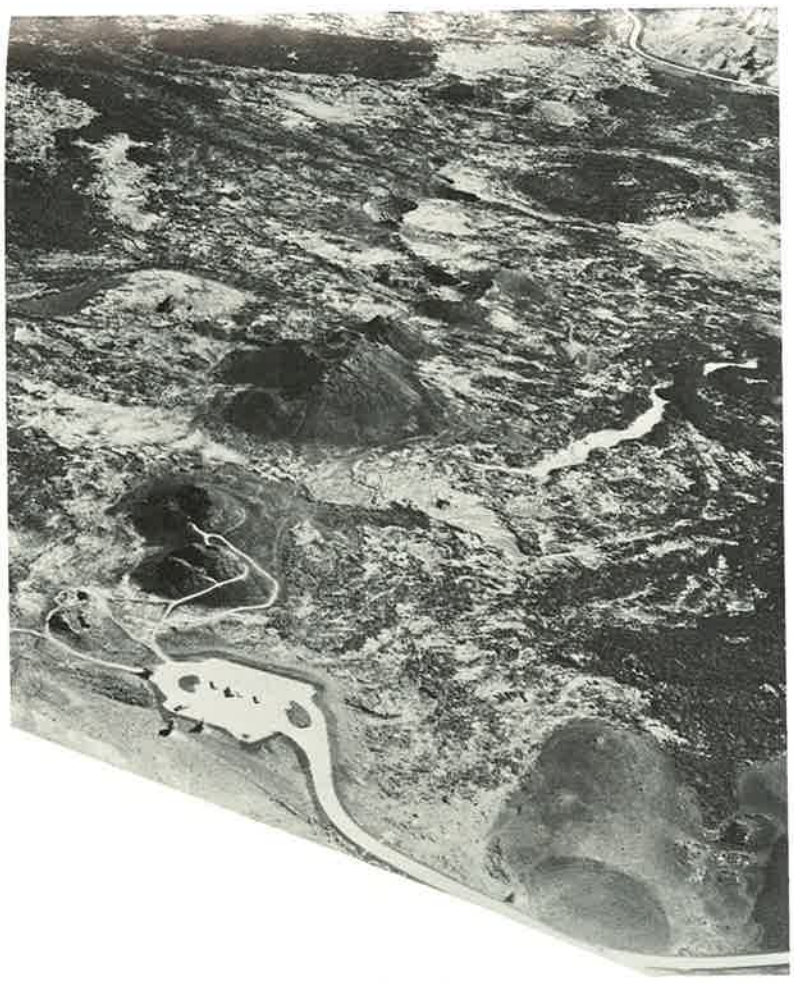

FIGURE 3-20. Low oblique aerial view of cinder-and-spatter cones aligned on a fissure in Craters of the Moon National Monument. (photograph by Ronald Greeley, University of Santa Clara, 1972).

FIGURE 3-21. Vertical aerial photograph of the main vent region (upper left) for the Shoshone Ice Cave lava flow, a compound lava flow consisting of pahoehoe and aa flow units, many of which were fed through lava tubes. Parts of the collapsed lava tube are visible as dark spots. Side road and parking area west (left) of the main highway (U.S. Highway 93) mark Shoshone Ice Cave, a segment of the lava tube open to the public. (U.S. Department of Agriculture photograph CVR-1KK-157, 158).

FIGURE 3-22. View of the interior of Bear Trap lava tube, part of a lava tube system more than 13 km long that fed a major compound lava flow.

is collapsed, there are two uncollapsed segments close to the Arco–Minidoka road that are readily accessible. Although the total extent of the flows associated with Bear Trap lava tube cannot be determined because the flanks of the tube-arch and distal end of the flows are buried, the exposed part of the flow is estimated to be about 60 km^2.

In contrast to the voluminous lavas in low shields and the large fissure-flows, major lava tube flows are small. However, these flows contribute substantially to maintaining the flatness of the plain in that they "fill-in" the low-lying region between adjacent, coalescing low shields (Fig. 3-12).

Intracanyon Flows

Several rivers cut the Snake River Plain, forming deep canyons (Fig. 3-23). Although the most notable is the canyon of the Snake River, several tributary canyons are also impressive. During the relatively short history of the plain, older canyons apparently existed, but their presence is now mostly

FIGURE 3-23. Low oblique aerial view northeastward of Twin Falls on the Snake River near Kimberley, Idaho. (NASA-Ames photograph by Ronald Greeley, 1969).

obscured by lava flows. Outcrops exposed by erosion along the present Snake River show that lavas spilled into the canyons, forming *intracanyon flows,* some of which ponded to depths exceeding 30 m. Columnar jointing and entablature structures are evidence for possible ponding of the flow prior to cooling. Sources for intracanyon flows may have been low shield, fissures, or major lava tubes. A tube-fed intracanyon flow occurs in the western Snake River Plain, mapped by Howard and Shervais (1973).

Because exposures of intracanyon flows in the central and eastern Snake River Plain are rather limited, their significance in the accumulation of lavas in the plain cannot be assessed fully. Intracanyon flows, however, are probably of relatively limited areal extent and may not be very representative for the plain as a whole.

Miscellaneous Vent Structures and Flows

Relatively minor accumulations of lava flows and other volcanic products occur on the plain and on the margins of the plain. These features include tuff-and-cinder cones, such as China Cap (Fig. 3-24), and maar craters such as Sand Crater (also known as Twin Buttes, Fig. 3-25), and Split Butte (see Chapter 12). Cinder and spatter cones are rare and appear to be associated with fissures, as discussed above. Some elongate vents and flows may be aligned over fissures and may be transitional between fissure flows and low shields associated with rift zones.

Some flows from tubes, central vents, or fissures formed natural levees and developed into lava lakes. The lakes may have been centered over the vent, as at King's Bowl (Fig. 3-18 and Chapter 11) and Split Butte (Chapter 12), or they may have formed "perched" lava ponds (Holcomb and others, 1974) on the flanks of construct (Figs. 3-17 and 3-26).

DISCUSSION AND SUMMARY

A style of volcanism, informally termed "plains" volcanism, is intermediate in character between eruptions of flood lava flows and of shield volcanoes. Distinctions of style are based on thickness, extent, and other properties of the flows for each type of eruption and on gross geomorphology of the three types of constructs.

As used here, the term *flood eruption* is restricted to the production of flows that exceed 20-30 m thickness and that are erupted at very high rates of effusion; flood eruptions produce "simple" flows that are single-body cooling units,

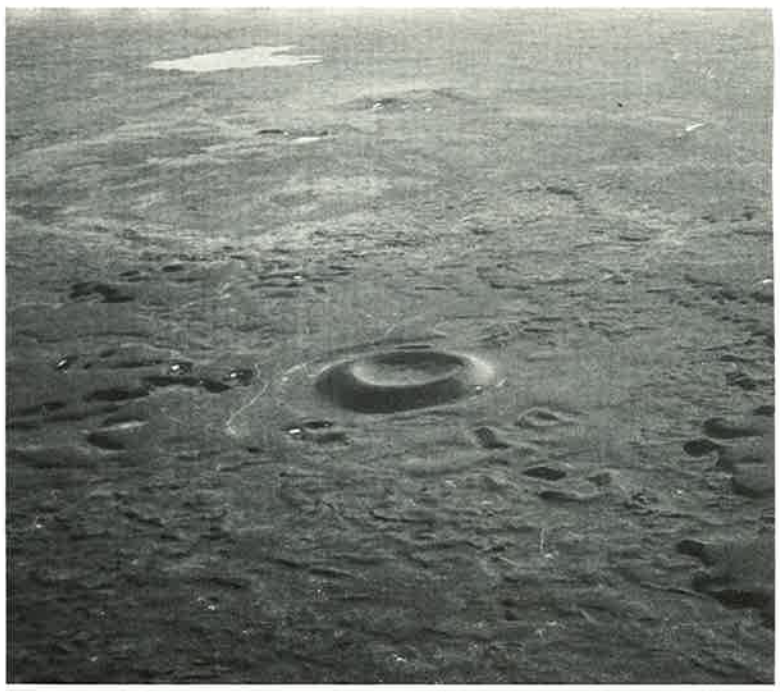

FIGURE 3-24. Oblique aerial view southwestward across China Cap, a small scoria cone about 385 m across that is 14 km southwest of Big Southern Butte. This nearly perfectly circular cone contains a crater 30 m deep. The rim is composed mostly of scoria with some blocks and bombs and at least one layer of agglutinate. Like Split Butte and Sand Butte, the flanks of China Cap have been partly buried by younger lava flows, creating a distinctive moat-like ring around the cone where the flow front solidified. (Photograph by R. Greeley, University of Santa Clara, 1970.)

typified by the Roza Member of the Yakima Basalt in the Columbia Plateau (Swanson and others, 1975). These flows lack well-defined surface flow features such as lava tubes and lava channels. Vent systems are long, narrow fissures that are seldom active for more than one eruption. Vent structures, such as cinder and spatter cones, typically are not preserved on the surface.

FIGURE 3-25. Oblique aerial view northeastward across Sand Butte, a tephra cone 1.2 km in diameter that contains a 650 m crater. Although most of the inner and outer slopes are covered with vegetation, several outcrops show the outward-dipping tephra layers that make up the cone. Sand Butte is astride a north-south fissure along which flow has occurred, and which has given rise to other vents, such as the series of low spatter ramparts in the upper left part of the photograph. The lower flanks of the cone have been covered by pahoehoe flows, identified here by the hummocky surface and pressure ridges. (From Greeley and King, 1975a.)

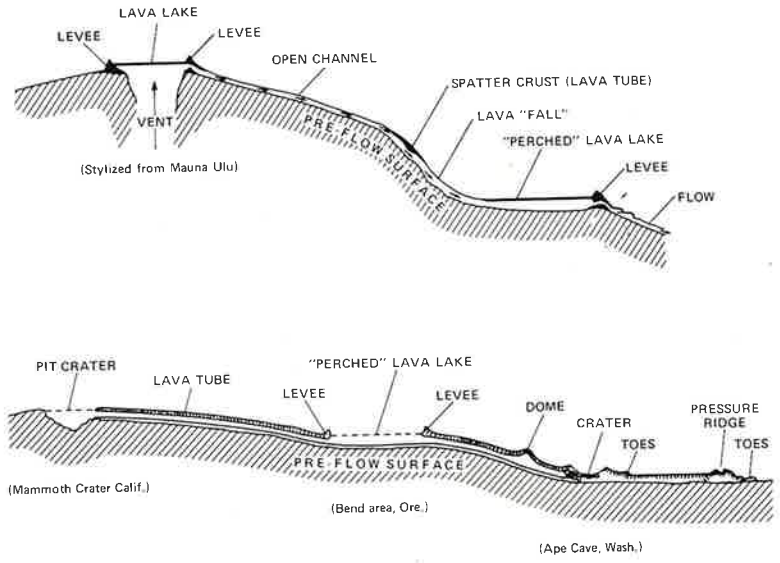

FIGURE 3-26. Hypothetical diagrams based on observations, showing "perched" lava ponds on steep and gentle slopes and their relation to lava tubes.

Large shield volcanoes of the Hawaiian and Iceland type are formed by relatively quiet lava outpourings, erupted more slowly than in flood eruptions. The flows typically are compound and emplaced through tubes. Flows are erupted predominantly from central vents–hence the formation of the shield–but can also emanate from fissures.

In contrast, basaltic "plains" regions, typified by the Snake River Plain, combine aspects of both flood eruptions and shield-forming eruptions. The Snake River Plain is built of four types of constructs: low shields (small, low profile, central vent volcanoes), major tube-fed lava flows, fissure-fed flows, and intracanyon flows, all of which coalesce and interweave in space and time. Although low shields are the predominant structure, eruptions appear to have been limited inasmuch as the shields never reached the enormous proportion of the large Hawaiian shield volcanoes.

The definition of "plains" volcanism is tentative and requires additional study to determine if the classification is warranted. The recognition of distinctive volcanic styles, and hence volcanic histories, is pertinent to planetary geology, and discrimination of "plains" volcanism may be useful for unravelling surface histories for the planets.

REFERENCES

Bullard, F. M., 1971. Volcanic history of the Great Rift, Craters of the Moon National Monument, South-central Idaho: Geol. Soc. Amer. Abs. with Programs, vol. 3, no. 3, p. 234.

Champion, D. E., 1973. The relationship of large scale surface morphology to lava flow direction, Wapi lava field, southeastern Idaho: Unpubl. Master's Thesis, Univ. New York at Buffalo, 44 p.

Eardley, A. J., 1962. *Structural Geology of North America:* Harper and Row, Publ., New York, 2nd ed., 743 p.

Greeley, R., 1971. Observations of actively forming lava tubes and associated structures, Hawaii: Modern Geology, vol. 2, p. 207-223.

Greeley, R., 1972. Additional observations on actively forming lava tubes and associated structures, Hawaii: Modern Geology, vol. 3, p. 157-160.

Greeley, R., 1976. Modes of emplacement of Basaltic terrains and an analysis of mare volcanism in the Orientale Basin: Proc. Lunar Sci. Conf. 7th, p. 2747-2759.

Greeley, R. and J. S. King, 1975a. Geologic field guide to the Quaternary volcanics of the south-central Snake River Plain, Idaho: Idaho Bur. Mines and Geology Pamphlet No. 160, 49 p.

Greeley, R. and J. S. King, 1975b. Rift zones in the south-central Snake River Plain, Idaho: Geol. Soc. Amer., Abs., vol. 7, p. 610-611.

Greeley, R., D. Storm, and C. Wilbur, 1976. Frequency distribution of lava tubes and channels on Mauna Loa volcano, Hawaii: Geol. Soc. Amer. Abs., vol. 8, p. 892.

Hatheway, A. W., 1971. Lava tubes and collapse depressions: Unpubl. Ph.D. dissertation, Univ. Arizona, 353 p.

Holcomb, R. T., D. W. Peterson, and R. I. Tilling, 1974. Recent landforms at Kilauea Volcano: A selected photographic compilation in Greeley, R., ed., Geologic Guide to the Island of Hawaii, NASA CR 152416, p. 49-86.

Howard, K. A. and J. W. Shervais, 1973. Geologic map of Smith Prairie, Elmore County, Idaho: U. S. Geol. Survey, Misc. Geol. Inv. Map I-818.

Jones, R. W., 1970. Comparison of Columbia River basalts and Snake River Plains basalts: Proc. Second Columbia River Basalt Symp., Eastern Wash. State College, p. 209-221.

LaPoint, P. J. I., 1975. Photogeologic study of volcanic and structural features of the eastern Snake River Plain, Idaho: Geol. Soc. Amer., Abs. with Programs, vol. 7, no. 5, p. 620.

LaPoint, P. J. I., 1977. Preliminary photogeologic map of the eastern Snake River Plain, Idaho: U. S. Geol. Survey, MF-850.

Leeman, W. P., 1974. Part I–Petrology of basaltic lavas from the Snake River Plain, Idaho, and Part II–Experimental determination of partitioning of divalent cations between olivine and basaltic liquid: Univ. Oregon, Ph.D. dissertation, 337 p.

Leeman, W. P., 1975. Petrology and origin of Snake River Plain (SRP) olivine tholeiites: Geol. Soc. Amer., Abs. with Programs, vol. 7, no. 5, p. 621-622.

Macdonald, G. A., 1972. *Volcanoes:* Prentice-Hall, Englewood Cliffs, New Jersey, 510 p.

Murtaugh, J. G., 1961. Geology of Craters of the Moon National Monument: Moscow, Idaho Univ., M. S. thesis, 99 p.

Niccum, M. R., 1969. Geology and permeable structures in basalts of the east central Snake River Plain near Atomic City, Idaho: Pocatello, Idaho State Univ., M. S. thesis, 137 p.

Nichols, R. L., 1936. Flow units in basalt: J. Geol., vol. 44, p. 617-630.

Noe-Nygaard, A., 1968. On extrusion forms in plateau basalts. Visindafelag Islendinga, Anniv., vol., Reykjavik, p. 10-13.

Peterson, D. W. and D. A. Swanson, 1974. Observed formation of lava tubes during 1970-71 at Kilauea Volcano, Hawaii: Studies in Speleology, vol. 2, pt. 6, p. 209-224.

Powers, H. A., 1960. A distinctive chemical characteristic of Snake River Basalts of Idaho: U. S. Geol. Survey Prof. Paper 400-B, p. 298.

Prinz, M., 1970. Idaho rift system, Snake River Plain, Idaho: Geol. Soc. Amer. Bull., vol. 81, p. 941-947.

Protska, H. J., P. Eaton, and S. Oriel, 1976. Cordilleran Thermotectonic Anomaly: II. Interaction of an intraplate chemical plume mass and related mantle diapir (abs.): Geol. Soc. America Ann. Mtg., Abs. with Programs, p. 1055.

Russell, T. C., 1902. Geology and water resources of the Snake River Plains of Idaho: U. S. Geol. Survey Bull. 199, 192 p.

Stearns, H. T., 1928. Craters of the Moon National Monument, Idaho: Idaho Bur. Mines and Geology Bull. 13, 57 p.

Stearns, H. T., L. Crandall, and W. G. Steward, 1938. Geology and groundwater resources of the Snake River Plain in southeastern Idaho: U. S. Geol. Survey Water Supply Paper 774, 268 p.

Stearns, H. T., L. L. Bryan, and L. Crandall, 1939. Geology and water resources of the Mud Lake region, Idaho, including the Island Park area: U. S. Geol. Survey Water Supply Paper 818, 125 p.

Swanson, D. A., 1973. Pahoehoe flows from the 1969-1971 Mauna Ulu eruption, Kilauea Volcano, Hawaii: Geol. Soc. Amer. Bull., vol. 84, p. 615-626.

Swanson, D. A., T. L. Wright, and R. T. Heltz, 1975. Linear vent systems and estimated rates of magma production and eruption for the Yakima Basalt on the Columbia Plateau: Amer. J. Sci., vol. 275, p. 877-905.

Trimble, D. E. and W. J. Carr, 1961. Late Quaternary history of the Snake River Plain in the American Falls region, Idaho: Geol. Soc. America Bull., v. 72, no. 12, p. 1739-1748.

Walker, G. P. L., 1972. Compound and simple lava flows and flood basalts: Bull. Volcan., vol. 36, p. 579-590.

Waters, A. C., 1961. Stratigraphic and lithologic variations in the Columbia River Basalt: Am. Jour. Sci., vol. 259, p. 583-611.

Wentworth, C. K. and G. A. Macdonald, 1953. Structures and forms of basaltic rocks in Hawaii: U. S. Geol. Surv. Bull. 994, 98 p.

4. REGIONAL SETTING OF THE SNAKE RIVER PLAIN, IDAHO

John S. King
Department of Geological Sciences
State University of New York at Buffalo
Amherst, New York 14226

4. REGIONAL SETTING OF THE SNAKE RIVER PLAIN, IDAHO

John S. King
Department of Geological Sciences
State University of New York at Buffalo
Amherst, New York 14226

Although lava flows and features of the central and eastern Snake River Plain are the focus of this field conference, examination of the regional setting may provide a perspective useful to those unfamiliar with the Plain. For convenience, the broad picture developed here will be concentrated on the State of Idaho with ultimate resolution to the Snake River Plain.

PHYSIOGRAPHIC FRAMEWORK

Idaho consists of some 216,300 km^2 of diverse physiography and geology (Fig. 4-1). It is best classified as mountainous, for areas of high relief dominate the northern, central, and far southern parts of the State. The irregular eastern boundary of Idaho, adjoining Montana, lies along the crest of mountain ranges. Throughout much of its course of more than 560 km, it follows the high peaks of the Bitterroot Mountains, and in the south, along the continental divide, a location which reflects the history of the Idaho Territory in the 1860's (Wells, 1974).

Mountain ranges in the panhandle region of the State extend southward to the generally west-flowing Salmon River at about 45°30' N latitude, about the middle of the State. To the south lie the Salmon River Mountains with many peaks in excess of 3050 m (10,000 ft). Due south of the Salmon River Mountains are the Sawtooth Mountains and extending southeast from the central Salmon River Mountain

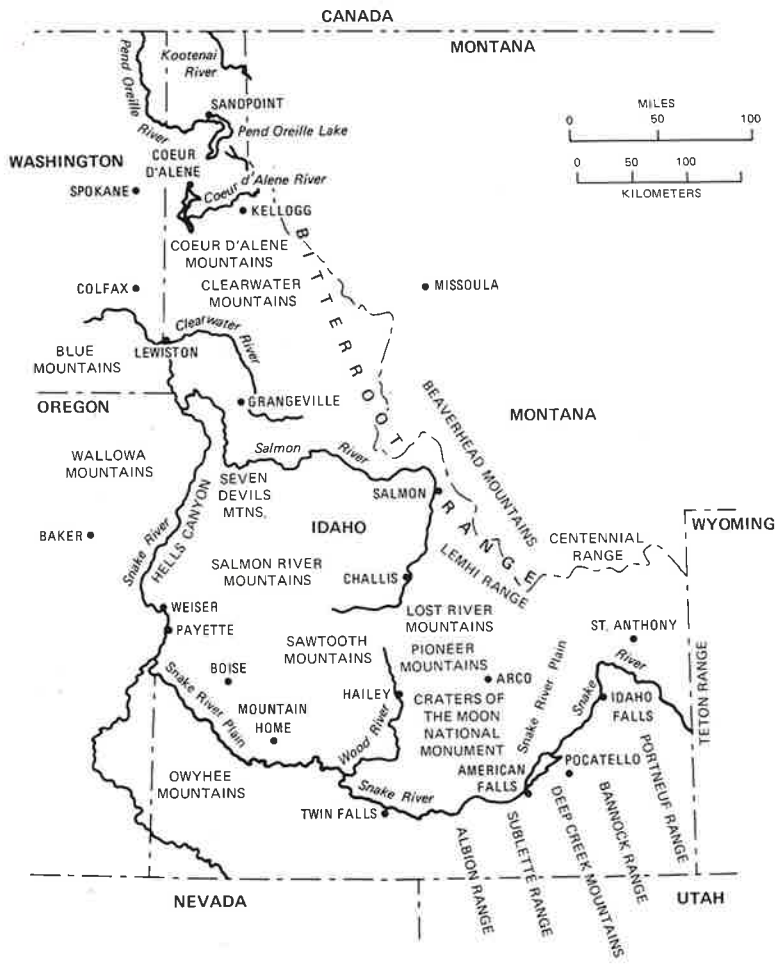

FIGURE 4-1. Map of Idaho showing Snake River Plain and other physiographic features (after McKee, 1972).

"core" is a series of parallel ranges which from west to east are the Pioneer, Lost River, Lemhi, and Beaverhead Ranges. The highest point in Idaho is Borah Peak (12,622 ft) in the Lost River Range. In the southeastern part of the State, south of the Snake River is a series of mountain ranges which trend generally northwest. From east to west these are the Portneuf Range, east of Pocatello, the Bannock Range, the Deep Creek Mountains, the Sublette Range, and the generally north-south trending Albion Range. Many elevations in this region exceed 2750 m. The Owyhee Mountains with high peaks ranging in elevation from 1825 to 2440 m are located in the southwestern part of the State.

Cutting a swath 65–100 km wide across this region of mountain terrain is the Snake River Plain physiographic province which dominates southern Idaho. This is a broad, flat, arcuate depression which is concave to the north and covers some 49,200 km^2, nearly one quarter of the total area of the State. It extends about 645 km west from the Yellowstone Plateau to the Idaho–Oregon border where it adjoins the Columbia Plateau. It is bordered on the south by the Basin and Range Province and on much of the north by the Northern Rocky Mountain Province. Elevations on the Snake River Plain diminish from the east (1350–1525 m) to the west (900–1200 m).

GEOLOGIC FRAMEWORK

A variety of rock types of all geologic ages crop out in Idaho and, although on first view a patchwork pattern emerges, there is nonetheless resolvable order. All of the rocks in the State may be placed in three general categories from Precambrian to Recent (Fig. 4-2).

1) Precambrian rocks occur mostly north of the Snake River Plain and are dominant in the northern panhandle region of the State. However, they also crop out to the south in the Bitterroot Range but are covered by younger rocks before coming in contact with volcanic rocks of the Snake

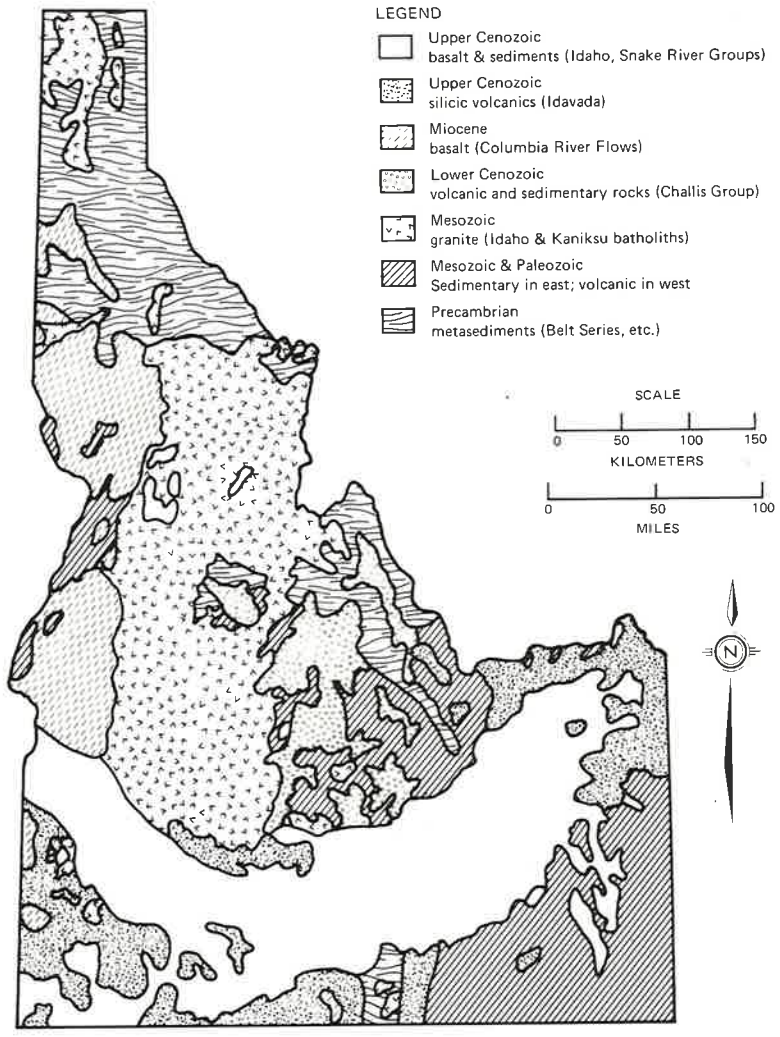

FIGURE 4-2. Geologic sketch map of Idaho (after McKee, 1972).

River Plain Province. Precambrian metamorphic and plutonic rocks south of the Snake River are generally confined to the Albion Range at about 113°30' longitude, although young Precambrian rocks are exposed in the Bannock Range. There are two types of Precambrian rocks in Idaho: a metamorphic basement complex of gneisses and schists, such as those which occur in the central and southern Albion Range (Armstrong and Hills, 1967), and younger, weakly to non-metamorphosed rocks such as the siltstones and argillites of the Belt Series and the quartzites and argillites of the younger Brigham Group. Belt-type rocks are the dominant Precambrian units in Idaho.

2) Paleozoic and Mesozoic sedimentary rocks crop out in the southeastern part of the state. They occur both north and south of the Snake River Plain and rocks representing every Paleozoic period are present in southeastern Idaho (McKee, 1972). Central Idaho is dominated by the Idaho batholith which is made up of granitoid rocks of Mesozoic and early Tertiary age. The Idaho batholith extends north from the Snake River Plain for more than 400 km and is 80–110 km wide.

3) The younger rocks of Idaho are dominated by several volcanic series, many of which are associated with interlayered fluvial and lacustrine sediments. The oldest of these series is the Challis Volcanics of probable Eocene age. The Challis Volcanics consist mainly of andesite but some associated basalts and rhyolites, as well as interlayered sediments are also present. For the most part, Challis Volcanics are located east of the Idaho batholith and north of the Snake River Plain (Fig. 4-2).

The Columbia River Basalts are younger than the Challis Volcanics and lie in western Idaho, mostly north of the Snake River Plain. This basalt contains interlayered lake beds.

The Idavada Volcanics are of Early to Middle Pliocene age and are composed primarily of welded ash flows. The Idavada Volcanics are exposed in the southwestern part of the State where they border the Snake River Plain Province. Silicic rocks of this age are generally considered to be the "basement" of the Snake River Plain (Stone, 1967).

Two younger volcanic series complete the generalized stratigraphic column: the Idaho Group of Early Pliocene to Middle Pleistocene age, and the youngest volcanic series, the Snake River Group of Late Pleistocene to Holocene age. The Idaho Group is made up of siliceous ash beds associated with some basalt flows while the Snake River Group is composed mainly of basalt flows. Both of these younger series contain intercalated lake and stream deposits. The Idaho and Snake River Groups are the dominant units of the Snake River Plain.

SNAKE RIVER PLAIN

The Snake River Plain was early concluded to be, because of its low relief, a regional downwarp that has been filled with basalt. Kirkham (1931) believed that subsidence of the plain may have been caused by removal of deep magma from both this region and the Columbia Plateau region to the west. Recent studies have demonstrated, however, that the Snake River depression is made up of two structurally dissimilar segments which join in the vicinity of Twin Falls at about 114°30' longitude.

The western Snake River Plain is a complex graben bounded on both the north and south by systems of normal faults (Malde and Powers, 1962; Hill and others, 1961). Malde (1965) estimated 2745 m of displacement since Early Pliocene along the faults on the north side of the western plain.

The structure of the eastern Snake River Plain is less clearly defined. The idea of a downwarp proposed by Kirkham has not been entirely dismissed. Malde (1965) located northeast trending faults on the north side of the plain in the vicinity of Twin Falls, but these are of limited extent and cannot be traced far to the northeast. Truncation of the southeast trending mountain ranges arrayed along the north side of the Snake River Plain suggests faulting. Hot

springs along both boundaries of the eastern plain compared to the lack of such springs in the interior region is suggested as evidence for the presence of bounding faults (Schoen, 1974). The gravity relief in the eastern plain is in marked contrast with high gravity anomalies characteristic of the western plain (LaFehr and Pakiser, 1962) and anomalies normal to the trend of the eastern Snake River Plain may reflect near-surface relief. The grain of this geophysically-defined structure agrees with structural trends in the Basin and Range Province to the south, and may mean that basin and range type structure is buried beneath the plain (Schoen, 1974).

Geological and geophysical data suggest that the eastern Snake River Plain is an extension of a zone defined by the alignment of the Yellowstone calderas and the Island Park caldera west of the Park. Eaton and others (1975) concluded that the Yellowstone plateau volcanic field and the eastern Snake River Plain were contiguous and shared a common ancestry of volcanism and tectonism (Fig. 4-3). They further suggested that a magma chamber may be present beneath the Yellowstone rhyolite plateau and have acted as a volcanic focus, perhaps related to a subcrustal plume, that has migrated northeastward relative to the North American plate and parallel to the axis of the eastern Snake River Plain over the last 15 million years (since Late Miocene). However, this interpretation has more recently been altered by Eaton and others (1976) and Protska and others (1976) who now include the region in a zone of high heat flow extending from southeastern California to Idaho and Montana. It is suggested that this anomaly is the result of late Cenozoic interaction between an uranium and thorium-rich plume and subducted oceanic lithosphere.

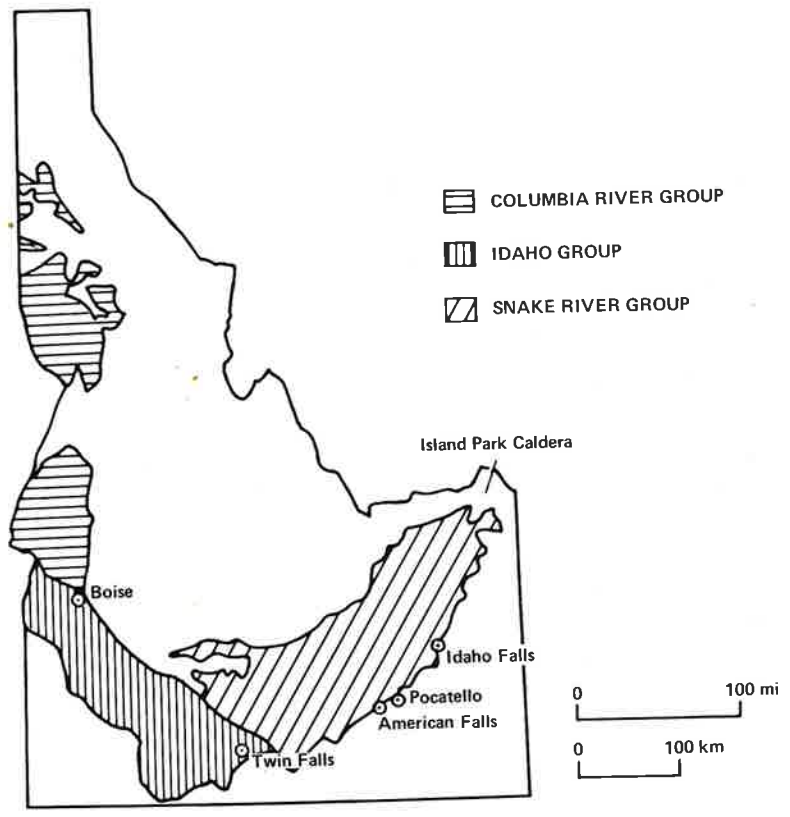

FIGURE 4-3. Idaho map showing the major Cenozoic basalt groups.

Idaho Rift System

The Idaho Rift System is a a series of aligned vents and discontinuous fractures that extend from the northern margin of the Snake River Plain in the vicinity of Craters of the Moon National Monument southeastward to the Wapi lava field (Fig. 4-4) where the fractures either terminate or are obscured by the young lavas of the Wapi flow. Many of the fractures of the Idaho Rift System have served as conduits for lava. The Idaho Rift System was originally referred to as the Great Rift but was redesignated by Prinz (1970) when he divided the system into several rift sets (Fig. 4-5) of differing trends:

1. The Great Rift set trends N 35°W and is defined within Craters of the Moon National Monument by an alignment of vents. No open cracks are exposed in the Monument;

FIGURE 4-4. ERTS image of the central Snake River Plain showing three of the youngest lava fields in the region, flows associated with Craters of the Moon National Monument, the Wapi lava field, and the King's Bowl lava field.

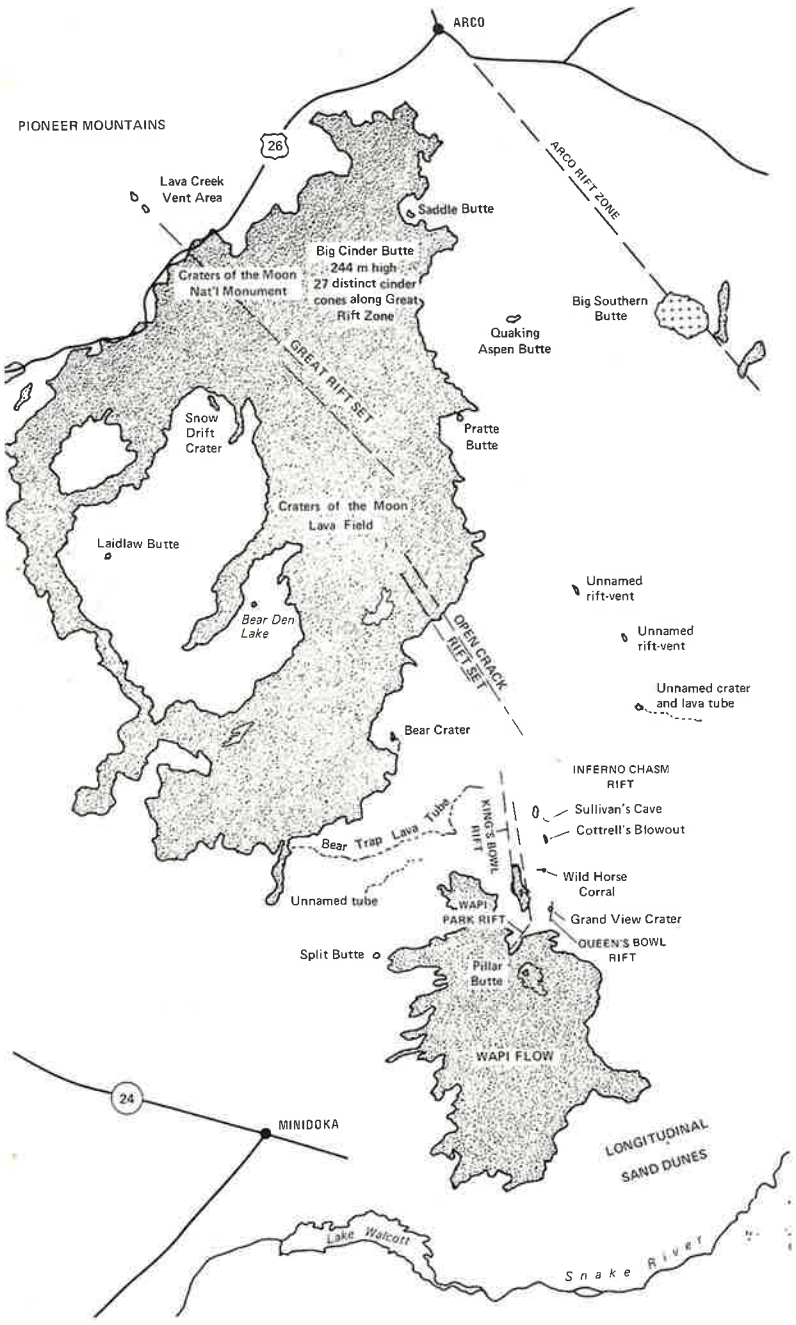

FIGURE 4-5. Map of the general area shown in Figure 4-4, showing the major features along the Idaho Rift System (after Prinz, 1970).

however, open fissures are present southeast of the Monument but lack associated lava flows. An open fissure located north of the Snake River Plain in the Pioneer Mountains which parallels the trend of the Great Rift set has been described by Anderson (1929). This fracture suggests extension of the Great Rift set beyond the limits of the Snake River Plain (Fig. 4-5).

2. The Open Crack rift set trends N 30°W and has no extrusives associated with it (Fig. 4-6).
3. The King's Bowl rift set trends N 10°W and has some small flows associated with it (Fig. 4-7). Prinz (1970) included the Queen's Bowl rift set here and projected it north into Inferno Chasm, Cottrell's Blowout and Wildhorse Corral (Fig. 4-5).
4. The Wapi rift set is inferred to trend north-south beneath Pillar Butte and extend parallel to the long dimension of the Wapi flow.

Several rift sets of different trends and ages have been recognized in the King's Bowl area (Greeley and King, 1975a):

1. The King's Bowl rift is the youngest of these rift sets and is defined by a discontinuous 1.5 m to 2.5 m wide fissure flanked on both sides by sets of narrow tensional cracks. The King's Bowl rift trends N 10°W. To the south of King's Bowl (Fig. 4-5), the flanking fractures on the east side of the rift are traceable to and beneath a tongue of the Wapi flow.
2. The Queen's Bowl rift, which trends N 10°E, is an older tensional set, as evidenced by greater weathering of basalt exposed in the fractures and a heavier cover of vegetation.
3. The Inferno Chasm rift which appears to be the oldest of these rift sets, is a zone defined by an alignment of several prominent volcanic vents including Inferno Chasm, Cottrell's Blowout and Wildhorse Corral. This set trends N 4°W.

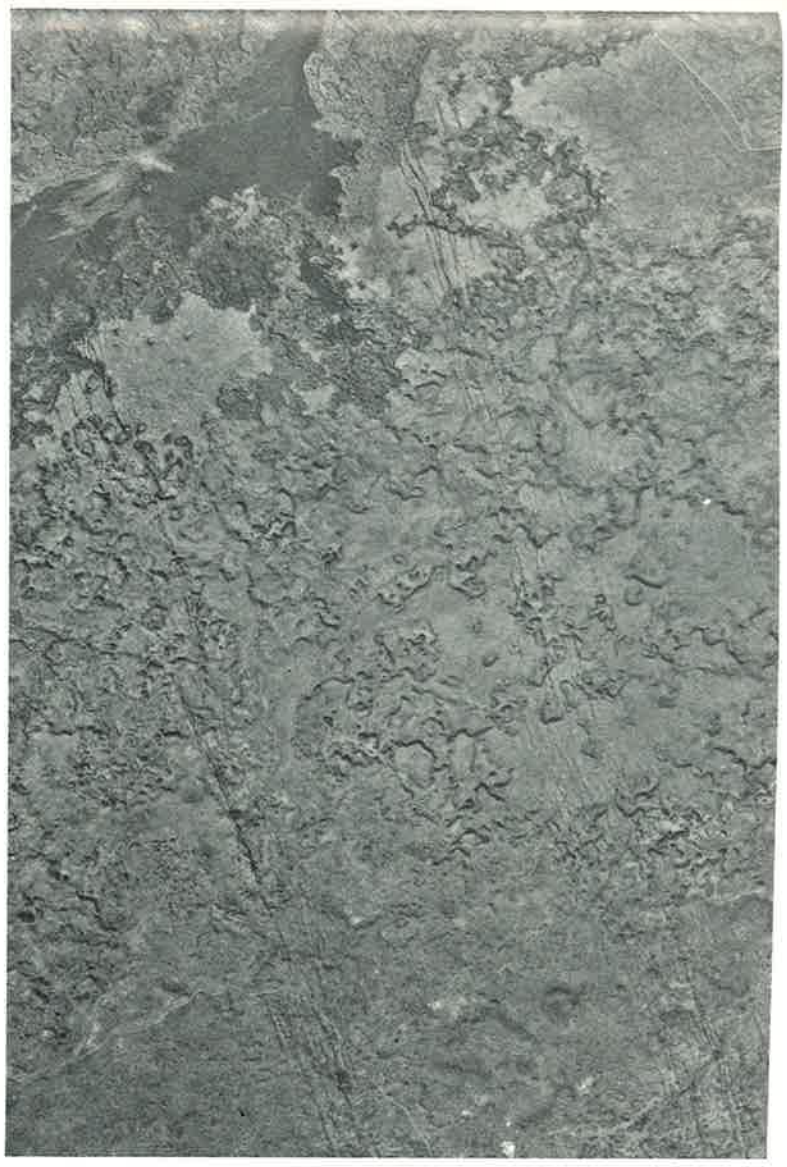

FIGURE 4-6. Vertical aerial photograph of the Open Crack rift set of the Idaho Rift System, south of Craters of the Moon National Monument. This rift set was apparently "dry" with no apparent eruption associated with it. Area of photograph 2.4 km by 3.6 km. (U. S. Geological Survey Photograph GS SWEZ 8-75, October 1971).

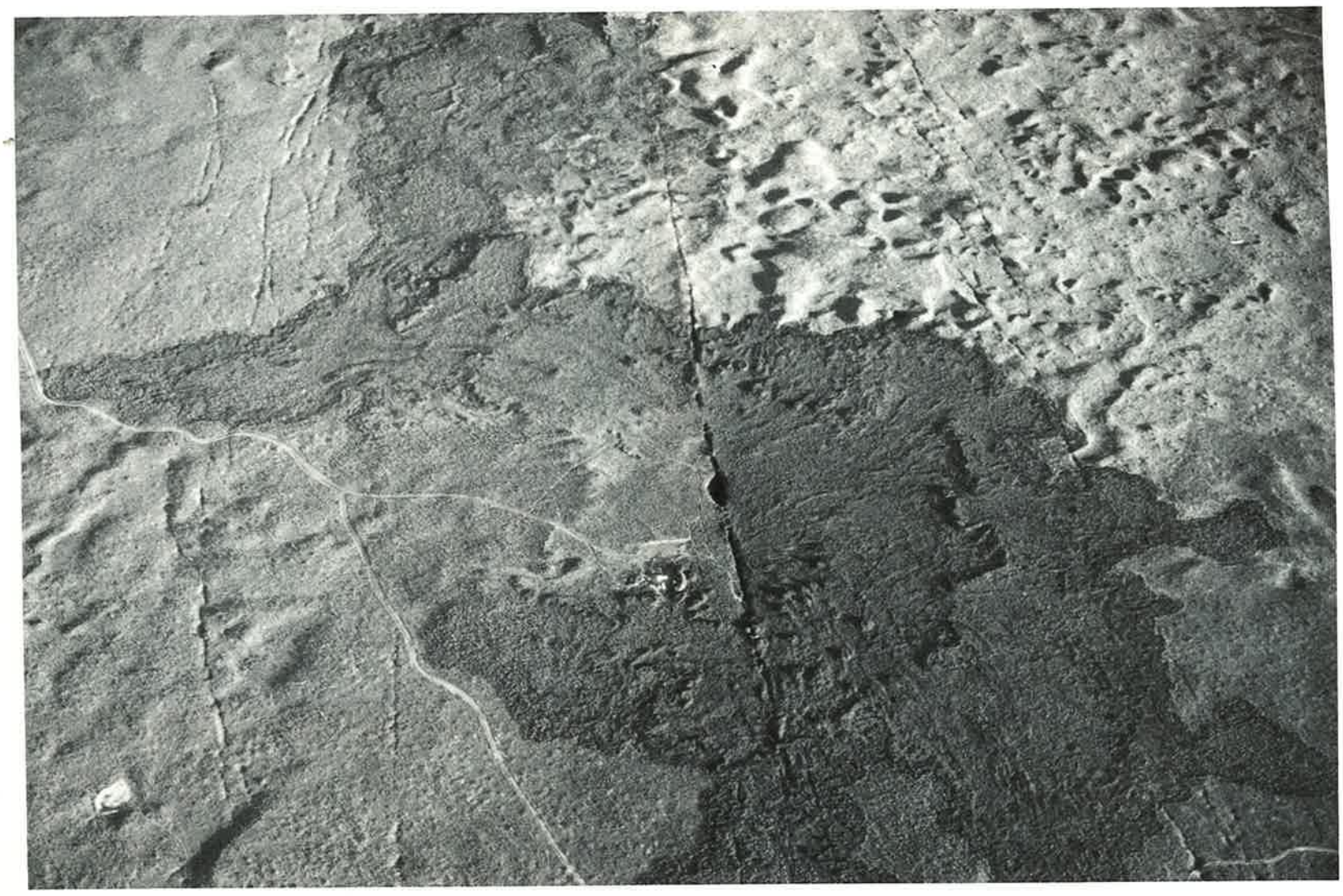

FIGURE 4-7. Low oblique aerial view of the King's Bowl rift, showing the young fissure-fed flows (dark area) and King's Bowl, a phreatic eruption crater on the fissure. Note the extensional fractures that parallel the fissure. (From Greeley and King, 1975b.)

A possible additional rift is defined by an alignment of vents in Wapi Park on the north side of the Wapi lava flow.

The trends of the rift sets range from N 10°E (Queen's Bowl rift of Greeley and King, 1975a) to N 35°W (Great Rift set of Prinz, 1970). The rifts are tensional fractures which collectively approximate the trend of basin and range structures north and south of the plain. In this sense they may be the surface expression of renewed basement faulting related to basin and range structure beneath the lava flows of the Snake River Plain (Leeman, 1974; Schoen, 1974).

Silicic Volcanic Constructs

Basalt is the dominant surface rock of the eastern and central Snake River Plain, but in a group of three prominent volcanic features close to the central axis of the plain south of Arco, two features are not basaltic, and the third, Middle Butte, is defined by tilted basalt which is believed to be a cap overlying a silicic plug. Big Southern Butte and East Butte are both composed of silicic rocks and their origin has long been controversial. They have been interpreted as kipukas or stoptoes (Russell, 1902) and as blocks of older rock faulted to their present position (Stearns and others, 1938). More recently, Schoen (1974) has suggested that these features were emplaced as viscous silicic domes, possibly derived from remobilized silicic material underlying the basalt of the Snake River Plain. He points out that the tilted basalt flow which caps Middle Butte stands at an anomalously high elevation compared to surrounding flows. The nearest location of a flow showing equal elevation and similar attitude to the Middle Butte flow is 128 km distant to the northeast. From this Schoen concludes that the basalt cap on Middle Butte is a plate which has been pushed up to its present elevation and orientation by emplacement of a plug of younger silicic rock. More attention will be given to East, Middle, and Big Southern Buttes in another paper in this conference guide (Chapter 6).

Snake River Basalts

All of the features which will be seen during the Volcanic Conference are developed in basalts of the Snake River Group which are of late Pleistocene to Holocene age. These basalts differ markedly in origin from the Miocene basalts of the Columbia River Group to the west. The Columbia River basalts were extruded from fissures whereas Snake River Group lavas erupted from centers which were probably rift controlled, but which changed locations repeatedly through time. Thus the present build up of the basaltic succession represents a composite of overlapping and coalescing flows from a variety of vents (Fig. 4-8). The distinction between the two basaltic provinces is discussed in Greeley (1976) and Chapter 3.

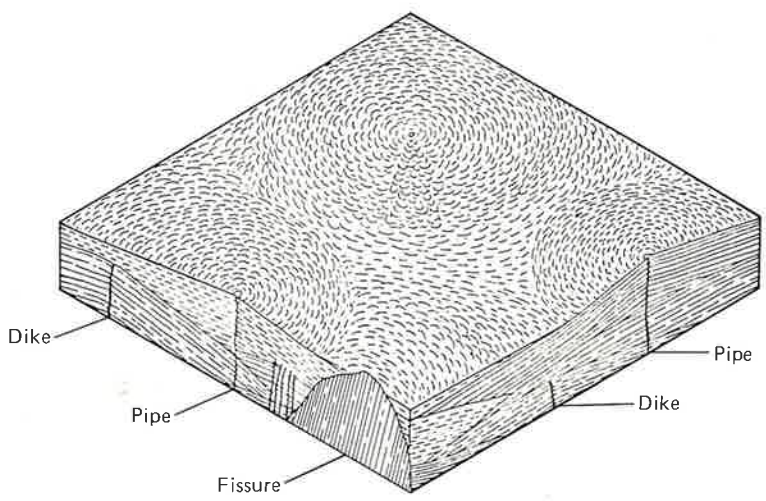

FIGURE 4-8. Diagram illustrating the structure of a typical lava plain or plateau. (From Macdonald, 1972, after Rutten, 1964.)

Most of the Snake River basalts represent highly mobile pahoehoe flows (Stone, 1967). Snake River lavas must have been extremely fluid as the flows spread great distances from their vents (Lindgren, 1898). Furthermore, shields of many of the vents are large (up to 16 km) but of low relief (60–90 m) reflecting discharge of a very fluid lava (Russell, 1902). Stearns and others (1938) noted an abundance of low shields (about 30 m high) with associated flows which cover areas up to 77 km^2 also suggesting a very fluid lava. However, it has recently been pointed out that the rate of effusion is an important variable which must be considered in the evaluation of the extent of lava flows. Thus even viscous material can be carried farther from the vent if the effusion rate is continuously high (Walker, 1972).

The Snake River Group lavas are olivine tholeiites which are fairly uniform in mineralogy, chemistry, and texture (Stone, 1967). They are characterized chemically as being low in SiO_2 and total alkalis and having a high total iron content. The average Snake River lava apparently began to crystallize at about 1175°C and crystallization was complete with a reduction of 150°C (Stone, 1967). Leeman (1974) indicated from a study of the McKinney basalt, which is a member of the Snake River Group, that the lavas were erupted at 1190° to 1200°C. According to Stone (1967), the first phase to crystallize was olivine, but it was quickly joined by plagioclase and all principal phases were crystallizing simultaneously with a temperature drop of 35°–50°. The texture of the basalt indicates that crystallization generally occurred subsequent to termination of movement of the flow. Had crystallization taken place during flow, subalignment of elongate grains such as feldspar laths would be expected. However, such alignment is not common and, for the most part, the inequant mineral grains show random orientation.

The total thickness of basalts of the eastern Snake River Plain is not known. LaFehr and Pakiser (1962) suggest thickness variations of the basalts of from several hundred to over 1500 m. Test holes drilled at the National Reactor Testing Station south of Arco penetrated 456 m below the surface and were still in Snake River Group basalts (Walker, 1964). Electrical resistivity data determined on a line between Blackfoot and Arco are interpreted to indicate a maximum depth of 1830 m for basalts of the eastern Snake River Plain (Zohdy and Stanley, 1972, 1973).

Estimates of the thicknesses of individual flows of Snake River Group basalts are variable. Russell (1902) estimated flows to be from 45–75 m thick. Stone (1967) states that "the flows range in thickness from 10–60 feet (3–18 m), averaging 30 feet (9 m), but may reach several hundred feet in thickness where they fill canyons." Champion (1973) estimated the average thickness of the Wapi field (made up of several flow units), which is one of the most recent of the Snake River Group lavas, at about 32 m, and Leeman (1974) characterized the Snake River basalts as thin flows from 3 to 10 m in thickness. Accurate flow thicknesses are difficult to establish in light of the petrologic similarity of the lavas as well as the overlap of flows from different vents. Coupled with this, flow units, representing different but overlapping surges of material from the same vent tend to mask any textural boundary differences between flows. The areal extent of many flows which have spread out on a low gradient surface indicate that the flows were extremely fluid and this, in turn, suggests that the average thickness of the flows is not great, possibly in the range of 1 m to 10 m.

The uniformity of petrology and the lack of widespread natural incisions through the flows as well as a lack of well data makes correlation of all but the younger surface flows of the eastern Snake River Plain difficult. Stratigraphic columns can be determined locally as at the King's Bowl or in Wildhorse Corral, but it is difficult to extend that control laterally. Moreover, flow thicknesses determined near their vents are probably not typical of the main part of the flow. Most flows have vesicular tops and narrower vesicular bases (Stone, 1967) which is a useful criterion for differentiation of flows. Soil horizons are also useful as flow dividers but are not always continuous. Also, Stearns and Macdonald (1942),

based on observations at Haleakala in Hawaii, have shown that "pseudo" soil horizons can result from the migration of ground water through rubbly zones within a single lava flow. Such a pseudo horizon, marked by an abundance of reddish friable material would, in such a case, not indicate a flow contact, but rather a physically distinct zone within a single flow. Additionally, the present surface of the flows is undulating and significant local relief is found around pressure ridges and collapse depressions. Assuming a similar surface expression for earlier flows and noting the present accumulation patterns of windborne deposits, a significant period of time appears to be necessary to develop a widespread, continuous soil horizon. Loess accumulates in low and protected regions on the surface and builds up slowly. If insufficient time intercedes between flows, the loessal accumulation remains discontinuous and of only local significance in flow correlation. Some success at correlation of the surface flows has been made by intensive stereoscopic study of aerial photos noting slopes, textural variations, and flow fronts. This type of analysis allows geologic mapping of the surface units and provides insight into the complex overlap and coalescence of flows from various vents (Greeley and King, 1975b; LaPoint, 1975).

Stearns and others (1938) mapped some 300 vents on the Snake River Plain east of 115° longitude and extrapolated this figure to a total of 400 for the entire plain. In their mapping they were unable to locate any widespread structural patterns defined by the vents although many short chains of vents were found. Most of the vents are low shields from which lava erupted quietly. There are notable local exceptions to this pattern of eruption, however, which indicate more violent phreatic eruptions. King's Bowl on the King's Bowl rift set is one of these. It has an extensive field of ejecta as well as an area of ash accumulation. Split Butte is another such vent and, although apparently less explosive than the King's Bowl event, the Split Butte mound is made up dominantly of a rampart of layered tephra (Greeley and King, 1975b; Womer, 1977 and Chapter 12). Both of these vents no doubt erupted as they did owing to interaction of the lava with ground water.

Age of the Plain and Lavas

The Snake River Plain is interpreted by Stone (1967) to have developed since the Pliocene Epoch. Eaton and others (1975), based largely on K-Ar dating of volcanic units along the margins of the eastern plain (Armstrong, Leeman and Malde, 1975), project the volcanic and tectonic history of the eastern plain back about 15 million years. They suggest that a magma body, which is still molten, underlies the Yellowstone Plateau, and, in their interpretation, this present position of volcanism ". . . represents the active end of a system of similar volcanic foci that has migrated progressively northeastward for 15 million years. . . " This migration is envisioned to have started at the southwestern end of the eastern Snake River Plain and followed slowly along the trace of the eastern plain. The parallelism of the structural grain of exposed Precambrian rocks elsewhere in the Rocky Mountain region with the direction of movement has suggested control by Precambrian structures (Eaton and others, 1975).

Age determinations for the younger flows of the eastern Snake River Plain are not abundant. Bullard (1976) reports two dates from burned sage destroyed by one of the Holocene flows in Craters of the Moon National Monument which bracket in a 2100–2300 year age range. Flows which issued from the King's Bowl rift have also been dated by C^{14} methods on burned sage roots found in the base of the flow at the Crystal Ice Cave as 2130 ± 130 years (Prinz, 1970). Kuntz (1977) has obtained C^{14} dates from disseminated charcoal and organic material in soils beneath the older North Robbers and Cerro Grande flows as 11,940 ± 300 and 10,780 ± 300 C^{14} years respectively and an age of 4100 ± 200 C^{14} years on the Hell's Half Acre flow. He also feels that at least 10 other flows in the same vicinity are less

than 50,000 years old. These ages are all considerably younger than the youngest eruptive events in the Yellowstone region (150,000–70,000 years) indicated by Eaton and others (1975). Although their hypothesized eruptive sequence has been qualified by suggesting that rhyolitic volcanism followed eruption of tholeiitic lava at each focus and was followed in turn by basalts which have ". . . continued to erupt virtually to the present," there seems to be some lack of supporting evidence for this in many of the basalt and rhyolite sequences of the central plain.

SUMMARY

The Snake River Plain is a prominent physiographic region which occupies nearly one fourth of the total area of the State of Idaho. It contrasts markedly with the surrounding terrain in that it is characterized by low topographic relief and stands at low elevation in respect to the surrounding ranges. The Snake River Plain has developed since Late Miocene–Pliocene. The base of the Snake River depression can be considered to be the Idavada Volcanic Series or time-equivalent silicic rocks which crop out along the edge of the plain.

The Snake River Plain is structurally divisible into two parts. The western plain is interpreted on both geophysical and geological evidence to be a graben. The eastern plain, however, is more difficult to interpret; it may be a regional downwarp at least partially bounded by faults, or it may be the result of the migration of some shallow subsurface volcanic focus over the past 15 million years or possibly a combination of these causes.

REFERENCES

Anderson, A. L., 1929. Lava Creek Vents, Butte County: Northwest Science, vol. 3, p. 13-19.

Armstrong, R. L. and F. A. Hills, 1967. Rb-Sr and K-Ar Geochronologic Studies of Mantled Gneiss Domes, Albion Range, Southern Idaho, USA: Earth and Planetary Letters, vol. 3, p. 114-124.

Armstrong, R. L., W. P. Leeman and H. R. Malde, 1975. K-Ar dating Quaternary and Neogene volcanic rocks of the Snake River Plain, Idaho: Amer. Jour. Sci., vol. 275, p. 225-251.

Bullard, F., 1976. Volcanoes. University of Texas Press, Austin, 330 p.

Champion, D. E., 1973. The relationship of large scale surface morphology to lava flow direction, Wapi lava field, southeastern Idaho: Unpublished M. A. Thesis, State Univ. of New York, Buffalo, 44 p.

Eaton, G. P. and R. L. Christiansen, H. M. Iyer, A. M. Pitt, D. R. Mabey, H. R. Blank, Jr., I. Zietz, M. E. Gettings, 1975. Magma beneath Yellowstone National Park: Science, vol. 188, p. 787-796.

Eaton, G. P., H. Protska, S. Oriel, and K. Pierce, 1976. Cordilleran Thermotectonic Anomaly: I. Geophysical and geological evidence of coherent late Cenozoic intraplate magmatism and deformation (abs.): Geol. Soc. America Annual Meeting, Abstracts with Programs, p. 850.

Greeley, R., 1976. Modes of emplacement of basalt terrains and an analysis of mare volcanism in the Orientale Basin: Proc. Lunar Sci. Conf. 7th Annual, p. 2747-2759.

Greeley, R. and J. S. King, 1975a. Rift zones in the south-central Snake River Plain, Idaho: Geol. Soc. America, Abs. with Program (Rocky Mountain Section), vol. 7.

Greeley, R. and J. S. King, 1975b. Geologic field guide to the Quaternary volcanics of the south-central Snake River Plain, Idaho: Pamphlet No. 160, Idaho Bureau of Mines and Geology, 49 p.

Hill, D. P., H. L. Baldwin, Jr., and L. C. Pakiser, 1961. Gravity, volcanism and crustal deformation in the Snake River Plain, Idaho: U. S. Geol. Survey Prof. Paper 424-B, p. B248-B250.

Kirkham, V. R. D., 1931. Snake River Downwarp: Jour. Geol., vol. 39, p. 465-482.

Kuntz, M. A., 1977. Extensional faulting and volcanism along the Arco Rift Zone, eastern Snake River Plain, Idaho (abs.): Geol. Soc. America, Rocky Mountain Sectional Meeting, Missoula.

*LaFehr, T. R. and D. H. Pakiser, 1962. Gravity, volcanism and crustal deformation in the eastern Snake River Plain, Idaho: U. S. Geol. Survey Prof. Paper 450D, p. D76-D78.

LaPoint, P. J. I., 1975. Photogeologic study of volcanic and structural features of the eastern Snake River Plain, Idaho (abs.): Geol. Soc. America, Rocky Mountain Sectional Meeting, Abstracts with Programs, p. 620.

Leeman, W., 1974. Petrology of basaltic lavas from the Snake River Plain, Idaho, Ph.D. Dissertation, Univ. of Oregon, 337 p.

Lindgren, W., 1972. Geologic Atlas of the U. S.: Boise Folio No. 45, 11 p.

Macdonald, G. A., 1977. Volcanoes: Prentice-Hall, Englewood Cliffs, 510 p.

Malde, H. E., 1965. Snake River Plain: in Wright, H. E. and D. G. Frey, eds., The Quaternary of the United States, p. 255-263.

Malde, H. E. and H. A. Powers, 1962. Upper Cenozoic stratigraphy of western Snake River Plain, Idaho: U. S. Geol. Survey Prof. Paper 596, 52 p.

McKee, B., 1972. Cascadia: McGraw Hill Book Co., 394 p.

Prinz, M., 1970. Idaho rift system, Snake River Plain, Idaho: Geol. Soc. America Bull., vol. 81, p. 941-947.

Protska, H. J., G. P. Eaton and S. S. Oriel, 1976. Cordilleran Thermotectonic Anomaly: II. Interaction of an intraplate chemical plume mass and related mantle diapir (abs.): Geol. Soc. America Annual Meeting, Abstracts with Programs, p. 1055.

Russell, T. C., 1902. Geology and water resources of the Snake River Plains of Idaho: U. S. Geol. Survey Bull. 199, 192 p.

Schoen, R., 1974. Part III. Geology, in Robertson, J. B., R. Schoen and J. T. Barraclough, Influence of liquid waste disposal on the geochemistry of water at the National Reactor Testing Station, Idaho: U. S. Geol. Survey Open File Report, IDO 22053, 231 p.

Stearns, H. T., L. Crandall and W. G. Steward, 1938. Geology and groundwater resources of the Snake River Plain in Southeastern Idaho: U. S. Geol. Survey Water Supply Paper 774, 268 p.

Stearns, H. T. and G. A. Macdonald, 1942. Geology and ground water resources of the island of Maui, Hawaii: Hawaii Division of Water and Land Development, Bull. 7, p. 61-113.

Stone, G. T., 1967. Petrology of Upper Cenozoic basalts of the Snake River Plain, Ph.D. Dissertation, Univ. of Colorado, 392 p.

Walker, E. H., 1964. Subsurface geology of the National Reactor Testing Station, Idaho: U. S. Geol. Survey Bull. 1133E, 22 p.

Walker, G. P. L., 1972. Compound and simple lava flows and flood basalts: Bull. Volcanologique, vol. 35, p. 1-12.

Wells, M. W., 1974. Origins of the name "Idaho" and how Idaho became a territory in 1863: in Etulain, R. W. and B. W. Marley, The Idaho Heritage, Idaho State University Press, 230 p.

Womer, M. B., 1977. A study of the ash rings of Split Butte, a maar crater of the south-central Snake River Plain, Idaho: Unpubl. Master's Thesis, State Univ. of N. Y. at Buffalo, 53 p.

Zohdy, A. A. R., and W. D. Stanley, 1972. Profiles of deep electrical soundings on the Snake River Plain, Idaho, (abs.): Geol. Soc. America, p. 423.

Zohdy, A. A. R. and W. D. Stanley, 1973. Preliminary interpretation of electrical sounding curves obtained across the Snake River Plain from Blackfoot to Arco, Idaho: U. S. Geol. Survey Open File Report, 3 p.

THE GEOLOGY OF BRUNEAU DUNES STATE NATURAL PARK

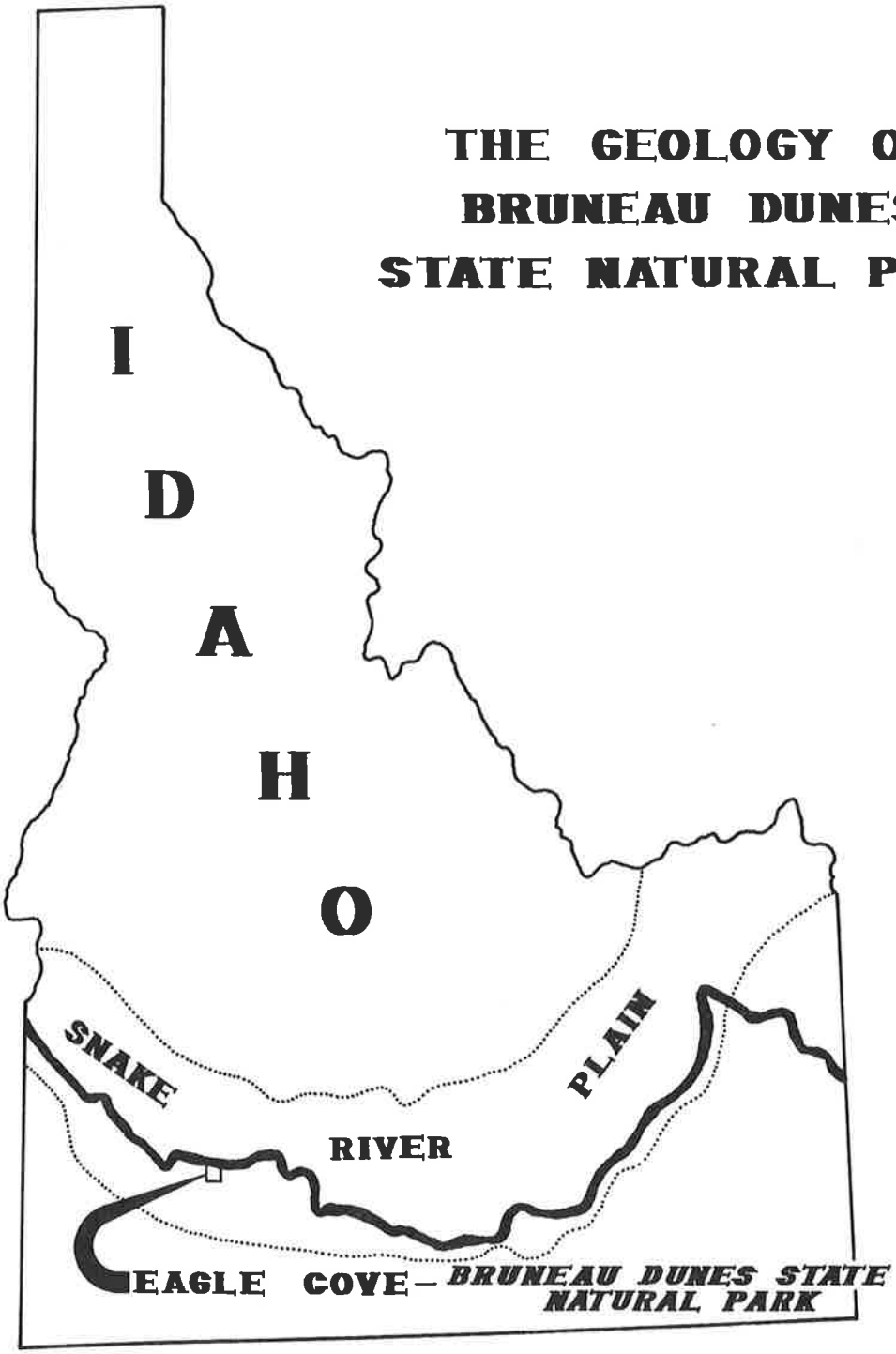

CONDENSED FROM THE THESIS

OF JAMES D. MURPHY, GEOLOGIST

"THE GEOLOGY OF EAGLE COVE" at Bruneau, Idaho

M.S. Thesis

STATE UNIVERSITY OF NEW YORK AT BUFFALO

77p.

(1973)

What is the chronological combination of natural happenings that created and maintain the unique Bruneau Sand Dunes?

To answer this question, you will take a trip back in time when our planet Earth was a bit younger. Let's go back to when the Snake River Plain (area from Pocatello to Ontario) was being filled with upper cenozoic sediments and occasional lava flows. The lava flows intermittently dammed the Snake River Canyon in various locations causing the accumulation of water in the resulting reservoirs. These lakes, like our modern man-made reservoirs, accumulated thick layers of sediments. (Lacustrine Sediments, Plate 1). When the lava dams eventually washed out, flood plain situations occurred downstream resulting in another form of deposition. (Fluvial Sediment, Plate 2). The most important geological strata for the sand dunes area formed by these occurrences are termed the Glenns Ferry formation, the Bruneau formation, and tauna gravel. (Plate 3).

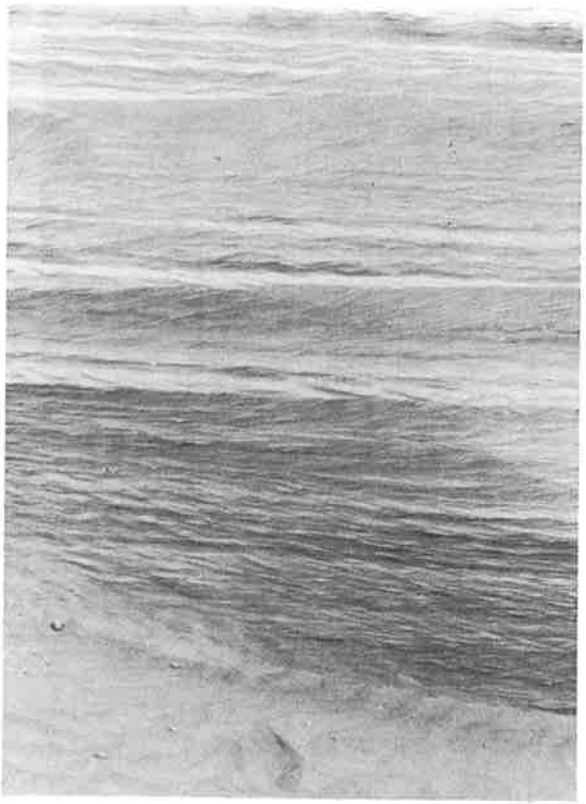

Plate 1 - Lacustrine Sediments

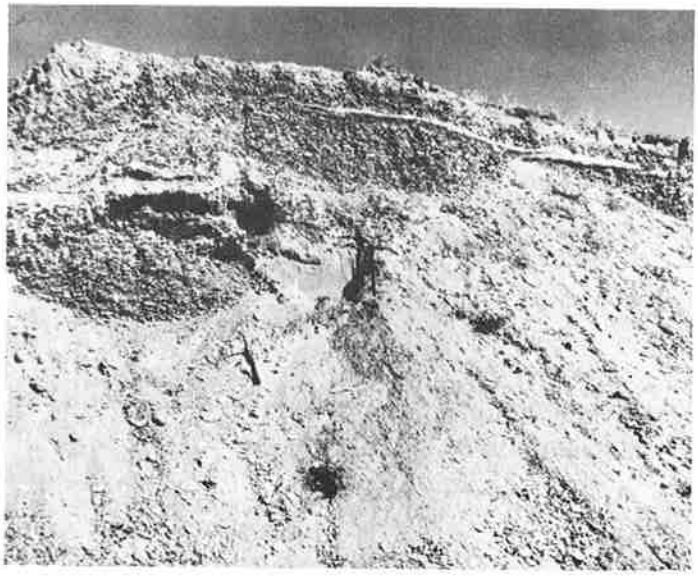

Plate 2

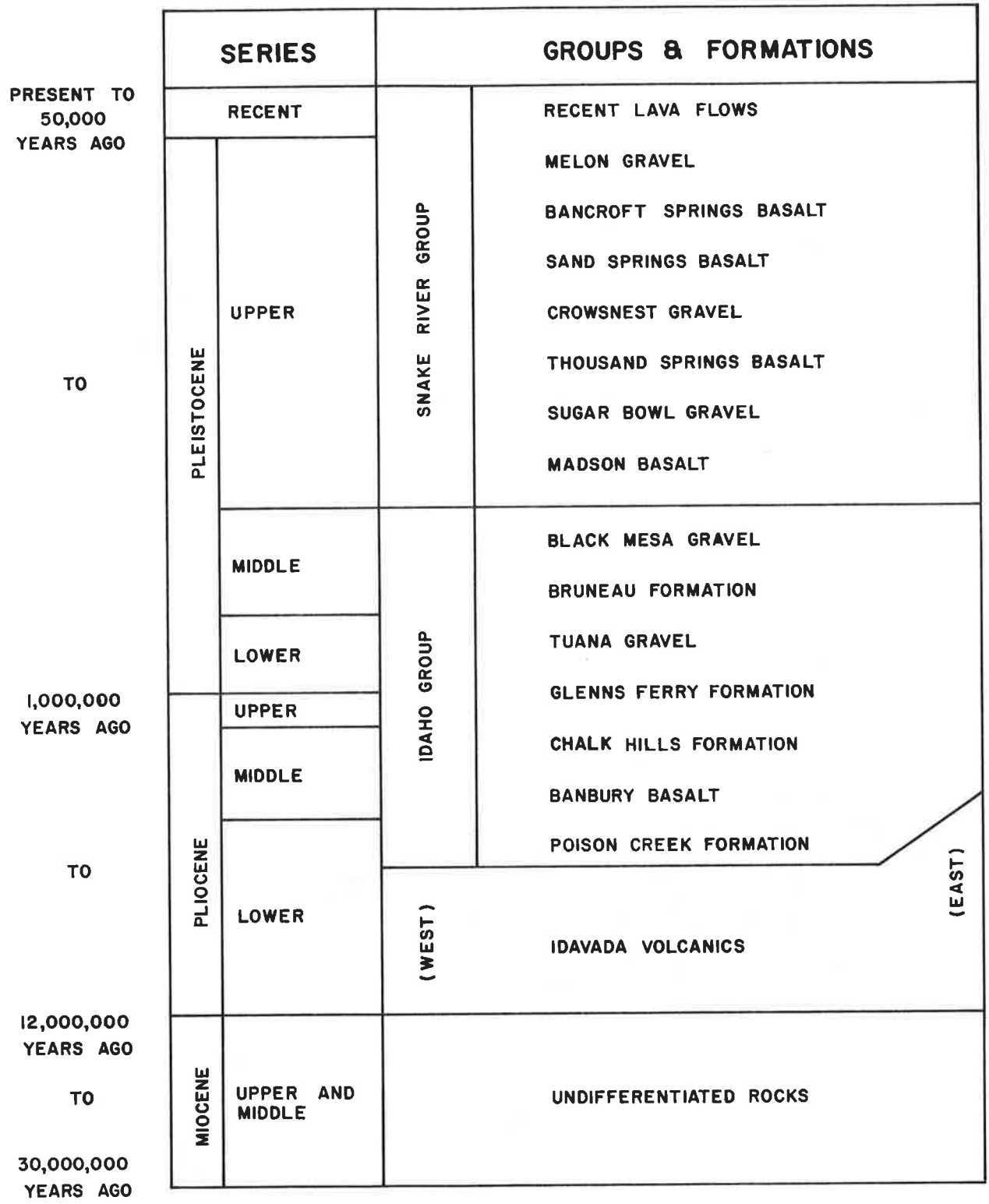
SERIES
GROUPS & FORMATIONS
PRESENT TO 50,000 YEARS AGO
RECENT
RECENT LAVA FLOWS
PLEISTOCENE
UPPER
SNAKE RIVER GROUP
MELON GRAVEL
BANCROFT SPRINGS BASALT
SAND SPRINGS BASALT
CROWSNEST GRAVEL
THOUSAND SPRINGS BASALT
SUGAR BOWL GRAVEL
MADSON BASALT
TO
MIDDLE
IDAHO GROUP
BLACK MESA GRAVEL
BRUNEAU FORMATION
LOWER
TUANA GRAVEL
GLENNS FERRY FORMATION
1,000,000 YEARS AGO
PLIOCENE
UPPER
CHALK HILLS FORMATION
MIDDLE
BANBURY BASALT
POISON CREEK FORMATION
TO
LOWER
(WEST)
(EAST)
IDAVADA VOLCANICS
12,000,000 YEARS AGO
TO
MIOCENE
UPPER AND MIDDLE
UNDIFFERENTIATED ROCKS
30,000,000 YEARS AGO

Plate 3

The ancient Snake River Meander Scar, which is now Eagle Cove (Plate 4) was cut into the lacustcine facies of the aforementioned strata. The sands in Eagle Cove are similar in minerology to the sands in the Bruneau and Glenns Ferry formation. This suggests that the fluvial-lacustrine cenezoic deposits are the source of sand for these dunes. New supplies of sand for the maintenance and building of the dunes are blown in from the various gullies, draws, and plateaus immediately surrounding the dunes. Silt, clay, and organic particles are carried by the wind over the depression while the pebble and cobble sized materials remain in place regardless of the wind force. (Plate 5, Plate 6).

Plate 4

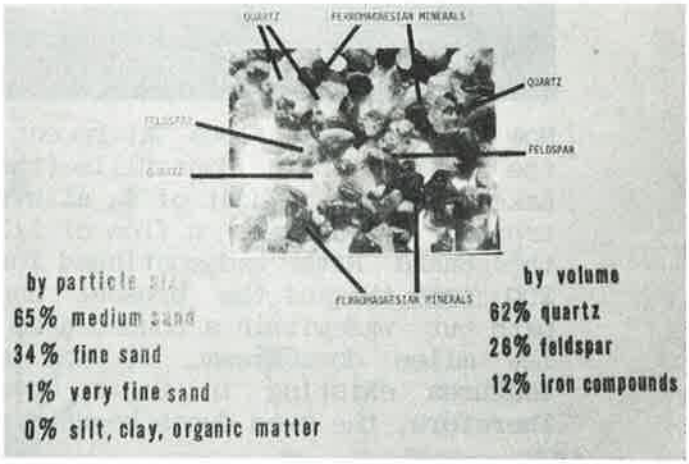

Plate 6
Sand Analysis

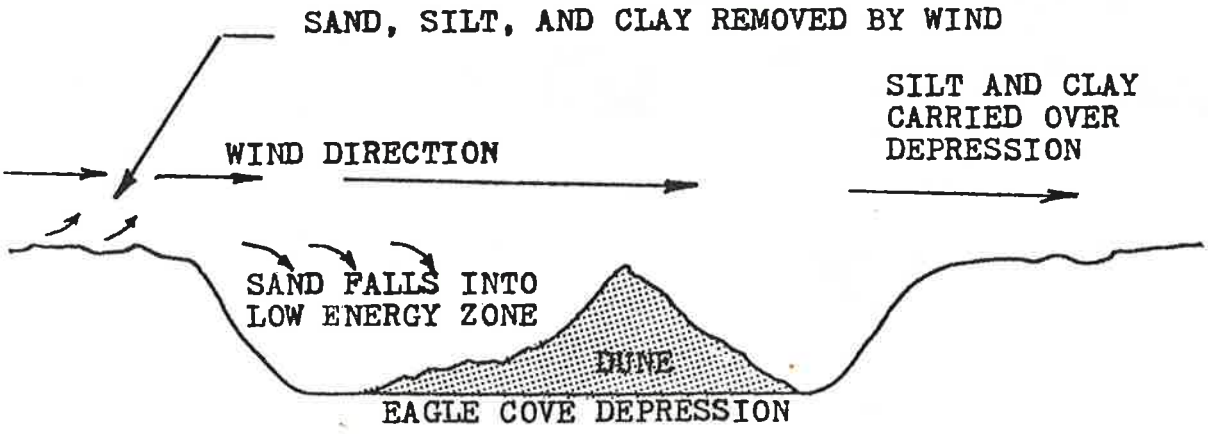

Plate 5

Some sand is carried to the floor of Eagle Cove by water during cloudbursts. As the redeposits dry, the wind again erodes these alluvial fans redepositing the sand grains in the dune formations. (Plate 7).

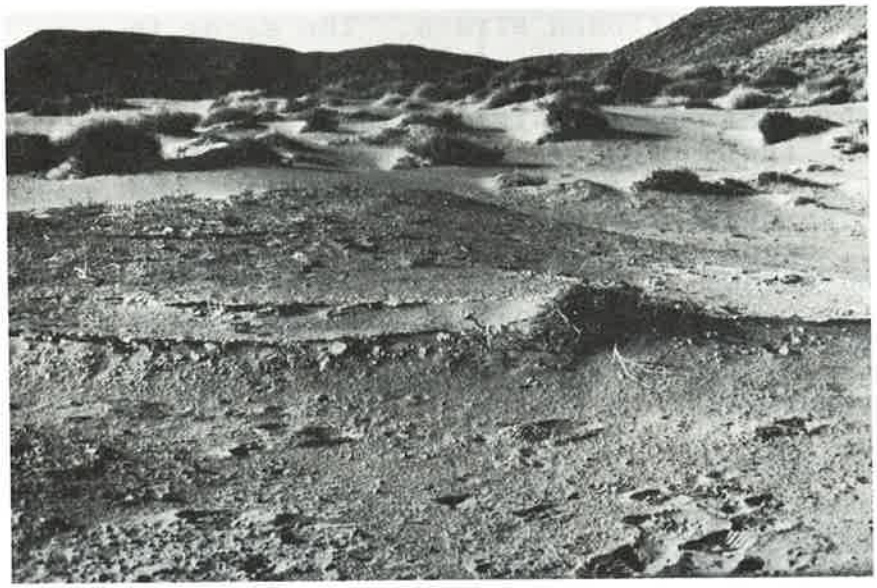

Plate 7

Now let's take a look at recent times. About 30,000 years ago, a rise in the level of Lake Bonneville (the remainder of this lake is the Great Salt Lake) caused a washout of an alluvial barrier near Preston, Idaho. A catastrophic flood with a flow of 1/3 cubic mile per hour hollowed the path of the Snake River and continued for at least six weeks. This flow was about 200 times that of the present Snake River. Eagle Cove was in the direct path but was within a ponded area due to the constriction at Crane Falls, a few miles downstream. It was suggested that any eolian (wind deposited) features existing in Eagle Cove at the time of the flood were destroyed. Therefore, the sand dunes began development 30,000 years ago.

Plate 8

The "Big Dune" with its renowned crater is actually a "dune complex" (Plate 8) or an aggregation of eolian features which is manifested in an apparent single structure. Why does this complex remain in the same area and same relative shape? The complex is created and maintained by long-term wind patterns. Wind records from Mountain Home Air Force Base clearly show that the wind is bimodal (2 prevailing directions) approximately 180^{o} apart. The winds are southeasterly 28 percent of the time, and northwesterly 32 percent of the time. These opposing winds apparently keep the central dune complex in place. (Plate 9).

WIND ROSE DIAGRAM, MOUNTAIN HOME AIR FORCE BASE, IDAHO.
FOR PERIODS 1932-33, 1943-1945, 1949, 1951-1965

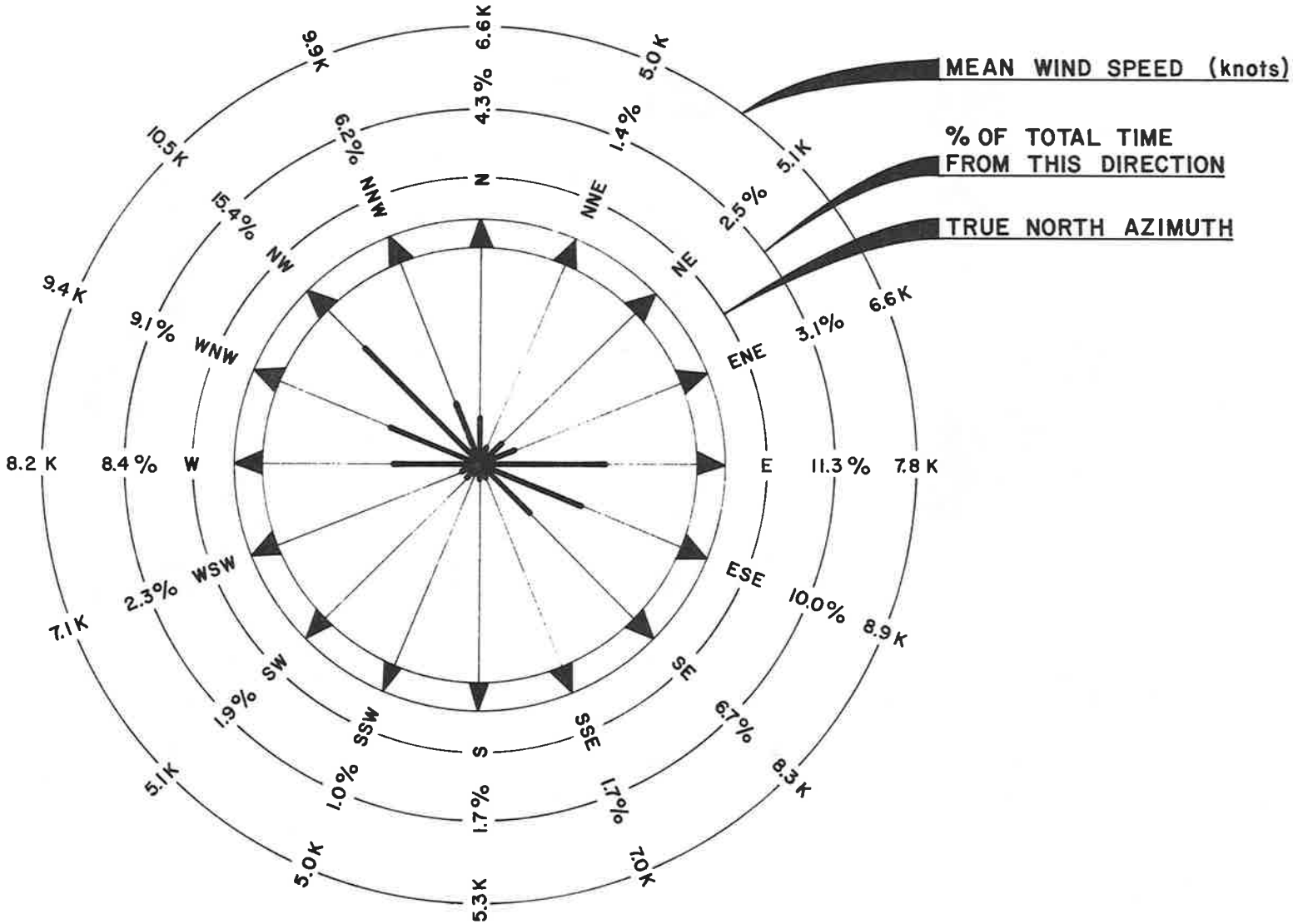

Plate 9

Wind patterns within and around the Bruneau Dunes Crater were studied. Smoke generating devices (Plate 10) and balloons marked the travel of the wind. The tests were photographed with both single frames and motion pictures. These tests showed eratic or apparently random behavior of southeasterly winds without any clear vortexing motion. Therefore, it is suggested that there are two separate dunes (Dune L and Dune S, Plate 11) of the transverse type which interact with one another to produce the crater. Therefore, the crater is an area of no deposition surrounded by the interacting ends of the two dunes.

Plate 10

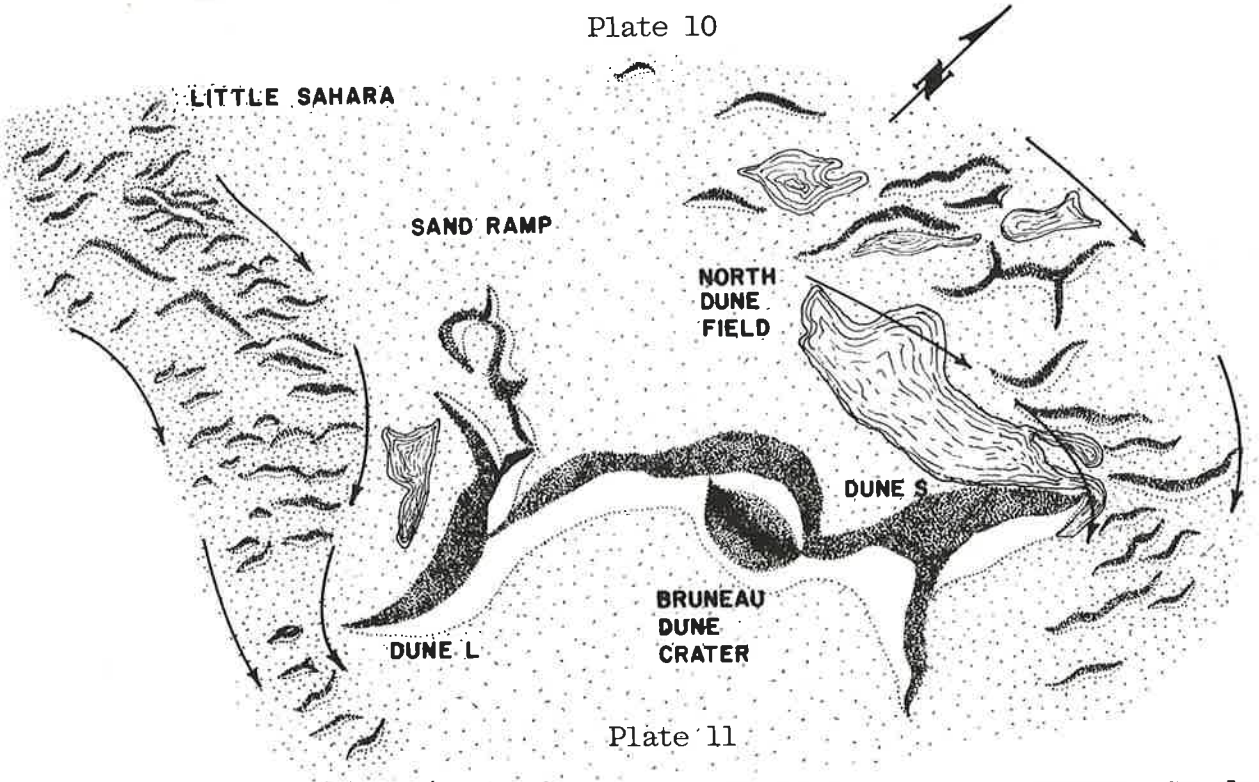

Plate 11

Migration of Little Sahara Dunes and North Field Dunes around Central Complex showing characteristic arcuate patterns due to deflection of wind by the Central Dune Complex.

Today, the dunes are being affected by the higher water table in the area. The water is stablizing many of the dunes by wetting the sand. Water is promoting heavier plant growth throughout the area, which slows surface winds and disrupts local wind patterns. These alterations will probably cause the complete stablization and eventual elimination of the sand dunes sometime in the geological future. In the meantime, the water-caused habitat has increased the beauty, wildlife populations, and human interest in this desert area with its unique dunes. It will remain as an Idaho Natural State Park for your study and enjoyment for hundreds of years. (Plates 12, 13, and 14).

Plate 12

Plate 14

Plate 13

Icarus 230 (2014) 29–37

Contents lists available at ScienceDirect

Icarus

journal homepage: www.elsevier.com/locate/icarus

Precision topography of a reversing sand dune at Bruneau Dunes, Idaho, as an analog for Transverse Aeolian Ridges on Mars

James R. Zimbelman *, Stephen P. Scheidt

Center for Earth and Planetary Studies, National Air and Space Museum, MRC 315, Smithsonian Institution, Washington, DC 20013-7012, USA

ARTICLE INFO

Article history:
Available online 13 August 2013

Keywords:
Mars, Surface
Mars
Earth
Geological processes
Data reduction techniques

ABSTRACT

Ten high precision topographic profiles across a reversing dune were created from a differential global position system (DGPS). The shapes of the profiles reveal a progression from immature to transitional to mature characteristics moving up the dune. When scaled by the basal width along each profile, shape characteristics can be compared for profiles whose horizontal scales differ by orders of magnitude. The comparison of width-scaled Bruneau Dunes profiles to similarly scaled profiles of Transverse Aeolian Ridges (TARs) on Mars indicates that many TARs are likely similar to transitional or mature reversing sand dunes.

Published by Elsevier Inc.

1. Introduction

A reversing sand dune is defined to be "a dune that tends to develop unusual height but migrates only a limited distance because seasonal shifts in direction of the dominant wind cause it to move alternately in nearly opposite directions" (Jackson, 1997, p. 545). The seasonal wind pattern is therefore bidirectional for reversing dunes, where the two dominant winds from nearly opposite directions are balanced with respect to strength and duration (McKee, 1979). The Bruneau Dunes in central Idaho are an excellent place to conduct a study of reversing sand dunes because here the dunes have grown to impressive heights in a wind regime that supports the development of reversing dunes rather than horizontally migrating dunes. The dunes are protected from off-road vehicular traffic because the main dune complex is located within the boundaries of the Bruneau Dunes State Park (Zimbelman and Williams, 2007). The Bruneau Dunes are a 1.5-h drive SE from Boise, and they are only 29 km (18 mi) south of the city of Mountain Home.

Recent data from Mars has stimulated interest in the collection of detailed topographic information about reversing dunes. The High Resolution Imaging Science Experiment (HiRISE) camera on the Mars Reconnaissance Orbiter spacecraft has returned over 20,000 images that reveal the martian surface in exquisite detail, with many of the images achieving a ground spatial resolution of 25 cm per pixel (McEwen et al., 2007). Early HiRISE images included some dramatic examples of aeolian bedforms that have been given the non-genetic name 'Transverse Aeolian Ridges' (TARs), a general term proposed for linear to curvilinear aeolian features that could be the result of either dune or ripple formation processes (Bourke et al., 2003). Profiles derived from photoclinometry of TARs in HiRISE images showed that TARs larger than 1 m in height compared favorably to profiles of reversing dunes at Coral Pink Sand Dunes State Park in southern Utah, while TARs less than 0.5 m in height were very distinct from the reversing dune profiles but consistent with measured profiles of megaripples (Zimbelman, 2010).

In order to provide a test of the reversing dune hypothesis for large TARs on Mars, we collected a series of precision topographic profiles across one of the large reversing dunes at the Bruneau Dunes, as first reported at the Third Planetary Dunes workshop (Zimbelman and Scheidt, 2012). The resulting profiles provide valuable new information about probable stages of formation encountered during the growth of reversing dunes, as well as a possible tool for evaluating the relative state of evolution of reversing dunes. The profile series provides a template for evaluating the possible stages of evolution of individual TARs on Mars, under the working hypothesis that large TARs have profile shapes comparable to that of reversing dunes.

2. Background

The Bruneau Dunes State Park was formed in order to preserve a very unique natural area, as well as provide protection for the wildlife that make use of two lakes on the northwest side of the dunes (inset, Fig. 1). Established in 1970, the park covers 19.4 km^2 (4800 acres), including the tallest single-structured (i.e., not braced against other dunes or mountains) sand dune in North

* Corresponding author. Fax: +1 202 786 2566.
E-mail addresses: zimbelmanj@si.edu (J.R. Zimbelman), sscheidt77@gmail.com (S.P. Scheidt).

0019-1035/$ - see front matter Published by Elsevier Inc.
http://dx.doi.org/10.1016/j.icarus.2013.08.004

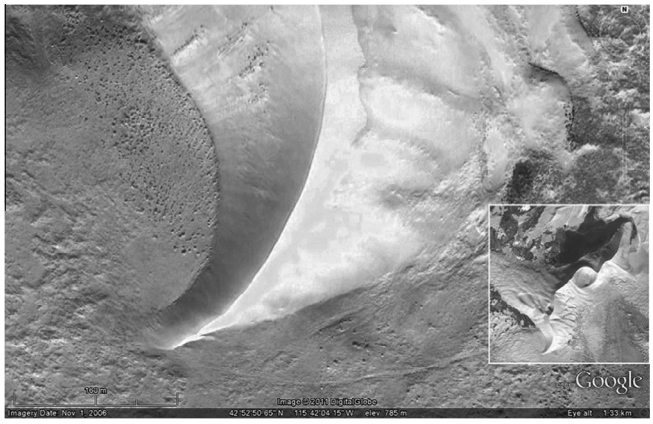

Fig. 1. Google Earth image mosaic of the study location at the southern end of the Bruneau Dunes, Idaho (11/1/06). North is to the top. Inset shows all of the largest dunes, and the lakes at their northern end.

America, which has 143 m (470 ft) of relief from the summit of the tallest dune to the lake level (for information about the park, see parksandrecreation.idaho.gov/parks/bruneau-dunes or www.idahoparks.org/state-parks/bruneau-dunes-state-park). The largest dunes are interpreted to be reversing dunes (Murphy, 1973), but features on the sides of the largest dunes suggest possible form flow interactions that can move sand in directions at large angles relative to the regional wind direction (Howard et al., 1978). There are some visual similarities between features observed on the Bruneau Dunes and patterns present on the arms of star dunes (e.g., Lancaster, 1989), where sand transport occurs oblique to crest orientation. The sheer size of the main Bruneau Dunes may induce complex local wind patterns on the sides of dunes.

The Bruneau Dunes are located approximately in the center of an old cut-off meander of the Snake River, now called Eagle Cove, that was carved into lacustrine sediments of the Glenns Ferry and Bruneau Formations, which are from Upper Pliocene to Middle Pleistocene (respectively) in age (Murphy, 1973). The close proximity of Eagle Cove to the present day channel of the Snake River contributes significantly to a constraint for the probable initiation of the sand accumulation represented by the current large sand dunes.

The Snake River is the main drainage pathway for water to exit the southern portions of Idaho. This large river has carved a substantial canyon into the basalt lava flows that comprise the surface materials of the Snake River Plains, the largest physiographic province within southern Idaho. There is abundant geologic evidence that the present day Snake River is but a mere shadow of the major flood that passed through this river system during the Pleistocene (Malde, 1968). Glacial Lake Bonneville attained a level that overtopped its rim at Red Rock Pass in southeastern Idaho, leading to rapid downcutting at the site of the breach and the rapid release of 4700 km^3 of water onto the Snake River Plains; erosional features and flood deposits along the Snake River Canyon indicate that the peak discharge during this catastrophic flood was most likely ~935,000 m^3/s, so that a minimum duration of about 8 weeks was needed to move the total volume of released water through the canyon at the peak discharge rate (Jarrett and Malde, 1987; O'Connor, 1993). The massive Bonneville Flood occurred about 15,000 years ago (Jarrett and Malde, 1987), and it is presumed that the flood would have easily removed any aeolian sand deposits from Eagle Cove that pre-dated the flood (Murphy, 1973). The sand at the Bruneau Dunes consists (by volume) of 62% quartz, 26% feldspar, and 12% basaltic (iron-rich) particles, indicating a closer affinity to the nearby Bruneau and Glenns Ferry Formation sediments than to the basalts and other rocks exposed upstream of Eagle Cove (Murphy, 1973). Aeolian or fluvial activity would not have needed to transport the sand very far to get it into Eagle Cove. However, once sand got into Eagle Cove, the wind pattern is such that it likely could not have easily exited later.

Reversing sand dunes form under a bidirectional wind regime, where two dominant winds come from directions that are almost directly opposite of each other (McKee, 1979). The Remote Automated Weather Station (RAWS) system, operated by the U.S. government, has >1900 individual instrumented weather stations (as of 2002) spread throughout the conterminous United States, Alaska, and Hawaii (Zachariassen et al., 2003, p. 2). The Mountain Home Air Force Base (MHAFB) RAWS station is located about 21 km NW of the Bruneau Dunes. Using a web-based access page, we obtained MHAFB RAWS data from 2010, which clearly demonstrates a strong bimodal annual wind regime for the region, although minor winds can blow from a variety of directions during spring and fall (Fig. 2). It is justifiable to ask whether wind records obtained 21 km away from the study site reflect the wind conditions experienced at the dunes. We attempted to address this issue by installing an inexpensive weather-proof timelapse digital camera (known commercially as a 'GardenWatchCam') to obtain hourly images of the study site at the Bruneau Dunes. Use of timelapse digital cameras has proved to be a cost-effective method for monitoring sand mobility in previous aeolian studies (Lorenz, 2011; Lorenz and Valdez, 2011). During more than 2 years of GardenWatchCam monitoring of the study site (from April 27, 2011, through August 31, 2013), images of bidirectional intense saltation occurring at the south end of the dunes (Figs. 3 and 4) correlate very well with strong wind events (taken here to be >6 m/s average winds sustained for >3 h) recorded at the MHAFB RAWS site, providing on-site validation that the bimodal wind pattern that dominates the RAWS data (Fig. 2) is consistent with the major sand-driving events observed to take place at the dunes.

In order to obtain precise topographic profiles of the sand dunes, we utilized a Differential Global Positioning System (DGPS). The equipment used in this project was a Trimble R8 Total Station, a carrier-phase DGPS system consisting of a stationary base receiver and a roving receiver to collect the individual survey points; this system provides horizontal accuracy of 1–2 cm and vertical accuracy of 2–4 cm, relative to the base station location (Zimbelman and Johnston, 2001). When combined with field notes and photographs tied to survey point locations, DGPS topographic data have proved to be very useful in addressing diverse geomorphic topics (e.g., Zimbelman and Johnston, 2001; Irwin and Zimbelman, 2012; Zimbelman et al., 2012). Precise topographic profiles across aeolian depositional features at diverse scales has proved to be very helpful in distinguishing between alternative formation mechanisms that have acted to generate the features (Zimbelman et al., 2012).

Topographic information for TARs on Mars have recently been derived from HiRISE image data (Zimbelman, 2010; Shockey and Zimbelman, 2013), generating profiles that can be compared to the measured profiles of aeolian features on Earth (Zimbelman et al., 2012). The study project at the Bruneau Dunes was carried out specifically in order to obtain a well constrained topographic data set for a reversing sand dune, to serve as a guide for evaluating the hypothesis that TARs > 1 m in height are most similar to reversing dunes (Zimbelman, 2010).

3. Methodology

The DGPS surveys were carried out across the southernmost reversing dune at the Bruneau Dunes (Fig. 1). This location was chosen for the study because this dune progresses steadily from a low sand ridge into a large reversing dune (going north),

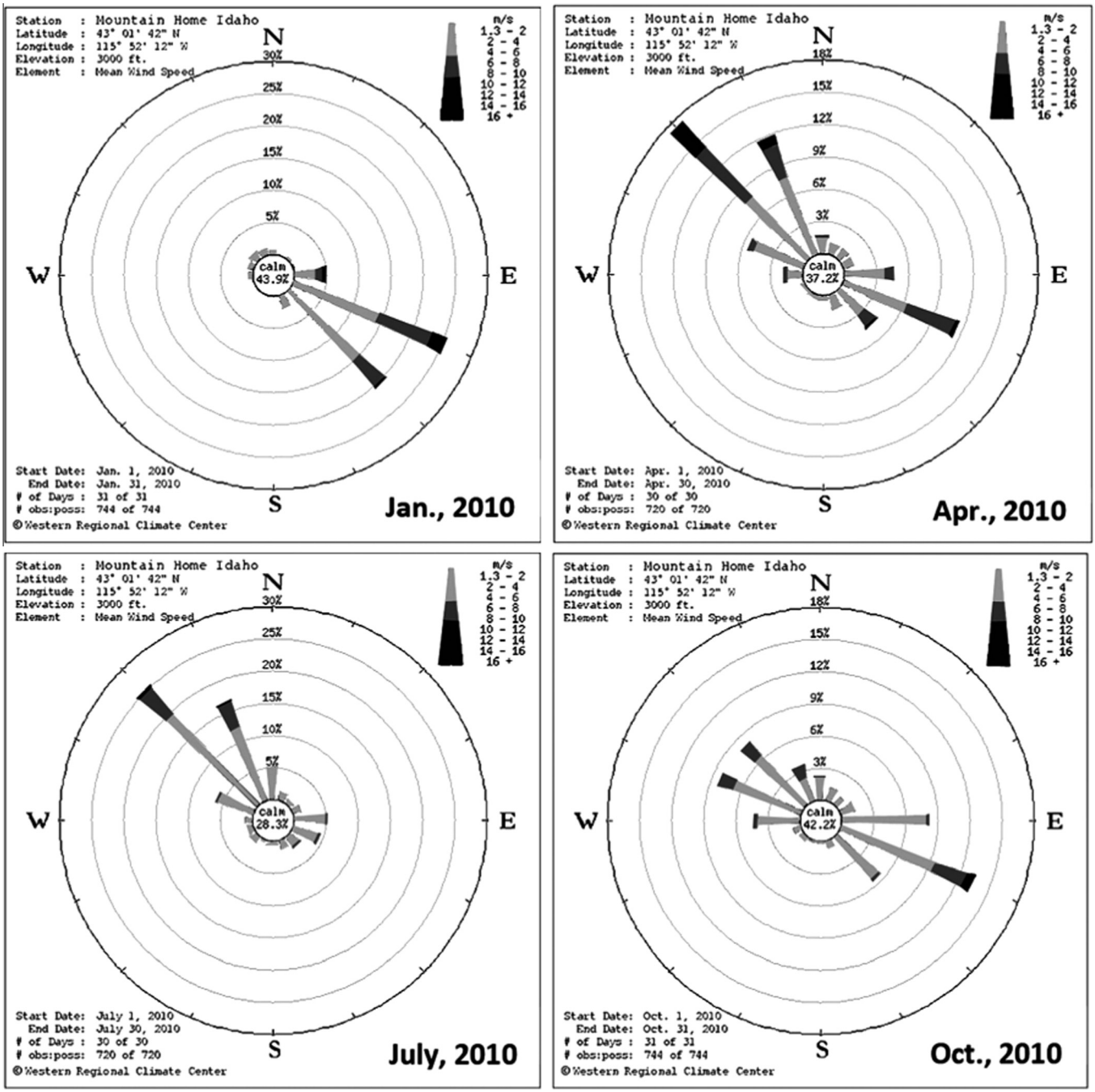

Fig. 2. Wind roses derived from RAWS data (Zachariassen et al., 2003) from station at the Mountain Home Air Force Base, located ~21 km NW of the Bruneau Dunes. Diagrams show the average wind strength and azimuth in four monthly averages during 2010. A seasonal bimodal wind pattern is evident, with spring and fall being transitional between oppositely directed winter and summer winds. Wind strength scale is simplified to three shades of gray; the two darkest gray shades are winds above the saltation threshold.

providing the opportunity to document the cross-sectional topography as it varies across the dune crest at a single site. The study location is well removed from the parking areas within the state park, which minimizes the public foot traffic at this part of the dune field, and thus maximizes the potential to document undisturbed dune morphology. Approximately a 1 h hike is required to go from a vehicle parking area (N42°54′2″, W115°41′40″; WGS84) to the study site (N42°52′50″, W115°41′57″) by traversing around the east side of the main dunes. The northern tip of the Bruneau Dunes extends into a lake present near the parking areas (Fig. 1, inset), which would have required the surveys to end at the waterline rather than extend onto the surrounding terrain. Intermediate portions of the Bruneau Dunes display substantial interactions between two main lines of reversing dunes, which would have complicated distinguishing the attributes of a single reversing dune at these locations.

On April 27, 2011, the authors conducted a series of ten DGPS traverses across the southern dune (Fig. 5). Traverse directions alternated between going W to E and going E to W as the surveys progressed upward in height along the dune crest. Labels in Fig. 5 indicate the start of each survey line. However, all topographic profiles presented below have been adjusted to represent distance across the dune beginning at the west side. The surveyed dune has a broad arcuate shape (Fig. 1), possibly influenced by some

Fig. 3. GardenWatchCam image of the southern end of the Bruneau Dunes showing strong saltation caused by wind from the NW (5/9/11).

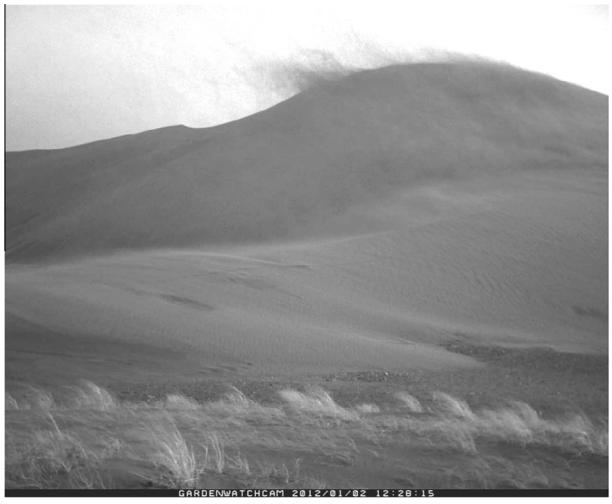

Fig. 4. GardenWatchCam image of the southern end of the Bruneau Dunes showing strong saltation caused by wind from the SE (1/2/12).

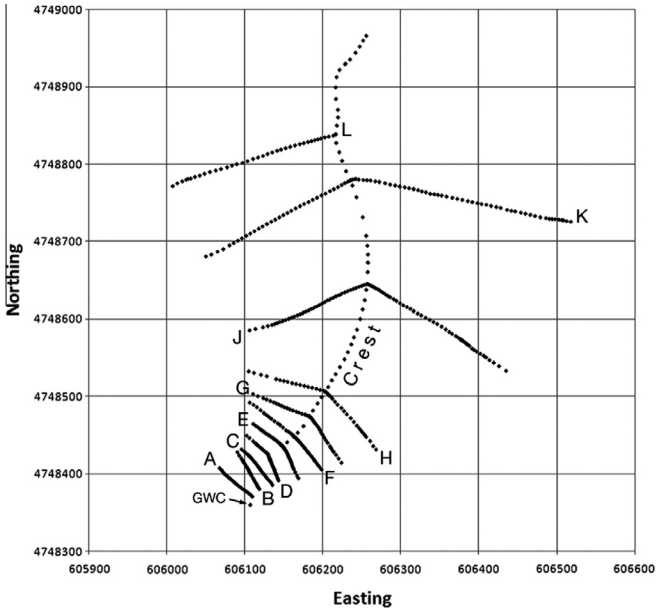

Fig. 5. Differential Global Positioning System (DGPS) transects across the southern end of the Bruneau Dunes, shown in UTM coordinates (Zone 11N). Profiles are labeled near the end of each line where that transect started. 'Crest' indicates points surveyed along the sharp crest after completing the profile transects. 'GWC' indicates the location of GardenWatchCam, looking NNE toward the summit of the southernmost large dune.

Table 1
Average slopes for the Bruneau reversing dune determined from DGPS surveys.

Profile	Slope (°) removed	h (m)	h/x W side	Slope (°)	h/x E side	Slope (°)
A	3.4W	1.0	0.0895	5.1	0.0342	2.0
B	3.3W	3.3	0.2157	12.2	0.1224	7.0
C	4.1W	4.7	0.2260	12.7	0.2185	12.3
D	4.2W	8.0	0.3627	19.9	0.3269	18.1
E	3.4W	13.1	0.3817	20.9	0.3098	17.2
F	3. 2W	16.3	0.3286	18.2	0.3683	20.2
G	3.4W	24.7	0.4970	26.4	0.4495	24.2
H	2.3W	34.8	0.4184	22.7	0.4439	23.9
J	1.7W	76.1	0.5614	29.3	0.4158	22.6
K	1.4W	106.6	0.5602	29.3	0.3938	21.5
L	0	122.2	0.5478	28.7	–	–

subtle local topography revealed during the DGPS surveys. For traverses D to K, the survey line orientation was adjusted at the dune crest so that the line always followed the local path of maximum increase or decrease in height, which was perpendicular to the crest orientation encountered along each line. During each survey, one person operated the R8 roving receiver while the other person took notes and photographs keyed to the number assigned to each point along the survey line.

Ten survey lines (labeled A to K, skipping I) were collected across the dune, after which points were collected following the sharp crest going north along the dune. After completion of the crest survey, transect L was obtained going down the west side of the dune, starting at the highest point on the dune; this survey line passed close to an abandoned fence line, so a few of the fence posts were surveyed as possible control points for future DGPS surveys in this area. Surveys A through J were carried out using real time kinematic (RTK) DGPS where the rover and base stations had a clear line of sight between them. Surveys K through L and the crest survey were conducted using post processing kinematic (PPK) DGPS techniques using the same base station location as that of the RTK surveys. The accuracy of the individual DGPS positions (<4 cm horizontal and vertical) means that differences between two surveyed points will be accurate to better than a decimeter, so relative distances and elevations reported here are listed to the nearest 0.1 m. Individual transect points were processed into profiles by calculating the distance between two adjacent points, then associating surveyed elevations to each point along the distance-based profile line. After a raw profile was generated, the local underlying slope could be determined, assisted by field notes that documented the points corresponding to the base of the dune. The local slope, determined by assuming a straight line between the base points on both sides of the dune (listed in Table 1), was then subtracted from each profile. Because profile L only covers the western side of the dune, no local slope was removed from it.

A GardenWatchCam timelapse digital camera was mounted 1.5 m above the sand surface on a post near the southern end of the surveyed dune ('GWC' in Fig. 5, which corresponds to the GPS location given above for the survey site) during the same trip used to collect the DGPS data. This camera has recorded hourly images of the surveyed dune that have documented major sand-driving events (e.g., Figs. 3 and 4) at the site since the surveys were

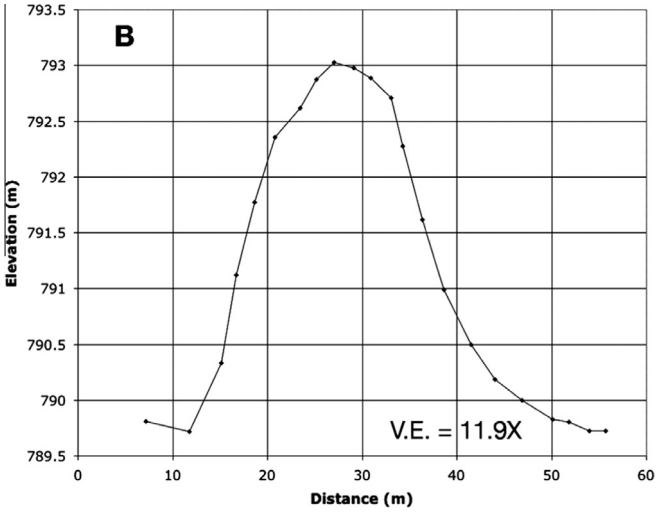

Fig. 6. DGPS survey B, showing a profile across an immature low sand ridge. Profile is shown going W to E, and a 3.3° West-dipping slope has been removed. Vertical exaggeration is 11.9×.

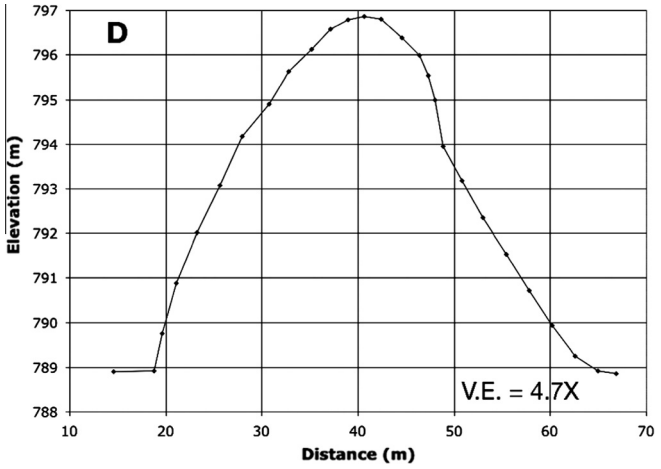

Fig. 7. DGPS survey D, showing a profile across a transitional part of the dune. Note subtle break in slope at ~48 m distance. Profile is shown going W to E, and a 4.2° West-dipping slope has been removed. Vertical exaggeration is 4.7×.

conducted, starting on April 27, 2011. More than 2 years of time-lapse image data (through August 31, 2013) have shown a close correlation between sand-driving events at the study site and strong winds recorded at the MHAFB RAWS station. It is beyond the scope of the present project to explore the RAWS wind records in depth, but the GardenWatchCam data increase our confidence that RAWS data from the MHAFB station are representative of the major wind activity experienced at the Bruneau Dunes.

4. Results

The DGPS data provide an interesting series of profiles that document how the topography of the reversing dune changes with distance up the axis of the dune. Local slopes removed from the profiles indicate that this portion of the dune has been built upon a shallow westward dipping slope (Table 1). Also, the surveyed elevations at the western base of the dune decrease by a cumulative 24.6 m going north from profiles A to L. The underlying local slopes and the decreasing elevations to the north suggest that the southern end of the dune likely lies across the southern margin of the shallow depression represented by Eagle Cove, with the lakes at the northern end of the dunes likely corresponding to the lowest part of the depression. It is at least possible that the subtle relief of the underlying depression may have contributed to the broad arcuate shape of the southern end of the dune (Fig. 1).

Profiles A to C cross the southern tip of the dune, where all three profiles are distinguished by low overall relief and the lack of a slip face; this part of the dune is essentially a low sand ridge. Profile B (Fig. 6) is typical of this immature section of the dune, the long axis of which is aligned with the axis of the main dune crest. During the collection of all three of these profiles, no field evidence was observed to indicate that flow separation was taking place as the sand moved over the sand ridge. However, following a few very strong wind events, a transient small (<15 cm high) sharp crest was visible in some GardenWatchCam images for the portion of the dune covered by profiles A to C, but such a feature rarely remained visible longer than a few days. Bagnold (1941, p. 183) observed in his wind tunnel that fully developed saltation induces a drag on the wind profile that resulted in sand deposition ~6 m downwind from where the intense saltation began; he inferred that this distance represented the minimum size of a dune, because over a distance smaller than this size sand is preferentially removed, whereas a sand patch larger than this size will tend to grow through deposition. Today numerical models can investigate the physics of grain motions in the air and grain-to-grain interactions, so that a continuum saltation model provides the theoretical basis behind the minimum size of a sand dune (e.g., Sauermann et al., 2001). The three profiles across the immature sand ridge portion of the dune are $\geqslant$40 m in width, well in excess of Bagnold's minimum dune size. The presence or absence of a slip face should not be the defining characteristic for deciding whether or not a sand deposit can be considered to be a 'dune'.

Starting with profile D (Fig. 7), the sand ridge begins a transition toward the development of a sharp crest. While still lacking even a small slip face, profile D reveals that the top of the sand ridge has a broad pile of sand superposed on the smooth slope that typifies both of the lower flanks of the ridge (note the inflection point at ~48 m distance in Fig. 7). This feature is far too subtle to be readily apparent from visual inspection alone; a precision topographic transect was required to identify its presence. This low mound of sand at the top of the sand ridge may be better situated to respond to the alternating wind directions resulting from the bimodal wind regime associated with reversing dunes (e.g., Fig. 2), than would be the sand ridge itself.

The mound on top of the sand ridge finally has a small but distinct crest in profile E (Fig. 8). An inflection point similar to the one in profile D (Fig. 7) is present at ~53 m distance in profile E, but here the magnitude of the change in slope at the inflection point is considerably greater than the inflection point lower on the dune. Inflection points on the E side of both profiles D and E suggest that the most recent strong wind was from the west, consistent with the RAWS data for the weeks immediately preceding the survey work. Profile F has a good sharp crest, but it does not have an inflection point like the ones in profiles D and E, nor is the magnitude of its average flank slopes (Table 1) quite as large as those of a mature reversing dune, discussed next, so it appears to be transitional between mound-topped and mature profiles.

Profile G (Fig. 9) is the first profile that illustrates the main attribute of a mature reversing dune. Both sides of profile G are remarkably constant in slope away from the very sharp crest, giving a strong sense of symmetry to the profile. The average slope angle exceeds 24° on both sides of profile G (Table 1), but the average slope value ranges from 22° to 29° for the other mature profiles. As steep as these slope values are, they are still well below the angle of repose, which is the maximum angle (measured from horizontal) at which loose, cohesionless material will come to rest on

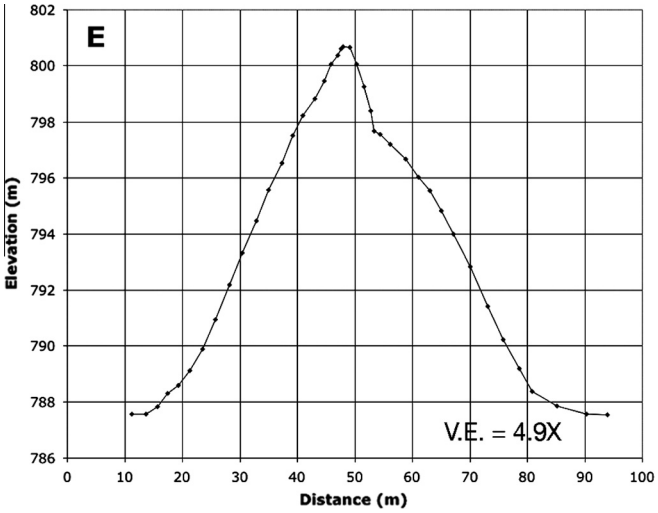

Fig. 8. DGPS survey E, showing a profile across a transitional part of the dune, with a mound present on top of a sand ridge base. Profile is shown going W to E, and a 3.4° West-dipping slope has been removed. Vertical exaggeration is 4.9×.

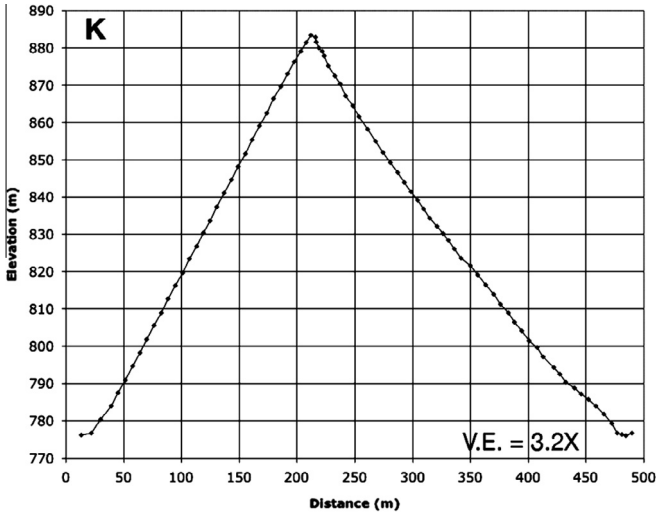

Fig. 10. DGPS survey K, showing a profile across a mature symmetric part of the dune, with 106.6 m of total relief. Profile is shown going W to E, and a 1.4° West-dipping slope has been removed. Vertical exaggeration is 3.2×.

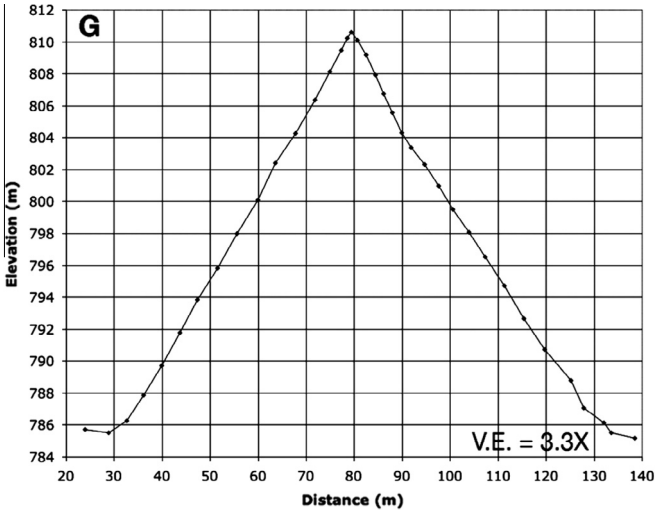

Fig. 9. DGPS survey G, showing a profile across a mature symmetric part of the dune, with 24.7 m of total relief. Profile is shown going W to E, and a 3.4° West-dipping slope has been removed. Vertical exaggeration 3.3×.

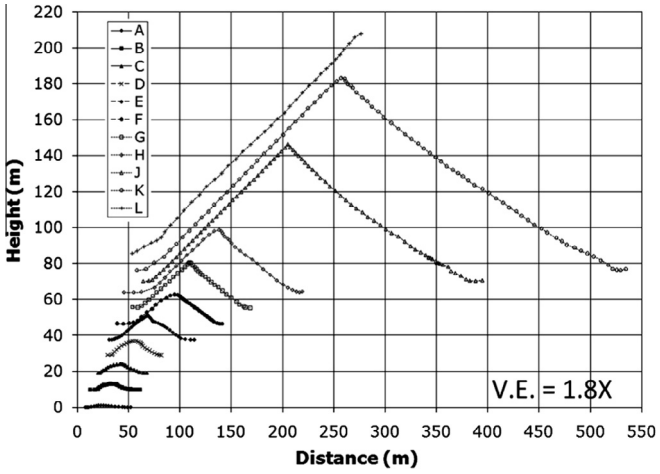

Fig. 11. All DGPS profiles at the Bruneau reversing dune, shown at the same scale. Successive profile starting points are offset 5 m horizontally and 10 m vertically, for clarity. Vertical exaggeration is 1.8×.

a pile of similar material (Jackson, 1997, p. 25). The angle of repose reported in the literature for dry sand on dune slip faces varies little from 33 ± 1° (Cooke and Warren, 1973, p. 276). Hence, the slopes of reversing dunes are not really very close to the slope found on a slip face, which is not surprising since sand will be moving back and forth across the dune crest, and thus cannot be near the angle of repose on both flanks at the same time. The sense of symmetry continues through profile K (Fig. 10) even as the total height and total width of the dune has steadily increased by more than a factor of four from profile G to K (Table 1). While not a complete profile, transect L documents that this reversing dune attains a maximum height of 122.2 m (Table 1).

It is difficult to appreciate the large change in scale that takes place across the surveyed profiles. When shown at the same horizontal and vertical scales (Fig. 11), the very low relief of the immature sand ridge profiles makes them almost indiscernible, although the large size of the mature profiles is readily apparent. Previous work has demonstrated that scaling both the horizontal and vertical dimensions by the feature width (defined as the distance between the basal breaks in slope on both sides of the feature) is an effective way to preserve profile detail while comparing features that may differ by more than three orders of magnitude in absolute scale (Zimbelman et al., 2012). Fig. 12 shows the ten complete profiles for the Bruneau reversing dune when they have been scaled by the feature width (listed for each profile inside parentheses in the symbol key). Symbols and line styles help to distinguish between the three classes of profiles discussed above: immature sand ridge profiles in solid symbols and solid lines, transitional profiles in large dashed lines, and mature profiles in open symbols and small dashed lines. Along with preserving shape detail for each profile, this representation shows the steady increase in the scaled height for each profile; maximum height divided by feature width is therefore a key parameter for determining where along the 'maturity' continuum any single profile may lie, aided by details of the profile shape. It is particularly interesting to see how similar the four mature profiles appear, particularly on their west (left) side, which is consistent with the west being the windward side for the most recent strong winds. There is considerable variation in where the dune high point occurs along the scaled distance axis,

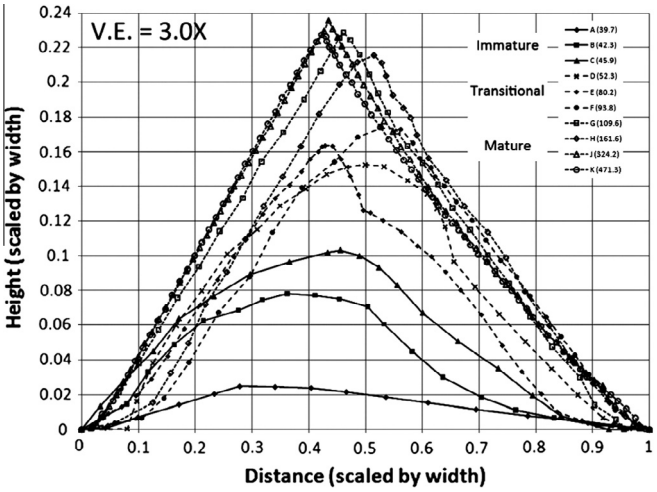

Fig. 12. Ten complete DGPS profiles from the Bruneau reversing dune, with both horizontal and vertical values scaled by the feature width for each profile (width values in m are listed in parentheses). Vertical exaggeration is 3.0×.

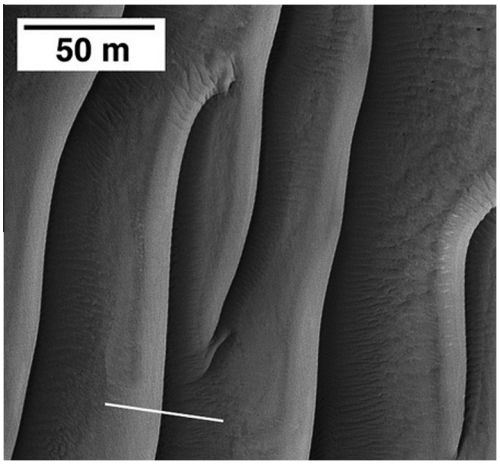

Fig. 13. Transverse Aeolian Ridges (TARs) on Mars. White line shows location of one profile (45.3 m width) that is included in Fig. 14. Portion of HiRISE image TRA_000823_1720, 7.7 S, 279.5 E, 25 cm/pixel. NASA/JPL-Caltech/U of A.

most likely due to local intensification or weakening of winds blowing over a feature as large as the Bruneau Dunes. Profiles in a composite width-scaled figure like Fig. 12 can serve as a general template to assess the relative maturity of features that are suspected of being reversing sand dunes, as discussed below.

The widely spaced points that followed the sharp crest line (Fig. 5) were sufficient to show a monotonic increase in elevation going up the dune, all the way to the local high point on transect L. From this local high, the elevation of the crest was broadly undulatory, gradually increasing 7.8 m in height while traversing 152 m north of transect L, so overall height of the biggest dunes slowly increases going north. At the same time, the topography on which the dunes are emplaced decreases toward the center of Eagle Cove, leading to the tallest dune (adjacent to the large lake) having a reported relief of 143 m. The surveyed DGPS points were imported into Google Earth following the conclusion of the field work, where we noted that the surveyed crest points did not correspond to the crest locations visible in the Google Earth images. Although the offset between some of the survey points and commercial images may be a result of a mismatch between coordinate systems or image geolocation accuracy, some parts of the survey lines matched up well with the image data. It is equally as likely that the crest location shifted in horizontal position between the times of image collection and the DGPS survey, raising the possibility that precise monitoring of crest location throughout the year may serve as a proxy for annual adjustments caused by fluctuations in seasonal wind patterns.

5. Discussion

The motivation for obtaining the topographic profiles at the Bruneau Dunes was to make use of the field data in evaluating the probable origins for TARs on Mars. HiRISE images finally show TARs with sufficient detail (Fig. 13) to make inferences about their shape from the way that the pixel brightness varies across an individual TAR. Three TAR profiles, corresponding to profiles A, C, and D of Zimbelman (2010), were scaled by their basal width to facilitate their direct comparison with three Bruneau profiles representing immature, transitional, and mature states of a reversing dune (Fig. 14). Two of the TAR profiles are most consistent with the transitional profile in terms of scaled height, although the martian features have much sharper crests than does the transitional profile. One TAR compares quite well with a mature profile from Bruneau,

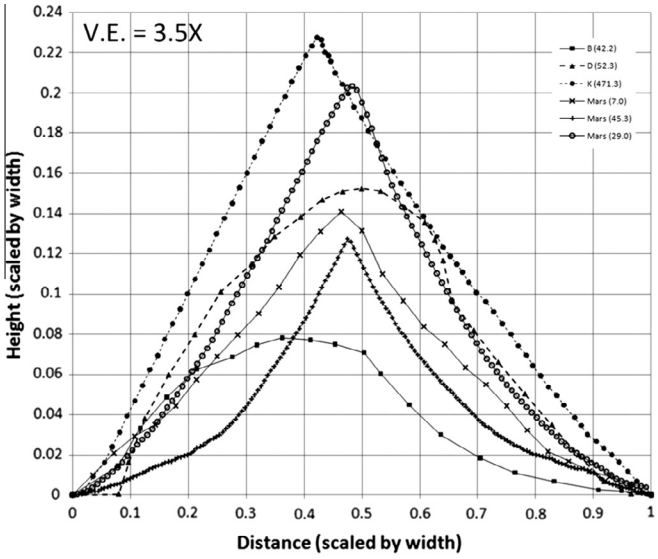

Fig. 14. Profiles of three Bruneau Dunes DGPS transects (closed symbols, profiles B, D, and K, this work) and three Mars TAR features (profiles A, C, and D, from Table 1 of Zimbelman (2010)), all scaled by feature width (width values in m are listed in parentheses). TARs are most similar to transitional and mature Bruneau profiles. Vertical exaggeration is 3.5×.

both in terms of profile shape and in maximum scaled height. Both profile shape and scaled height therefore suggest that TARs are generally more evolved than that of an immature sand ridge. Indeed, the overall shape of the sand ridge section of the Bruneau Dune (Fig. 6) is very similar to a profile across a broad sand patch on Mars (Fig. 6 of Zimbelman (2010)), consistent with the lack of either a sharp crest or a slip face visible on the martian sand patch. We interpret all of the above to suggest that large TARs (those larger than 1 m in height) are most similar to the transitional to mature parts of a growing reversing dune. This conclusion is also supported by observations that the topography across reversing dunes is measurably distinct from that of other transverse dunes, as well as from the topography across ripples, megaripples, and draa (Zimbelman et al., 2012). However, it is important to note that reversing dunes form under rather specific wind conditions, wind patterns that may be difficult to reconcile with the nearly planet-wide distribution of TARs on Mars (e.g., Balme et al., 2008; Berman et al., 2011).

The high degree of symmetry of most TAR profiles (Shockey and Zimbelman, 2013) argues strongly that bimodal winds of comparable strength and intensity may have been involved in their formation. Dramatic temperature extremes are generated globally on Mars by the thin martian atmosphere, whose relatively small heat capacity means that it cools and heats much more rapidly than our own atmosphere throughout the course of a day (Carr, 1981, p. 27). Possibly the dramatic diurnal temperature extremes on Mars may cause strong tidal winds, particularly where those winds become channeled within a valley or between broad topographic highs. Still, it is difficult to reconcile the wide distribution of TARs across Mars with the global wind patterns that exist at present (e.g., Zurek et al., 1992). The annual bimodal winds typical of the Bruneau area (Fig. 2) might be more similar to seasonal changes in wind patterns on Mars, but such relationships need to be explored by meteorological investigations well beyond the scope of the present study.

Maximum height scaled by width appears to be an important topographic parameter for evaluating the likely origin of aeolian bedforms (Zimbelman et al., 2012). Fig. 15 compares height/width values as a function of width for measured profiles from dozens of megaripples and transverse dunes on Earth (data from Fig. 5 of Zimbelman et al. (2012)) to values derived from the ten Bruneau profiles (large filled circles), and also to more than seventy TARs on Mars (small dots; data from Zimbelman (2010), and Shockey and Zimbelman (2013)). Several interesting trends are apparent from all of these data; we will first examine the track followed by points derived from the ten Bruneau profiles.

For the immature sand ridge section of the Bruneau reversing dune, values of height/width increase steadily as the profiles progress up the dune while overall width remains nearly constant. In general, height/width <0.13 appears to represent the immature phase of reversing dune development, where vertical growth entirely dominates over any significant increase in the width of the feature. The transitional phase of the Bruneau profiles begins at a point consistent with the trend followed in the immature section, but now the height/width values increase from 0.15 to 0.18 while at the same time width more than doubles. Vertical growth continues in this section, but now dune width also grows at roughly half the rate as the growing height. Once the mature stage is reached, height/width remains between 0.21 and 0.24 while height and width now change in lock step; height/width changes relatively little while width increases by more than a factor of five. Only reversing dunes (open and closed circles in Fig. 15) experience vertical growth sufficient to raise their height/width values well above ~0.15, which is the maximum value attained by transverse dunes (× in Fig. 15).

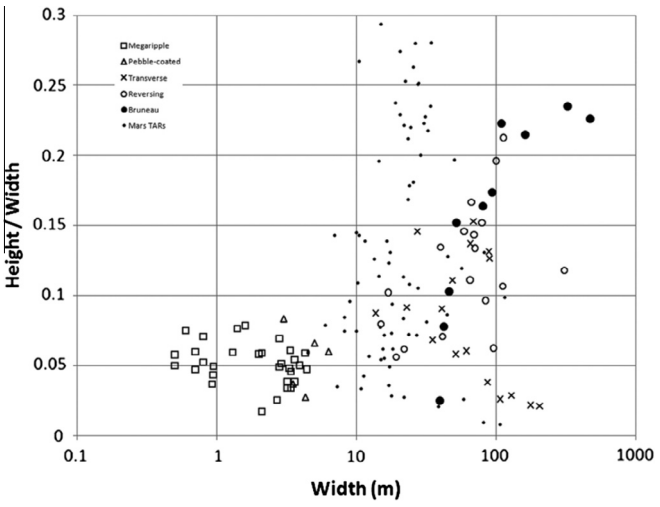

Fig. 15. Height/width as a function of log width, for features on Earth and Mars. Megaripple (open squares), pebble-coated megaripple (open triangle), transverse dune (×s), and reversing dunes (open circles) data are from the supplementary data file of Zimbelman et al. (2012). Bruneau reversing dune data (large filled circles) are from this work. Mars TAR data (small dots) are from Table 1 of Zimbelman (2010) and the supplementary data file of Shockey and Zimbelman (2013). See Section 5 of text.

The overall trend outlined above is consistent with measurements that are less precise than what is obtained through DGPS; the two largest height/width values previously reported for reversing dunes also come from the Bruneau Dunes, where a less precise laser inclinometer (precision of individual measurements was 0.3 m) produced values that fall along the trend between the transitional and mature DGPS points. Physical dimensions of dune-like features obtained from laboratory or numerical studies (e.g., Reffet et al., 2010; Taniguchi et al., 2012) should be amenable to comparison with the measured attributes shown in Fig. 15. Kocurek et al. (1992) documented the seasonal construction and destruction of sand dunes on Padre Island, Texas, with dunes growing from small patchs of sand into regular dunes, which were subsequently removed by winter storm winds, a situation that may warrant comparison to the Bruneau Dunes. We believe that the DGPS data from Bruneau reveal an evolutionary path that can be followed in a plot of height/width as a function of width, a path that might be explored through comparison with reversing dunes developed in a variety of formational settings.

Next consider the cloud of data points that represent measurements from dozens of TARs (small dots in Fig. 15) from locations scattered across Mars. The Mars TAR data come from measured heights and widths given in Table 1 of Zimbelman (2010; 13 TARs) and in the supplementary data file of Shockey and Zimbelman (2013; 60 TARs). In Fig. 15, the TAR data fill a gap between the fields representing values for megaripples (open squares) and pebble-coated megaripples (open triangles) and the values for transverse (×s) and reversing (open circles) dunes. The height–width distribution of TARs is generally similar to that of reversing dunes, but the measured height/width values of TARs extend to as much as twice that of transverse dunes, but are similar in shape to the overall trend for reversing dunes. While some of the TAR data points do overlap with the immature portion of the Bruneau trend, we do not believe this superposition indicates that most TARs are good matches to the immature part of the Bruneau reversing dune, particularly when the sharp-peaked symmetric profile shape for TARs (Fig. 14) is considered. Instead, the similarity of the overall range of height/width values between TARs and reversing dunes, but at widths scales generally 1/3 that of reversing dunes on Earth, raises the intriguing possibility that the reduced gravity of Mars (38% that on Earth) somehow contributes to the development of smaller symmetric TAR features on Mars relative to comparable features on Earth. We are unaware of a physical explanation for how the lower gravity on Mars should somehow result in martian landforms smaller than terrestrial counterparts, particularly since the low gravity and low atmospheric pressure cause sand saltation path lengths to be >10 times longer on Mars than they are on Earth (White, 1979). It is unwise to speculate too extensively on what is still a relatively limited data set derived from cross-sectional profiles for the features on both Earth and Mars, but these initial comparisons suggest that the height/width as a function of width parameter space warrants further investigation for features on both planets.

The height/width values in excess of 0.25 come from TARs at relatively high latitudes (lat. >30°N or S on Mars). It seems possible that features at mid- to high latitudes may include ground ice that would facilitate vertical growth beyond that of unconsolidated sand alone (a pile of sand with a slope angle of 33° would have a height/width value of 0.325). Another possibility is that during

long periods of stability (~50–200 ka inactivity for megaripples in Meridiani Planum, Golombek et al., 2010), dust that settled out of the atmosphere may filter between the particles on TARs and increase the angle of internal friction beyond that of unconsolidated materials alone, although if this effect is significant, it should occur anywhere on Mars rather than preferentially at high latitudes. Long periods of stability for megaripples (and TARs) on Mars would mean that wind patterns inferred from such features could be related to winds generated by conditions quite different from the present state of the atmosphere.

6. Summary

Ten precision profiles of a reversing dune show a progression from immature (lacking a sharp crest or slip face) sand ridge to mature (symmetric) reversing dune, for which both slopes are near the angle of repose. When scaled by the basal width of the feature, the Bruneau profiles can be compared to profiles of Transverse Aeolian Ridges (TARs) on Mars; this comparison suggests that many TARs are similar to either transitional or mature reversing dune profiles.

Acknowledgments

Comments by two anonymous reviewers were very helpful during revision of the manuscript. This research was supported by funds from the Becker portion of the Smithsonian Endowments.

References

Bagnold, R.A., 1941. The Physics of Blown Sand and Desert Dunes. Chapman and Hall, London, UK, 265p.
Balme, M., Berman, D.C., Bourke, M.C., Zimbelman, J.R., 2008. Transverse aeolian ridges (TARs) on Mars. Geomorphology 101, 703–720.
Berman, D.C., Balme, M.R., Rafkin, S.C.R., Zimbelman, J.R., 2011. Transverse aeolian ridges (TARs) on Mars II: distributions, orientations, and ages. Icarus 213, 116–130.
Bourke, M.C., Wilson, S.A., Zimbelman, J.R., 2003. The variability of Transverse Aeolian Ridges in troughs on Mars. Lunar Planet. Sci. XXXIV. Abstract #2090.
Carr, M.H., 1981. The Surface of Mars. Yale Univ. Pr., New Haven, 232p.
Cooke, R.U., Warren, A., 1973. Geomorphology in Deserts. Univ. Calif. Pr., Berkeley, CA, 394p.
Golombek, M. et al., 2010. Constraints on ripple migration at Meridiani Planum from Opportunity and HiRISE observations of fresh craters. J. Geophys. Res. 115, E00F08. http://dx.doi.org/10.1029/2010JE003628.
Howard, A.D., Morton, J.B., Gad-el-Hak, M., Pierce, D., 1978. Sand transport model of barchan dune evolution. Sedimentology 25, 307–338.
Irwin, R.P., Zimbelman, J.R., 2012. Morphometry of Great Basin pluvial shore landforms: Implications for paleolake basins on Mars. J. Geophys. Res. 117, E07004. http://dx.doi.org/10.1029/2012JE004046.
Jackson, J.A. (Ed.), 1997. Glossary of Geology, fourth ed. Am. Geol. Inst., Alexandria, pp. 769.
Jarrett, R.D., Malde, H.E., 1987. Paleodischarge of the late Pleistocene Bonneville Flood, Snake River, Idaho, computed from new evidence. Geol. Soc. Am. Bull. 99, 127–134.
Kocurek, G., Townsley, M., Yeh, E., Havholm, K.G., Sweet, M.L., 1992. Dune and dune-field development on Padre Island, Texas, with implications for interdune deposition and water-table-controlled accumulation. J. Sed. Res. 62 (4), 622–635.
Lancaster, N., 1989. The dynamics of star dunes: An example from the Gran Desierto, Mexico. Sedimentology 36, 273–289.
Lorenz, R.D., 2011. Observations of wind ripple migration on an Egyptian seif dune using an inexpensive digital timelapse camera. Aeol. Res. 3 (2), 229–234. http://dx.doi.org/10.1016/j.aeolia.2011.01.004.
Lorenz, R.D., Valdez, A., 2011. Variable wind ripple migration at Great Sand Dunes National Park and Preserve, observed by timelapse imagery. Geomorphology 133 (1–2), 1–10. http://dx.doi.org/10.1016/j.geomorph.2011.06.003.
Malde, H.E., 1968. The catastrophic late Pleistocene Bonneville Flood in the Snake River Plain, Idaho. U.S. Geol. Surv. Prof. Paper 596. 52p.
McEwen, A.S. et al., 2007. Mars Reconnaissance Orbiter's High Resolution Imaging Science Experiment (HiRISE). J. Geophys. Res. 112, E05S02. http://dx.doi.org/10.1029/2005JE002605.
McKee, E.D., 1979. Introduction to a study of global sand seas. In: McKee, E.D. (Ed.), A Study of Global Sand Seas. U.S. Geol. Surv. Prof. Paper 1052. Gov. Printing Office, Washington, DC, pp. 1–19.
Murphy, J.D., 1973. The Geology of Eagle Cove at Bruneau, Idaho. M.S. Thesis, State Univ. New York at Buffalo. 77p.
O'Connor, J.E., 1993. Hydrology, Hydraulics, and Geomorphology of the Bonneville Flood. Geol. Soc. Am. Sp. Paper 274. 83p.
Reffet, E., du Pont, S.C., Hersen, P., Douady, S., 2010. Formation and stability of transverse and longitudinal sand dunes. Geology 38 (6), 491–494. http://dx.doi.org/10.1130/G30894.1.
Sauermann, G., Kroy, K., Hermann, H.J., 2001. Continuum saltation model for sand dunes. Phys. Rev. E 64, 031305. http://dx.doi.org/10.1103/PhysRevE.64.031305.
Shockey, K.M., Zimbelman, J.R., 2013. Analysis of transverse aeolian ridge profiles derived from HiRISE images of Mars. Earth Surf. Process. Landforms 38, 179–182. http://dx.doi.org/10.1002/esp.3316.
Taniguchi, K., Endo, N., Sekiguchi, H., 2012. The effect of periodic changes in wind direction on the deformation and morphology of isolated sand dunes based on flume experiments and field data from the Western Sahara. Geomorphology 179, 286–299. http://dx.doi.org/10.1016/j.geomorph.2012.08.019.
White, B.R., 1979. Soil transport by winds on Mars. J. Geophys. Res. 84, 4644–4651.
Zachariassen, J., Zeller, K., Nikolov, N., McClelland, T., 2003. A Review of the Forest Service Remote Automated Weather Station (RAWS) Network. Gen. Tech. Rpt RMRS-GTR-119. U.S. Dept. Agric. and Forest Serv., Ft. Collins, CO. 163p.
Zimbelman, J.R., 2010. Transverse Aeolian Ridges on Mars: First results from HiRISE images. Geomorphology 121, 22–29. http://dx.doi.org/10.1016/j.geomorph.2009.05.012.
Zimbelman, J.R., Johnston, A.K., 2001. Improved topography of the Carrizozo lava flow: Implications for emplacement conditions. In: Crumpler, L.S., Lucas, S.G. (Eds.), Volcanology in New Mexico. New Mex. Mus. Nat. Hist. Sci. Bull. 18, Albuquerque, NM, pp. 131–136.
Zimbelman, J.R., Scheidt, S.P., 2012. Topographic profiles across a large reversing dune, to aid in evaluating the reversing dune hypothesis for TARs on Mars. In: Third International Planetary Dunes Workshop: Remote Sensing and Data Analysis of Planetary Dunes, LPI Contribution 1673, Lunar and Planetary Institute, Houston, pp. 105–106.
Zimbelman, J.R., Williams, S.H., 2007. Eolian dunes and deposits in the western United States as analogs to wind-related features on Mars. In: Chapman, M.G. (Ed.), The Geology of Mars: Evidence from Earth-based Analogs. Cambridge Univ. Pr., Cambridge, UK, pp. 232–264.
Zimbelman, J.R., Williams, S.H., Johnston, A.K., 2012. Cross-sectional profiles of sand ripples, megaripples, and dunes: A method for discriminating between formational mechanisms. Earth Surf. Proc. Landforms 37, 1120–1125. http://dx.doi.org/10.1002/esp.3243.
Zurek, R.W., Barnes, J.R., Haberle, R.M., Pollack, J.B., Tillman, J.E., Leovy, C.B., 1992. Dynamics of the atmosphere of Mars. In: Kieffer, H.H., Jakosky, B.M., Snyder, C.W., Matthews, M.S. (Eds.), Mars. Univ. of Arizona Pr., Tucson, pp. 835–933.